ASSURE A71 – Conduct Safety Risk Management Analysis on Unmanned Aircraft Detect and Avoid Systems

Task 2 Issue Report

June 04, 2025

v 1.0

NOTICE

This document is disseminated under the sponsorship of the U.S. Department of Transportation in the interest of information exchange. The U.S. Government assumes no liability for the contents or use thereof. The U.S. Government does not endorse products or manufacturers. Trade or manufacturers' names appear herein solely because they are considered essential to the objective of this report. The findings and conclusions in this report are those of the author(s) and do not necessarily represent the views of the funding agency. This document does not constitute FAA policy. Consult the FAA sponsoring organization listed on the Technical Documentation page as to its use.

LEGAL DISCLAIMER

The information provided herein may include content supplied by third parties. Although the data and information contained herein has been produced or processed from sources believed to be reliable, the Federal Aviation Administration makes no warranty, expressed or implied, regarding the accuracy, adequacy, completeness, legality, reliability, or usefulness of any information, conclusions or recommendations provided herein. Distribution of the information contained herein does not constitute an endorsement or warranty of the data or information provided herein by the Federal Aviation Administration or the U.S. Department of Transportation. Neither the Federal Aviation Administration nor the U.S. Department of Transportation shall be held liable for any improper or incorrect use of the information contained herein and assumes no responsibility for anyone's use of the information. The Federal Aviation Administration and U.S. Department of Transportation shall not be liable for any claim for any loss, harm, or other damages arising from access to or use of data or information, including without limitation any direct, indirect, incidental, exemplary, special, or consequential damages, even if advised of the possibility of such damages. The Federal Aviation Administration shall not be liable to anyone for any decision made or action taken, or not taken, in reliance on the information contained herein.

TECHNICAL REPORT DOCUMENTATION PAGE

1. Report No.	2. Government Accession No.	3. Recipient's Catalog No.
A11L.UAS.120_A71 – Detect and Avoid		

4. Title and Subtitle	5. Report Date
ASSURE A71 – Conduct Safety Risk Management Analysis on Unmanned System Detect and Avoid Systems: Issue Paper	August 30, 2024
	6. Performing Organization Code

7. Author(s)	8. Performing Organization Report No.
Tom Haritos, PhD., https://orcid.org/0000-0001-6546-383X Tim Bruner, https://orcid.org/0000-0002-7591-8823 Katie Silas, https://orcid.org/0000-0003-0647-4592 Kurt Carraway, https://orcid.org/0000-0002-1362-8177 Paul Snyder, https://orcid.org/0000-0003-2417-6388 Mark Askelson, https://orcid.org/0000-0002-8521-7158 James Cooley, Ph.D., https://orcid.org/0009-0004-2842-5892 Hever Moncayo, Ph.D., https://orcid.org/0000-0001-5088-9715 Richard Prazenica, Ph.D., https://orcid.org/0000-0001-6093-8891 Steven Weber Ph.D., https://orcid.org/0000-0002-9235-6922 Lifeng Zhou, Ph.D., https://orcid.org/0000-0001-7927-8504 Amirhosein Chahe, https://orcid.org/0009-0002-6883-2041 Sadia Afrin Ananna, https://orcid.org/0009-0003-6376-3275 Jorge Estupiñán, https://orcid.org/0009-0005-4922-3461 Rocio Jado-Puente, https://orcid.org/0000-0002-7567-1613	

9. Performing Organization Name and Address	10. Work Unit No.
Kansas State University University of North Dakota Embry Riddle Aeronautical University Drexel University	**11. Contract or Grant No.** A11L.UAS.120_A71 – Detect and Avoid

12. Sponsoring Agency Name and Address	13. Type of Report and Period Covered
Federal Aviation Administration UAS COE PM: Karen Davis, ANG-C2 UAS COE Dep. PM: Hector Rea, ANG-C2	Issue Report (…) **14. Sponsoring Agency Code** 5401

15. Supplementary Notes

Conducted in cooperation with the U.S. Department of Transportation, Federal Highway Administration.

16. Abstract

This issue paper explores DAA system functions and operations against the backdrop of the Safety Risk Management (SRM) process to identify issues and gaps that pose challenges to assessing risks associated with DAA systems. Framing this issue paper in terms of the SRM process – describing the system, identifying hazards, assessing risk, analyzing risk, and controlling risk – provides a rational way to look for issues and gaps that challenge effective SRM for DAA systems in each process step. This approach identifies issues and gaps that may be considered and addressed during the development of a DAA risk assessment framework in future research tasks.

17. Key Words	18. Distribution Statement
Safety Management Systems, Safety Risk Management, Detect and Avoid, Beyond Visual-Line-of-Sight,	No restrictions.

19. Security Classification (of this report)	20. Security Classification (of this page)	21. No. of Pages	22. Price
Unclassified	Unclassified	113	N/A

Form DOT F 1700.7 (8-72) Reproduction of completed page authorized

TABLE OF CONTENTS

TABLE OF FIGURES

TABLE OF TABLES

TABLE OF ACRONYMS

A1F	Alert Function
A2F	Avoid Function
ADS-B	Automatic Dependent Surveillance-Broadcast
ARC	Air Risk Class
ASTM	American Society for Testing and Materials
BQD	Bayesian Quickest Detection
BVLOS	Beyond Visual Line of Sight
CNS	Communication, Navigation, and Surveillance
CONOPS	Concept of Operations
CPA	Closest Point of Approach
DAA	Detect And Avoid
DCPA	Distance at Closest Point of Approach
DF	Detection Function
EASA	European Union Aviation Safety Agency
EC	Electronic Conspicuity
ETA	Event Tree Analysis
FAA	Federal Aviation Administration
FANET	Flying Ad Hoc Network
FTA	Fault Tree Analysis
GPS	Global Positioning System
ICAO	International Civil Aviation Organization
IDS	Intrusion Detection System
JARUS	Joint Authorities for Rulemaking on Unmanned Systems
LoWC	Loss of Well Clear
MIT LL	MIT Lincoln Laboratory
NMAC	Near Mid-Air Collision
OSM	OpenStreetMap
PMF	Probability Mass Function
PRA	Probabilistic Risk Assessment
RAP	Risk Assessment Point
RCS	Radar Cross-Section
ROS	Robot Operating System
RTP	Research Task Plan
RUVS	Risk Uncertainty-Validity Spheroid
SLRS	Safety Limit Risk Sphere
SME	Subject Matter Expert
SORA	Specific Operations Risk Assessments
SRM	Safety Risk Management
sUAS	Small Unmanned Aircraft System
SWaP	Size, Weight, and Power
TPC	Transpose time in Potential Conflict
UAS	Unmanned Aircraft System
USS	UAS Service Suppliers
UTM	Unmanned Traffic Management
YOLO	You Only Look Once

EXECUTIVE SUMMARY

This report is in partial satisfaction of the requirements of Task 2 of the ASSURE project "A71: Conduct Safety Risk Management Analysis on Unmanned Aircraft Detect and Avoid Systems." The report is divided into two parts, in alignment with the two subtasks identified in the Research Task Plan (RTP):

- *Task 2-1:* Hazard Identification and Risk Assessment Process for Detect And Avoid (DAA) Systems and Operations (Section 2)
- *Task 2-2:* Sensitivity Report for DAA Systems and Operations (Section 3).

Task 2-1. Task 2-1 identifies two proposed alternative Probabilistic Risk Assessment (PRA) methods suitable for use in the context of DAA systems and operations.

Proposed risk assessment method #1: Exposure-based approach to PRA. The proposed exposure-based approach to PRA expands traditional two-variable models by incorporating *exposure*, the duration an Unmanned Aircraft System (UAS) is subjected to a hazardous condition, as a third critical dimension alongside *potentiality* (the likelihood of a condition occurring at a specific moment) and *severity* (the potential consequences of an event). This approach allows for a more nuanced and dynamic understanding of risk by recognizing that the longer a UAS remains in a risky environment, the greater the overall threat becomes. Exposure is quantified in real time during potential conflict windows, such as proximity to other aircraft, and is considered only when potentiality is greater than zero. By framing risk as a point in three-dimensional space, represented by the Risk Assessment Point (RAP), this model provides a visualization of operational risk, which can be applied at both micro (individual encounters) and macro (fleet or mission-wide) levels. This method supports better-informed decision-making for both automated systems and human operators by capturing the time-dependent nature of real-world UAS risk scenarios.

Proposed risk assessment method #2: DAA timing distribution approach to PRA. The probability that a DAA system does not detect the other aircraft before a Near Mid-Air Collision (NMAC) in a Concept of Operations (CONOPS) is a vitally important but difficult to estimate risk measure. It is vitally important because DAA system performance (*e.g.*, the distribution on detection delay) is difficult to contextualize and interpret outside of specific CONOPS. That is, knowing the median and standard deviation of the detection delay are m and s seconds, respectively, does not by itself convey anything about the risk associated with using that DAA system. Rather, the risk acquires meaning only within the specific CONOPS, which includes *i)* characteristics of the flight of the *ownship* (the vehicle on which the DAA is mounted) and the *intruder* (the vehicle to be detected) such as the separation distance, *ii)* system characteristics (*e.g.*, the camera resolution), and *iii)* operating conditions (*e.g.*, fog and visual clutter). By leveraging probabilistic mathematical modeling, realistic flight trajectories, detailed detection algorithm simulation, machine learning techniques, and efficient Monte Carlo simulation, the proposed approach yields credible estimates of this risk measure.

Task 2-2. Task 2-2 studies the sensitivity of the proposed risk measures. Specifically, the approach described in proposed risk assessment method #2 in Task 2-1 yields a parameterized model for the instantaneous detection probability as a function of the instantaneous separation distance between the two aircraft, where the parameters capture system characteristics (*e.g.*, the camera resolution),

and operating conditions (*e.g.*, fog and visual clutter). This model is obtained by using standard machine learning techniques on datasets that combine realistic flight trajectories with a detailed detection algorithm simulation. Specifically, there is a parameter space for system characteristics and operating conditions sampled to estimate the probability of instantaneous detection under those particular conditions, and the machine learning algorithm yields a model of that detection probability over the entirety of the parameter space. The focus of this component of Task 2-2 is to explore the dependence risk measures of interest (*e.g.*, the instantaneous detection probability, the detection delay distribution, and the probability of detection before NMAC) upon operating conditions (camera resolution, fog, and visual clutter).

Summary of Findings:

- *Task 2-1:* The proposed risk assessment method #1, *i.e.,* the exposure-based approach to PRA, incorporating potentiality and severity, is a novel and promising approach to formally and intuitively integrate important components of a CONOPS into a risk assessment.
- *Task 2-1:* The proposed risk assessment method #2, *i.e.,* the DAA timing distribution approach to PRA, is a promising approach to integrating high-fidelity simulation tools (*e.g.*, Gazebo) with machine learning (*e.g.*, logistic regression) and statistical simulation (*e.g.*, Monte Carlo) methods to produce risk assessment of important risk assessment statistics, such as the probability of a NMAC.
- *Task 2-2:* the sensitivity analysis demonstrates both *i)* the importance of incorporating appropriate system characteristics (*e.g.*, camera resolution) and environmental operating conditions (*e.g.*, fog and visual clutter) for accurate risk assessment, and *ii)* the encouraging viability of the proposed risk assessment method in predicting the impact of those factors.

1 INTRODUCTION AND BACKGROUND

This report is structured as follows:

- Background and context and a summary of Subtasks 2-1 and 2-2 is in Section 1;
- Subtask 2-1 is addressed in Section 2;
- Subtask 2-2 is addressed in Section 3;
- An Appendix, containing technical content that complements the body of the report, follows the references.

1.1 Background and Context

This document is the second report for the ASSURE project entitled "A71: Conduct Safety Risk Management Analysis on Small Unmanned Aircraft Detect and Avoid Systems." It is a sequel to the first report, pursuant to the first task (Task 1). Quoting from the Task 1 report itself [A71 Task 1, 2024], the Task 1 report:

> *"...assessed past government, standards body, and industry work on current methods, protocols, and tools used by the Federal Aviation Administration (FAA) to evaluate the risk associated with DAA-enabled flight operations. This report highlights the benefits of current methods while identifying significant gaps and limitations when current qualitative methods are applied to assess UAS operational risk with DAA systems. This issue paper also underscores the importance of a migration towards quantitative methods for risk assessment. It sets the stage for exploring fault trees, conditional probabilities versus unconditional probabilities, and the stratification of likelihood or probability across specific use cases in later tasks. Last, this research aims to explore risk management documents for gaps, shortcomings, and misalignments and provide policy refinement recommendations."*

This report presents the findings and recommendations of the second task (Task 2) specified in the A71 RTP, entitled "Draft Hazard Identification and Risk Assessment Processes for Detect and Avoid (DAA) Systems and Operations." From the RTP:

> *"Task 2 builds upon Task 1, facilitating the development of hazard identification and risk assessment processes for (1) DAA systems and (2) operations. These templates should consider baseline DAA system functions and address issues identified in Task 1 to the greatest extent possible."*

From the RTP, the task exit criteria are the two subtasks named Subtask 2-1 and Subtask 2-2:

- *Subtask 2-1:* Hazard Identification and Risk Assessment Process for DAA Systems and Operations;
- *Subtask 2-2:* Sensitivity Report for DAA Systems and Operations.

1.2 Summary of Subtask 2-1: Hazard Identification and Risk Assessment Process for DAA Systems and Operations.

Pursuant to this subtask description, this report includes two distinct alternative risk assessment methods for DAA systems and DAA operational risk assessments, which are described in the following sections.

1.2.1 Summary of Proposed Risk Assessment Method #1: Exposure-Based Approach to PRA

This section contains a summary of the first proposed risk assessment method, *i.e.*, an exposure-based approach to PRA. The exposure-based approach to PRA represents a significant evolution in evaluating operational risk for UAS, particularly in DAA contexts. Traditional PRA models typically assess risk using two primary variables: *likelihood* (the probability that a hazardous event will occur) and *severity* (the impact or consequences if the event occurs). While effective in many aviation applications, this binary approach lacks the granularity needed to assess the dynamic nature of UAS operations, particularly in environments with variable and time-sensitive risk conditions. The exposure-based method addresses this limitation by introducing *exposure* as a third key variable, enhancing the fidelity and responsiveness of the risk assessment model.

In this paradigm:

- *Potentiality* replaces the traditional term "likelihood," and is defined as the probability of a hazard being present at a single moment in time.
- *Exposure* measures how long the UAS remains within a hazardous condition, such as a potential collision course with another aircraft, thus incorporating a temporal component into the risk evaluation. This addition allows the model to reflect how risk accumulates with time spent in dangerous conditions.
- *Severity* remains a measure of the possible consequences of a hazardous event.

The integration of these three variables creates a three-dimensional model in which risk is visualized as a single point in space, known as the RAP, defined by its coordinates in terms of potentiality, severity, and exposure.

This multidimensional model enables more accurate and actionable risk assessments. For example, two scenarios with similar likelihood and severity may present vastly different risk profiles if one involves prolonged exposure while the other does not. The system allows both automated algorithms and human operators to visualize risk more effectively and take appropriate mitigation steps. For automation, this enables machine learning models to process large volumes of real-time data and optimize flight paths or behaviors accordingly. For human users, the model can be translated into familiar red-yellow-green visual cues to support intuitive decision-making.

A critical advantage of this approach is its flexibility across both micro and macro scales. At a micro level, it allows for fine-grained risk analysis of specific events such as an NMAC. At the macro level, it facilitates fleet-wide risk profiling across time, geography, and operational contexts. Additionally, by overlaying this risk model with a “Safety Limit Risk Sphere” (SLRS) and a “Risk Uncertainty-Validity Spheroid” (RUVS), decision-makers can also visualize not just the calculated risk, but the confidence and uncertainty associated with that calculation. This is especially valuable when weighing whether a given mission’s benefits justify the associated risk.

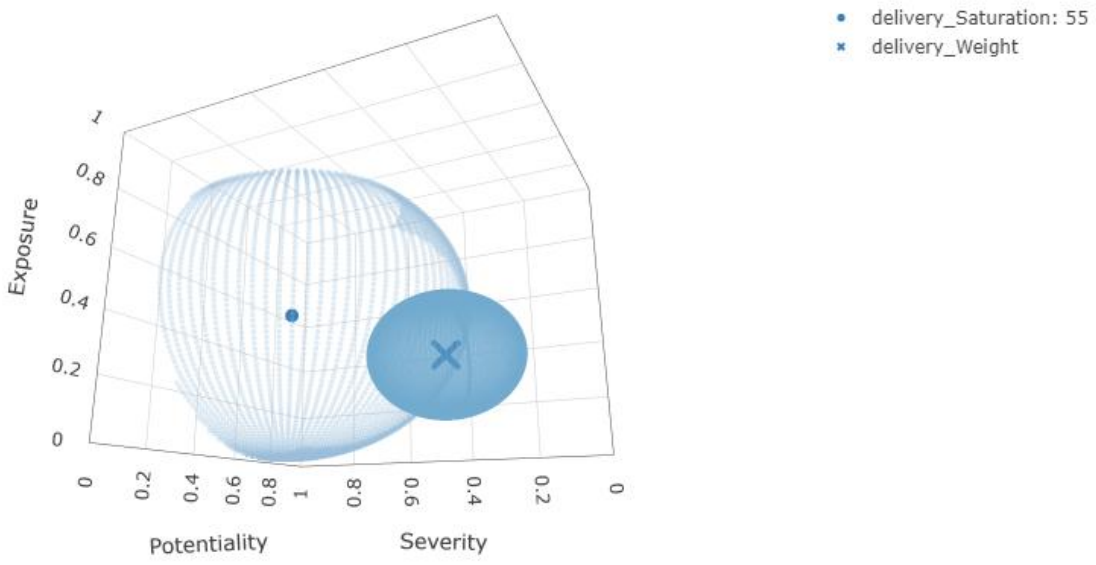

Figure 1. Example delivery mission RAP, RUBS, Weight, with Validity and Certainty spheroids.

Overall, the exposure-based PRA framework presents a forward-looking and comprehensive method for enhancing UAS operational safety. It is particularly well-suited for the increasingly autonomous and complex missions envisioned in the evolving national airspace, providing a foundation for more informed, adaptive, and mission-appropriate risk management. Details on this methodology are provided in Section 2.1.

1.2.2 Summary of Proposed Risk Assessment Method #2: DAA Timing Distribution Approach to PRA

This section contains a summary of the second proposed risk assessment method, *i.e.*, DAA timing distribution approach to PRA. Figure 2 shows a high-level summary of the methodology, including the three sets of inputs, the three tools, and the output.

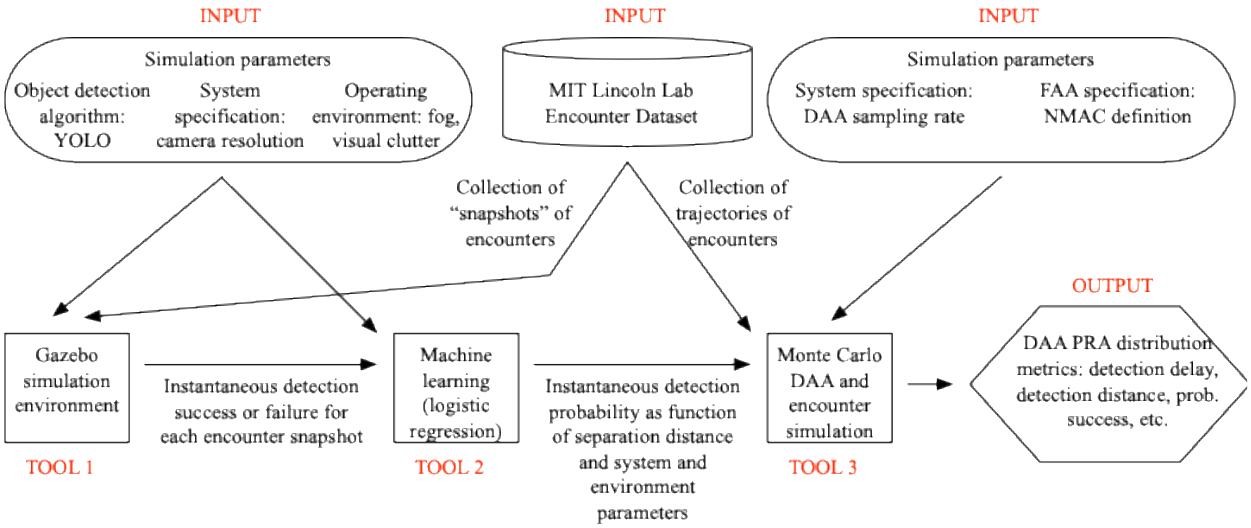

Figure 2. High-level overview of the second proposed risk assessment method.

The main idea of the proposed risk assessment method is to return a probability of successful detection by the DAA system for a specific encounter (*i.e.*, a pair of flight trajectories), for a DAA system with specific properties (*e.g.*, detection algorithm, camera resolution, and sampling rate), and for a specific operating environment (*e.g.*, fog, visual clutter). These terms may be roughly defined as follows:

- *Probability of successful detection:* the probability that the DAA system can detect the other aircraft before a NMAC;
- *Encounter:* a pair of aircraft trajectories that are collocated and concurrent, *i.e.*, the trajectories are such that the DAA system can nominally detect the other aircraft and the trajectories will admit one or more NMACs;
- *System properties:* the DAA system has specific properties that impact the detection probability, *e.g.*, the camera resolution;
- *Operating environment:* the trajectories take place in a specific operating environment, *e.g.*, a certain level of fog and a certain amount of visual clutter.

The methodology relies upon several inputs:

- *DAA and NMAC global parameters*, *e.g.*, the DAA system maximum detection distance, the NMAC distance threshold, and the DAA system sampling delay;
- *An encounter*, *i.e.*, a trajectory pair involving two collocated and concurrent aircraft, one of which is equipped with a DAA system;
- *An instantaneous detection probability model*, *i.e.*, a function that takes several inputs (instantaneous separation distance, DAA system properties, and relevant aspects of the operating environment) and returns a probability that the DAA system will detect the other aircraft under those conditions.

The DAA detection delay model works as follows:

- A random Bernoulli trial (*i.e.*, a success or failure) is conducted for each time instant in which the instantaneous separation distance between the two aircraft is below the DAA system maximum detection distance

- These trials are repeated at time offsets equal to the DAA system sampling delay until such time, if any, at which the random Bernoulli trial is a success, *i.e.*, the DAA system has detected the other aircraft.
- The detection delay is the total time between the earliest possible detection time for the encounter and the actual detection time, which is some nonnegative integer multiple of the DAA system sampling delay.
- The encounter is labeled as a success if the detection time is below the time at which the encounter has its first NMAC, else it is labeled as a failure.
- The above steps are repeated as many times as necessary using a Monte Carlo simulation paradigm to gain a suitably accurate approximation to the probability of a successful detection.

Several components are required for the above model to function correctly:

- *DAA system properties:* The uAvionix Casia X was used for this report;
- *Encounter database:* A database of encounters (trajectory pairs) was obtained from MIT Lincoln Labs;
- *Simulation of the instantaneous detection:* The Gazebo platform was used to simulate a detection algorithm You Only Look Once (YOLO) at randomly selected instants of a given trajectory pair under assumed DAA system parameters (*i.e.*, camera resolution) and under assumed operating conditions (*i.e.*, fog and visual clutter);
- *Simulation of the detection delay:* A simulator was written by the performers to simulate the detection delay using the instantaneous detection probability model.

The proposed methodology has the following advantages:

- *Realistic simulated encounters:* The encounters used to train the model are realistic.
- *Realistic simulated instantaneous detection:* The instantaneous detection probability of the DAA system is captured using a realistic simulated environment with a faithful representation of the detection algorithm.
- *Efficient approach to detection delay:* The detection delay can be efficiently simulated using the above instantaneous detection probability.
- *Parsimonious approach to a complex system in a complex environment:* The approach is computationally feasible but nonetheless is sufficiently flexible to accommodate variations in encounters, DAA system parameters, and operating conditions.

Details on this methodology are provided in Section 2.

1.3 Summary of Subtask 2-2: Sensitivity Report for DAA Systems and Operations.

The second subtask has the following description in the RTP:

> *"The performer will investigate the change in risk measures associated with DAA algorithms as caused by changes in the key model parameters of the DAA algorithm. The task will consist of conducting a sensitivity analysis, which may be performed in three distinct ways – using a mathematical model, simulation, or trial data. The resulting guidance from this task will drive model parameter selection and operating conditions for subsequent tasks/subtasks."*

This section contains summaries of the sensitivity analyses of the two proposed approaches to PRA.

1.3.1 Summary of Sensitivity Analysis for Proposed Risk Assessment Approach #1 (Exposure)

Several relevant components align with the second subtask guidance for investigating changes in risk measures due to variations in DAA algorithm parameters through sensitivity analysis. Specifically:

1.3.1.1 *Three-Dimensional Risk Model with Adjustable Parameters*

This task introduces a probabilistic risk model based on three key variables: *potentiality*, *severity*, and *exposure*, each ranging from 0 to 1 and designed to be dynamically adjustable. This structure inherently supports sensitivity analysis, as changes in any of these variables (representing DAA model parameters or environmental factors) directly influence the computed RAP. This makes the model well-suited for exploring how different DAA algorithm configurations affect overall risk.

1.3.1.2 *Simulation-Based Data and Transposition from Prior Models*

This task demonstrates the utility of simulation-derived data (*e.g.*, from the ASSURE A54 project) to feed their risk assessment framework. Variables such as "Closest Distance" and "Time in Potential Conflict" were transformed into the model's core parameters (potentiality and exposure), showing how simulation outputs can be adapted for sensitivity testing. This aligns with the directive to use simulation as one method for sensitivity analysis.

1.3.1.3 *Use of Modeled Risk Points and Risk Spheroids*

By visualizing risk as a point in three-dimensional space and enveloping it with a RUVS, the framework provides a way to assess not only the raw risk but also the *confidence* in those risk calculations. This offers a robust structure for identifying which model parameters (*e.g.*, exposure time thresholds, detection sensitivity, or algorithmic conflict resolution timing) introduce the most uncertainty—an essential element in sensitivity analysis.

1.3.1.4 *Application of a SLRS*

The SLRS defines a threshold for acceptable risk, enabling comparative analysis of how different parameter settings push the RAP in or out of acceptable bounds. This visual and computational tool is useful for assessing how operating conditions and algorithmic settings influence mission viability, providing a direct method for guiding future model parameter selection.

1.3.1.5 *Human and Automated System Adaptability*

The model accommodates both human-in-the-loop and fully automated DAA systems. This dual applicability means that sensitivity analysis can account for variations in DAA algorithm performance due to operator behavior or system autonomy, supporting a range of trial configurations.

1.3.2 Summary of Sensitivity Analysis for Proposed Risk Assessment Approach #2 (DAA Timing)

The sensitivity analysis for the second proposed risk assessment approach, *i.e.,* the approach focused on the distribution of the detection delay of the DAA system, focuses on the sensitivity of the instantaneous detection probability on the relevant system parameters and environmental operating conditions. The instantaneous detection probability gives the probability that the DAA

system on the ownship will successfully detect the intruder at a specific instant in time as a function of the separation distance, the relevant system parameters, and the relevant environmental operating conditions. This function is obtained by first sweeping these parameters across a set of discrete values in the Gazebo simulation environment and then using machine learning methods to estimate the value of the function for any parameter value(s). This approach is illustrated primarily for the level of fog, and the plots demonstrate both the importance of the fog level on the instantaneous detection probability and the accuracy of the methodology in estimating the impact of fog for other values beyond those tested within Gazebo.

2 SUBTASK 2-1: HAZARD IDENTIFICATION AND RISK ASSESSMENT PROCESSES FOR DAA

The first subtask has the following description in the RTP:

> *"The performer will explore alternative risk assessment methods and templates and propose new risk assessment methods and processes for DAA systems and DAA operational risk assessments. More than one method and process may be suggested to account for the different types of risk and different types of DAA systems (e.g., airborne, ground-based, UTM-supported, large UAS operations, sUAS operations, multi-vehicle operations, etc.).*
>
> *The team will identify potential metrics for evaluating DAA system performance. In doing so, the team will endeavor to answer questions regarding the broad deployment of systems (and associated impacts), although this is not the primary focus. Numerous metrics currently exist, such as risk ratios and conditional probabilities."*

Pursuant to this subtask description, this report includes two distinct alternative risk assessment methods for DAA systems and DAA operational risk assessments, which are described in the following sections.

2.1 Proposed Risk Assessment Method #1: Exposure-Based Approach to PRA

This section outlines the first proposed risk assessment methodology for DAA systems: an exposure-based approach to PRA, developed by the University of North Dakota. This method introduces a three-dimensional risk model—incorporating potentiality, severity, and exposure—to improve the accuracy of risk quantification in Small Unmanned Aircraft System (sUAS) operations. This contrasts with traditional two-variable approaches based only on likelihood and severity.

The following components are central to this method:

- *Potentiality:* the probability that a hazard exists at a given instant;
- *Severity:* the impact of the hazard if it results in a loss of safety;
- *Exposure:* the duration for which the system remains vulnerable to the hazard.

2.1.1 Safety Risk Assessment End Users

When developing a new method for risk assessment for DAA systems in UAS, it is crucial to identify and tailor the approach to the needs of the end users. This method must cater to two

primary users: pilot-operators and automated routines. Each audience has distinct requirements and characteristics that must be considered to ensure the system's effectiveness and usability.

2.1.1.1 *Pilot-Operators*

Pilot-operators are individuals who control and manage UAS operations. Their role is critical in ensuring safe and efficient flight operations, especially in complex and dynamic environments. For pilot-operators, the risk assessment method must be intuitive, easy to understand, and capable of facilitating quick and accurate decision-making. A human factors-friendly system for pilot-operators should incorporate principles of cognitive load management and user-friendly interfaces. One approach is to design a risk assessment method similar to the risk matrix commonly used in aviation today. This matrix uses a color-coded scheme with red, yellow, and green categories to indicate different levels of risk, as illustrated in Figure 3[1]:

- *Red* indicates situations that are too risky and unsafe, thus requiring operations to halt.
- *Yellow* denotes conditions that require mitigation before continuing, and even then, require an organization's higher authorities to accept extra risk with an operation.
- *Green* represents acceptable operating conditions where standard procedures can be followed without significant concern.

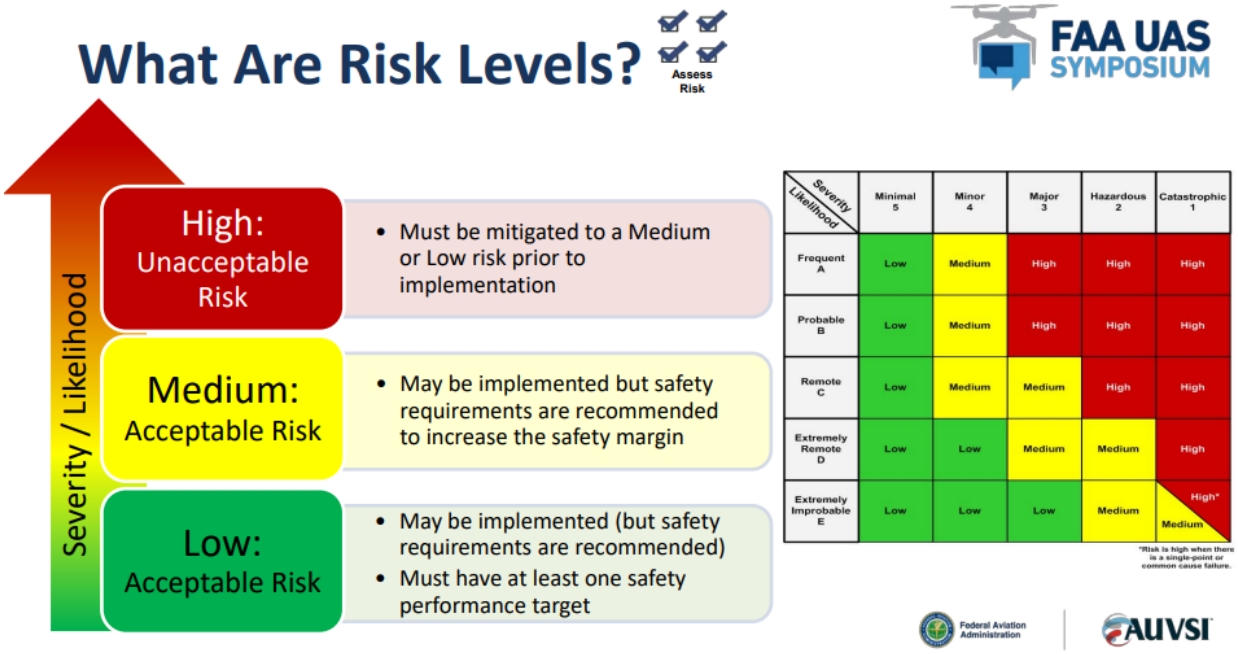

Figure 3. FAA risk level matrix by severity and likelihood.

The system should present information in a clear, concise manner, avoiding clutter and using visual aids like icons, charts, and graphs to help pilot-operators quickly grasp the situation. Interactive elements, such as touch screens or voice commands, can enhance usability and reduce the cognitive burden on the pilot-operator. Providing real-time updates and alerts is essential for maintaining situational awareness. The system should promptly notify pilot operators of any changes in risk

[1] From: https://www.faa.gov/sites/faa.gov/files/uas/resources/events_calendar/archive/Risk-Mitigation-in-UAS-Operations.pdf

status, allowing for timely decision-making. Comprehensive training programs should be developed to ensure that pilot-operators are proficient in using the new risk assessment method. Familiarization with the system through simulations and practical exercises can enhance confidence and competence.

2.1.1.2 *Automated Routines*

Automated routines refer to the algorithms and systems that enable UAS to perform tasks autonomously. These routines must be designed to assess risks accurately and respond to varying conditions without human intervention. For automated systems, the risk assessment method should prioritize efficiency, reliability, and adaptability. The algorithms must be capable of accurately assessing risks based on a wide range of data inputs, including sensor readings, environmental conditions, and flight parameters. Machine learning and artificial intelligence can be leveraged to improve the accuracy and predictive capabilities of these algorithms. Automated routines should include redundancy to ensure continuous operation even in the event of a system failure. Fail-safe mechanisms must be in place to safely land or return the UAS to a designated location if a critical risk is detected. The system should be scalable to accommodate various types and sizes of UAS, from small drones to larger unmanned aircraft, and adaptable to handle different operational environments, whether urban, rural, or remote.

The automated risk assessment system should integrate data from multiple sources, including onboard sensors, external databases, and real-time weather information. Advanced data analysis techniques can help identify patterns and trends, enabling proactive risk management. Continuous monitoring and evaluation of the system's performance are essential for identifying areas for improvement, and incorporating feedback from real-world operations can help refine the algorithms and enhance their effectiveness over time.

One major difference between the two end-users lies in the automated routines' ability to process much more robust and complicated mathematical probability calculations. This could allow for more accuracy, especially compared to the human-friendly and categorical red-yellow-green system, as more variables could be considered across a spectrum rather than trying to encapsulate risk into mere groupings of three (red, yellow, and green).

2.1.2 Traditional Risk Assessment

Traditional risk assessment methods in aviation typically utilize a matrix based on two main variables: likelihood and severity. Likelihood is the probability that a hazardous condition will occur, while severity measures the potential consequences of an accident if it occurs. This approach has been effective in managing risks by allowing operators to categorize and prioritize them based on their potential impact and probability.

However, as UAS DAA systems risk assessment methods are advanced, it is essential to refine this traditional approach to address the unique challenges and complexities in such operations. One significant enhancement to the conventional risk assessment model is the introduction of a third variable: exposure. Exposure is defined as the duration or time spent under a particular condition. In turn, exposure plays a crucial role in evaluating overall risk.

2.1.3 Potentiality

In this new risk assessment system, the traditional term "likelihood" will be replaced by "potentiality." Potentiality is defined as the probability that a condition will occur at a single instant in time. This subtle shift in terminology emphasizes the instantaneous nature of the risk factor, providing a more precise understanding of when a condition is present. This also dovetails with the exposure variable to obtain a more complete picture of risk.

2.1.4 Exposure

First, Exposure risk (and values between 0 and 1) is only applicable when there exists a non-zero Potentiality risk. In other words, if there is zero Potentiality of a risk, Exposure is moot.

The addition of exposure introduces a time-based dimension to risk assessment. Exposure measures how long the UAS is subjected to a particular condition. The longer the time spent in a hazardous condition, the higher the overall risk. For example, a UAS operating in a crowded urban environment for an extended period faces a higher risk compared to one that briefly passes through the same area.

As a more practical example, if a person were to pick up a coffee mug that was very hot but only kept their hand on the cup for a couple seconds (limited exposure), they will likely not experience any long-term negative consequences. However, if that same person were to hold that cup for several minutes, the person could be burned.

This analogy also highlights the difference between planned SRA and real-time SRA, both of which need to occur. In the case of real-time SRA, risk should be reassessed anytime the environment changes demonstrably from the planned conditions. Back to the example, exposure of a burn could be reduced if there was knowledge about the heat of the mug (a forecast). Additionally, the forecast for the mug heat may be dated, and when the person picks up the mug, they find it is surprisingly cool, thereby allowing the person to hold the mug longer without risk of burn; or in SRA parlance, the person could accept longer exposure without increased risk.

In the context of DAA systems, exposure can be quantified by the time a UAS spends within a defined encounter event window, such as the time during which the aircraft is on a trajectory that could potentially lead to a conflict. Standards and guidelines, such as those provided by American Society for Testing and Materials (ASTM), help define these encounter parameters, specifying how and when the exposure clock “starts” and “stops.” This research builds upon those definitions, incorporating them into a model that calculates exposure based on the real-time evolution of a potential conflict scenario. By precisely characterizing exposure time within these defined encounter boundaries, a more accurate representation of risk can be derived, ultimately aiding in safer and more informed operational decision-making.

Beyond the individual encounter scenario, exposure can also be considered at multiple scales. On a micro level, as with the DAA examples guided by ASTM standards, exposure focuses on the specific time interval during which a particular hazard or conflict scenario exists. This granular approach allows for precise calculations and targeted mitigation strategies. At a system-wide macro level, however, exposure can be aggregated across a broader operational landscape,

accounting for cumulative risks over entire fleets, specific missions, operational periods, or geographically expansive airspace systems. In this way, exposure serves not only as a tool for assessing individual conflict events but also as a key factor in understanding and managing cumulative, multi-dimensional risk profiles that evolve over time and space.

2.1.5 Severity

Severity remains a vital component of the risk assessment matrix, representing the probability that if an accident were to occur, it would result in serious consequences. It focuses on the impact or harm that could arise from a hazardous situation, helping to prioritize risks that could have significant negative outcomes. While severity pertains to any hazardous situation, a typical concern is of UAS NMACs. An NMAC is where there is a possibility of collision due to the proximity of less than 500 feet to another aircraft.

2.1.6 Integration of Three Variables

Integrating exposure into the traditional risk assessment model provides a more comprehensive evaluation of risk. The new system considers not just how likely and severe a condition might be, but also how prolonged the exposure is to that condition. This three-dimensional approach allows for a more nuanced and accurate assessment of risk.

To implement this enhanced risk assessment method, the matrix will now consist of three axes: potentiality, severity, and exposure. Each axis will have its own scale, which will follow the standard probability values (0 to 1) found in probability mathematics. The intersection of these variables will determine the overall risk value. For instance, a condition with high potentiality, high severity, and long exposure would be classified as extremely high risk and would necessitate immediate cessation of operations.

Potentiality focuses on identifying and quantifying the probability of encountering a specific hazardous condition at any given moment. It requires a thorough understanding of various operational environments and the factors that lead to potential hazards. Severity, on the other hand, emphasizes the need to analyze the possible outcomes and their impacts, ensuring that high-severity risks are given due consideration. Exposure, as a new variable, requires continuous monitoring and assessment of the UAS's operational environment to determine the duration of time respent in hazardous conditions. All three of these variables combine into a single RAP.

Table 1. Potentiality, severity, and exposure at values 0, 1/2, and 1.

	Values		
Variable	0	.5	1
Potentiality	Will not occur	Just as likely to occur or not occur	Will occur
Severity	No damage or injury	Some damage or injury	Severe damage or injury/death
Exposure	No amount of time	Moderate amount of time	Long or indefinite amount of time

Note: For illustration, these values are examples. Operational values will exist on a continuum ranging from 0 to 1.

By incorporating exposure into the risk assessment matrix and redefining likelihood as potentiality, the new system offers a more dynamic and accurate tool for managing risks in UAS operations. This approach enables operators to make more informed decisions, prioritize risks more effectively, and enhance the overall safety and reliability of UAS missions.

2.1.6.1 *Example 3D Risk Assessment Point*

To illustrate the integration of potentiality, severity, and exposure into a unified risk model, this subsection provides a detailed conceptual explanation and an applied example.

To visualize the risk as a single point in three-dimensional space, consider each axis representing one of the three key variables—Potentiality (P), Severity (S), and Exposure (E)—each ranging from 0 to 1.

- X-Axis: Potentiality (P)
- Y-Axis: Severity (S)
- Z-Axis: Exposure (E)

Choose the following example values for an NMAC:

- Potentiality (P): 0.6 (indicating the condition is more likely than not to occur at any given instant);
- Severity (S): 0.85 (indicating that if an NMAC does occur, the consequences are severe);
- Exposure (E): 0.7 (indicating the UAS remains within congested airspace for a substantial portion of the operational time).

Plotting this point in a 3D coordinate system gives:

Risk Point $R=(P,S,E)=(0.6,0.85,0.7)$

On a three-dimensional graph, the RAP can be depicted as shown in Figure 4.

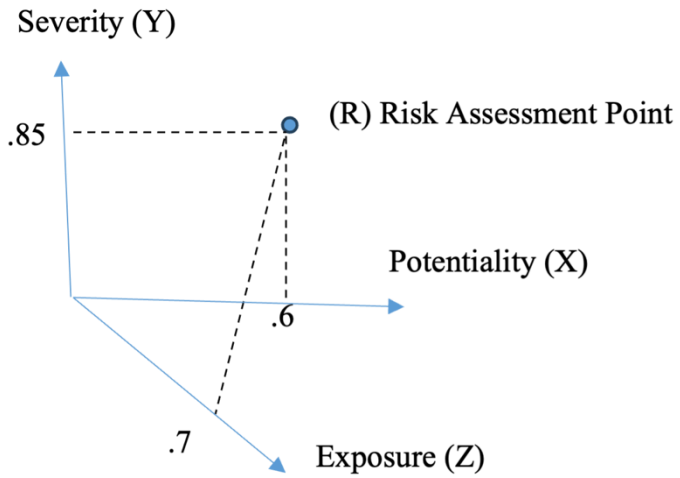

Figure 4. The potentiality, severity, and exposure axes and the RAP.

2.1.7 Deriving Values for the Risk Variables

One important aspect of safety risk assessment pertains to the accuracy of the associated variables: potentiality and severity. There are many methods used to derive these values, some more accurate than others. The chart in Figure 5 encapsulates these methodologies.

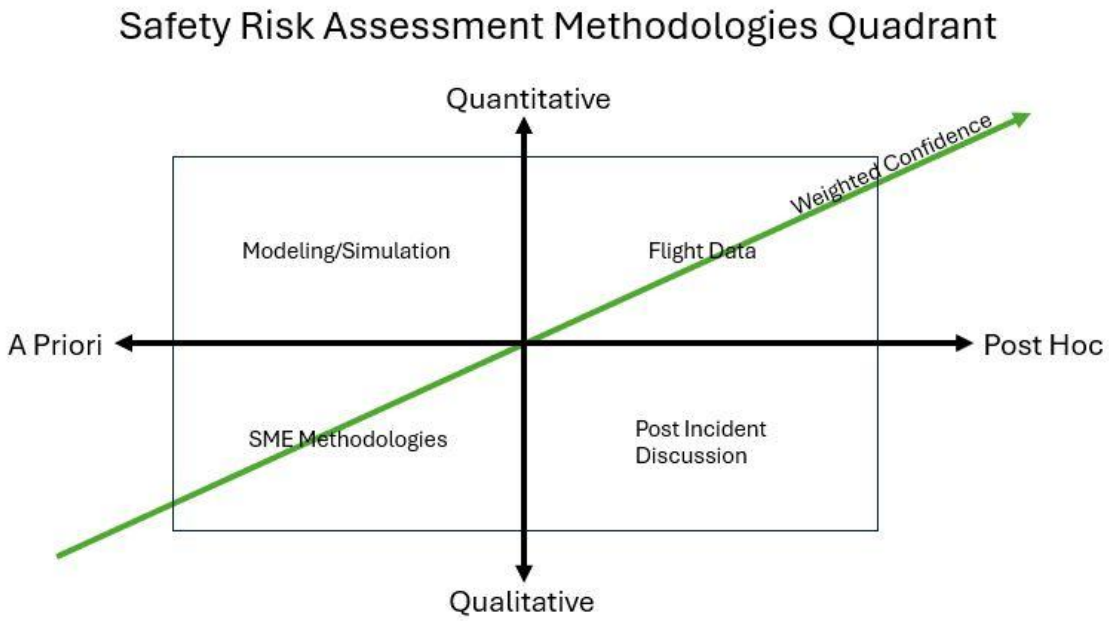

Figure 5. Safety risk assessment methodologies quadrant chart.

The "Safety Risk Assessment Methodologies Quadrant" chart provides a comprehensive overview of various risk assessment approaches based on two primary dimensions: the timing of the assessment (A Priori versus Post Hoc) and the type of data utilized (Qualitative versus Quantitative). Additionally, it introduces the concept of "Weighted Confidence," represented by a

green diagonal arrow, indicating the increasing reliability of risk assessments as one moves across the quadrants.

The horizontal axis distinguishes between A Priori and Post Hoc methodologies. A Priori methods are proactive, applied before an event occurs, aiming to predict and mitigate potential risks using theoretical models, expert opinions, and simulations. In contrast, Post Hoc methods are reactive, applied after an event to analyze past incidents and understand their causes and consequences, thereby preventing future occurrences.

The vertical axis differentiates between Quantitative and Qualitative approaches. Quantitative methods involve numerical data, metrics, and statistical analyses, offering objective and measurable insights into risk. Qualitative methods, however, rely on subjective assessments derived from expert judgment, interviews, and discussions, providing detailed insights that are not easily quantifiable. While qualitative methods do not inherently introduce a degradation in validity of data sources, they are resource-intensive, requiring Subject Matter Expert (SME) input along the way. Further, with every instance requiring SME input, there is an increased chance for errors to enter in the Safety Risk Management (SRM) calculations.

Each quadrant of the chart represents a combination of these dimensions. The top-left quadrant (A Priori and Quantitative) includes methodologies like Modeling/Simulation, which use mathematical models and computer simulations to predict risks before they happen. These models are based on theoretical frameworks, and where possible, will incorporate some historical data (Post Hoc), offering a quantitative basis for risk assessment.

The top-right quadrant (Post Hoc and Quantitative) focuses on methodologies like Flight Data analysis, where actual flight data is used to assess risks after an event. By examining data from past flights, analysts can identify patterns and trends, and thereby provide a robust quantitative understanding of risk, and inform future mitigation strategies.

In the bottom-left quadrant (A Priori and Qualitative), SME methodologies are prevalent. These rely on the expertise of SMEs to anticipate potential risks before they occur. SMEs use their knowledge and experience to provide qualitative assessments, identifying potential hazards and suggesting mitigation strategies based on their professional judgment.

The bottom-right quadrant (Post Hoc and Qualitative) includes Post Incident Discussions, which are qualitative analyses conducted after an incident. This approach involves debriefings, interviews, and discussions with stakeholders to understand the causes and impacts of the incident, providing valuable insights into preventing similar events in the future.

The green diagonal arrow labeled "Weighted Confidence" suggests that both the reliability and confidence in the risk assessment increase as one moves from the bottom-left quadrant (A Priori and Qualitative) to the top-right quadrant (Post Hoc and Quantitative). This implies that methodologies combining quantitative data with post-event analysis are generally viewed as more reliable and accurate in assessing risks.

It should be noted that as part of a robust safety system, the Post Hoc risk assessment data should be utilized a priori in a process of continual improvement from lessons learned. This type of process will help increase the accuracy of all variable calculations.

2.1.8 Validity, Uncertainty, and Weight

In advanced risk assessment methodologies, understanding and quantifying the confidence, weight, and uncertainty associated with each variable is crucial. These factors significantly influence the accuracy and reliability of the risk calculations. To represent this, an error spheroid is used to surround the risk calculation point, indicating the confidence of the data used to calculate each variable.

Validity: Validity refers to the degree of certainty in the data and methods used to assess risk variables. High validity indicates that the data are reliable and the methodology is robust, leading to more accurate risk assessments. Conversely, low validity suggests that there are potential inaccuracies or gaps in the data, increasing the uncertainty in the risk assessment. Validity levels are typically derived from the quality of data sources, the consistency of measurement methods, and the reliability of the analytical processes.

Uncertainty: Uncertainty quantifies the potential variability or error in the risk assessment. It encompasses the range of possible values that a risk variable might take, reflecting the inherent unpredictability of the conditions being assessed. Uncertainty arises from various sources, including measurement errors, data gaps, sensor specs, and the dynamic nature of the operational environment.

Weight: Weight represents the relative importance or influence of each variable in the overall risk calculation. Variables with higher weights have a greater impact on the risk assessment outcome. Weighting is determined based on the relevance and significance of each factor in the context of the specific risk scenario. For example, in a UAS risk assessment, exposure might be given more weight in a densely populated urban environment, whereas potentiality might be weighted higher in complex weather conditions.

To visualize these aspects, an error spheroid is employed, called the **Risk Uncertainty-Validity Spheroid (RUVS (pronounced like *grooves* without the g)).** This spheroid surrounds the risk calculation point on a 3D graph and represents the combined uncertainty in potentiality, severity, and exposure variables. The size and shape of the spheroid are determined by the validity and weight of the data for each variable. A larger spheroid indicates higher uncertainty and lower validity, whereas a smaller spheroid signifies lower uncertainty and higher validity.

For instance, if the potentiality of a risk event is based on comprehensive and accurate flight data, the validity level would be high, resulting in a smaller uncertainty range for this variable. Conversely, if the severity of potential consequences is based on limited historical data, the validity level would be lower, leading to a larger uncertainty range. Exposure might have varying levels of uncertainty depending on the consistency and coverage of operational time data.

The error spheroid not only provides a visual representation of the uncertainty but also helps in better understanding the risk landscape. By analyzing the size and orientation of the spheroid, stakeholders can identify which variables contribute most to the uncertainty and prioritize efforts to improve data quality and confidence in those areas. In turn, stakeholders can mitigate either the RUVS or the Severity, Potentiality, and Exposure variables, all while juxtaposing the operational gain of the flight/mission. Figure 6 depicts a sample RUVS.

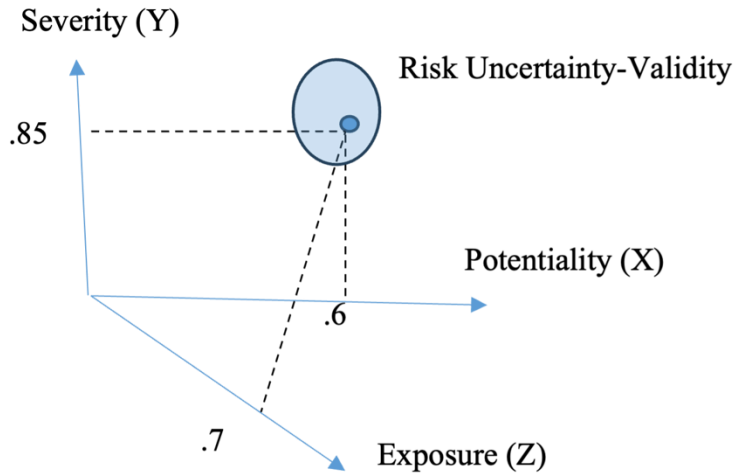

Figure 6. The error spheroid in the potentiality, severity, and exposure 3D space.

2.1.9 Acceptable Risks

The acceptable level of risk for any flight can be visualized through a concept known as the **Safety Limit Reward Sphere (SLRS).** This sphere represents the boundary within which the risk point must remain to be considered acceptable for a given mission. If the risk point, determined by the combined potentiality, severity, and exposure, falls within this sphere, the flight can proceed under normal conditions. **However, if the risk point exceeds this boundary, the flight can only be conducted with appropriate mitigation measures in place to reduce the risk to an acceptable level.**

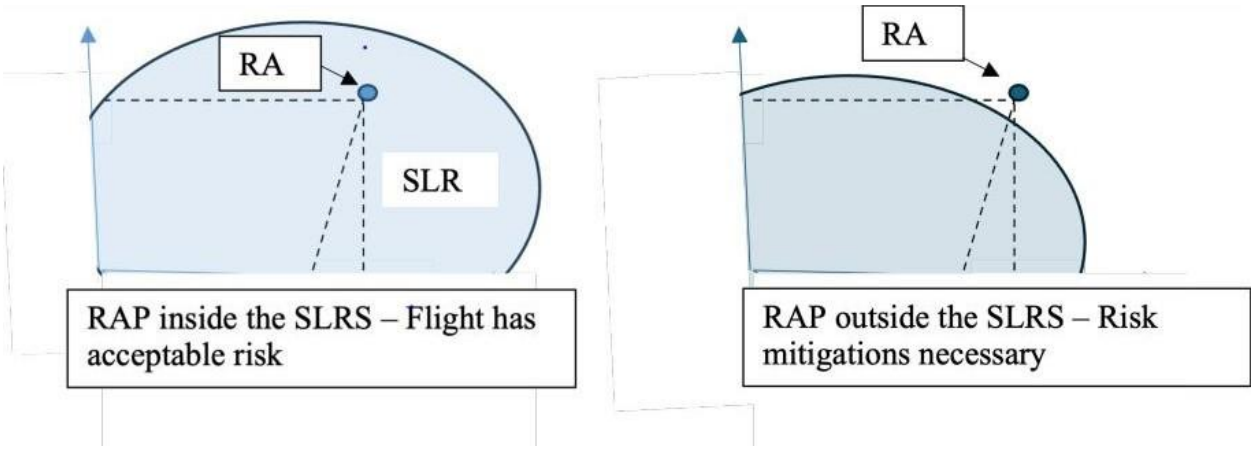

Figure 7. RAP inside (left) and outside (right) the SLRS.

In addition to the SLRS, the confidence spheroid also plays a crucial role in risk assessment. This spheroid surrounds the risk calculation point and reflects the uncertainty in the data used to determine the potentiality, severity, and exposure variables. If the confidence spheroid intersects or penetrates the SLRS, it indicates that there is a significant level of uncertainty in the risk assessment. **In such cases, even if the risk point itself is within acceptable limits, the presence of high uncertainty necessitates considering additional mitigation measures.**

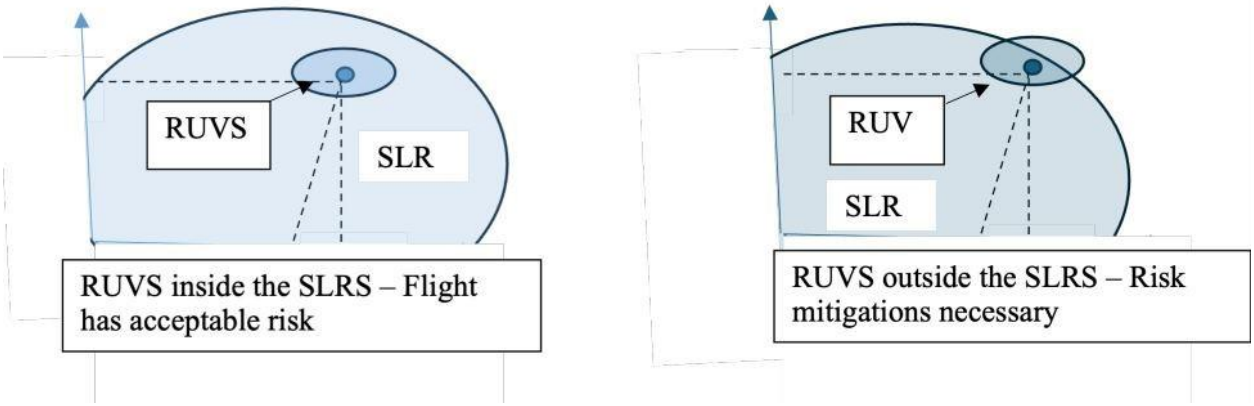

Figure 8. RUVS inside (left) and outside (right) the SLRS.

2.1.10 3-Dimentional Visualization

A repository of 3-dimensional graphs is available at this link: SRM-3D_graphs.zip

After clicking, download to view the .html files in your browser.

2.1.11 Risk Versus Reward

In the context of UAS operations, evaluating the balance between risk and reward is a critical aspect of decision-making. Acceptable risk levels vary with the mission's importance–for instance, a flight delivering critical medical supplies during an emergency may warrant higher risk tolerance

than a routine surveillance mission. The SLRS reflects this variability: it expands for high-stakes missions to allow greater risk tolerance and contracts for lower-stakes missions where safety margins must be tighter. This dynamic framework acknowledges that mission objectives can justify different levels of acceptable risk based on operational context and consequences of failure.

2.1.12 Human-Friendly Translation

Translating actual flight risk to the tradition two-by-two risk matrix, if the RAP and RUVS remain inside the SLRS, then the flight condition would be green. If the RAP is inside the SLRS, but the RUVS extends outside the SLRS, the flight condition would be yellow. If the RAP is outside the SLRS, then the flight risk condition would be red.

Table 2 is a tabular representation of the conditions relative to the SLRS.

Table 2. Conditions relative to the SLRS.

Condition	RAP Position Relative to SLRS	RUVS Position Relative to SLRS	Resulting Flight Condition Color
RAP and RUVS fully inside SLRS	Inside	Inside	Green
RAP inside SLRS but RUVS extends outside SLRS	Inside	Partially Outside	Yellow
RAP outside SLRS	Outside	N/A (RUVS position irrelevant)	Red

2.1.13 Simulated Data for SRM Model Decisions

This subsection presents the simulation data sources and processing methodology used to evaluate the proposed exposure-based PRA framework. To test this proposed model, data was created and graphed. Some data was created unique to this project, while other data leveraged a historic ASSURE project. The rationale to use A-54 data was merely for scientific continuity in research, incrementally advancing ideas in a previous project.

2.1.13.1 *Use of ASSURE A54 Simulated Data*

A previous ASSURE project, A54, simulated UAS traffic and collision potential, resulting in simulated data that was relevant to A71. A54 variables, such as Mission type, Closest Distance, and Time in Potential Conflict, were transposed into data for this project. Specifically, the 0 to 1 Potentiality variable used here in A71, was drawn from A54's Closest Distance variable. A71's Exposure variable was transposed from A-54's Time in Potential Conflict variable.

2.1.13.2 *Potentiality*

In A54, the researchers multiplied the closest distances (in feet) by .1 to normalize for graphing purposes. To start this transposition, these values were multiplied by 10, resulting in a new variable: Closest Point of Approach (CPA).

The next step was to normalize CPA into Potentiality values between 0 and 1. This step incorporated parameters from A54, specifically small UAS interacting with other small UAS, requiring 15 vertical feet and 50 horizontal feet. In A54, small NMAC thresholds were expanded to 25' vertical and 100' horizontal due to Global Positioning System (GPS) inaccuracies, but in A71, GPS accuracy was accounted for in the Certainty variable. Of note, A54 data was simulated at co-altitudes, a two-dimensional plane. As such, vertical separation parameters were moot. For this data transposition, if the CPA value was greater than or equal to 50', the Potentiality value was set to 0 (zero Potentiality risk). For CPA values less than 50, Potentiality was calculated wherein a CPA of 0' (a mid-air collision) resulted in a Potentiality value of 1 (absolute/full risk), and the rest of the CPA values between 0' and 50' were transposed to Potentiality values between 0 and 1.

2.1.13.3 ***Exposure***

The Exposure variable was calculated using the minimum and maximum values of A54's Time in Potential Conflict (seconds) variable as the benchmarks for A71's Exposure values of 0 to 1, respectively. Limitations with this method are captured below. The formula to Transpose time in Potential Conflict (TPC) to Exposure is:

$$min\text{-}TPC - TPC \,/\, (min\text{-}TPC - max\text{-}TPC)$$

2.1.13.4 ***Limitations***

"Well clear" is defined differently based on operating area and if other aircraft are crewed or not. While this research used 50 horizontal feet as a limitation to assist in calculating Potentiality, the horizontal (and vertical, if used) limitations can be adjusted based on context and SME input.

Using min/max TPC values to calculate Exposure is imperfect, but was a best effort given previous ASSURE research simulated data. However, as real data, and more data, are accrued, this model will become more robust and externally valid.

Further, with SME input as to how many seconds of potential conflict is considered "acceptable risk," the specificity of the Exposure variable will become more valid. Any time longer than this tolerable risk threshold, it can be assumed that the density and exposure time is so large that mid-air collisions are bound to occur.

There are limitations with the Severity variable as well. For now, this is merely a SME-determined value. Future work can incorporate the mass of the UAS and what UAS are overflying. Further AI modeling can incorporate accident reports' narratives (*i.e.* ASRS, ASAAP databases) to learn a multitude of severities from historic mishaps.

2.1.14 Advantages and Disadvantages

The advantages of incorporating a three-dimensional risk model with exposure, severity, and potentiality over a traditional two-variable approach are significant. By adding exposure as a third variable, the system not only improves accuracy, providing a clearer picture of risk during prolonged hazardous conditions, but it also resolves the long-standing debate over how to normalize flight segments (the so-called "denominator issue") by directly factoring the duration of risk into the calculation. This enhancement allows for more precise and nuanced assessments that

are ideal for algorithmic processing, enabling automated DAA systems to easily integrate complex environmental and temporal data. At the same time, the sophisticated three-dimensional model can be distilled into a human-friendly interface, such as a stoplight-style warning system, ensuring that pilots and operators can quickly understand, trust, and act upon the risk information provided.

While this enhanced three-dimensional model offers substantial improvements, it also comes with notable drawbacks. The fundamental challenge of accurately determining potentiality and severity remains largely unresolved, as these inputs often hinge on a priori expert judgment and SME methodologies rather than purely objective data. This inherent subjectivity can limit the precision and repeatability of the model. Additionally, despite providing a simpler stoplight-style interface for operators, the underlying complexity of the three-dimensional model may still be more difficult to explain to a user-oriented audience accustomed to more traditional two-variable risk matrices. Modeling exercises and extensive real-world testing are necessary before widespread adoption, ensuring that the theoretical advantages translate into safer, more effective UAS operations in practice.

2.1.15 Conclusion

The risk versus reward assessment in UAS operations is essential for making informed decisions about flight missions. By considering the mission's importance and utilizing the SLRS, operators can determine acceptable risk levels and necessary mitigation measures. The confidence spheroid adds another layer of assessment, highlighting the need to address uncertainty in risk evaluations. This comprehensive approach ensures that UAS missions are conducted safely and effectively, balancing the need to achieve mission objectives with the imperative to manage and mitigate risks.

2.2 Proposed Risk Assessment Method #2: DAA Timing Distribution Approach to PRA

Following the first proposed risk assessment method described in Section 2.1, this section describes the second method in support of Subtask 2-1, namely, a DAA timing distribution approach to PRA.

The subsections that follow primarily describe both the methods the researchers have implemented and tested to date, as well as extensions and enhancements that could be pursued with further resources. Where relevant, there is a distinction between what is part of the current implementation and what is aspirational for a full implementation. These future-facing elements are clearly identified using labels such as “Possible Future Direction,” distinguishing them from the methods already applied.

2.2.1 Overview of Proposed Risk Assessment Method #2

The method is best described through the following *overview*, which is simplified and abstracted to highlight the important components of the concept. The overview is described in terms of the inputs, the three tools, and the outputs (recall Figure 2):

- *Inputs:* Parameters and encounter dataset (Section 2.2.1.1);
- *Tool #1:* Gazebo flight, environment, and detection simulation environment (Section 2.2.1.2);
- *Tool #2:* Machine learning (logistic regression) (Section 2.2.1.3);

- *Tool #3:* Monte Carlo DAA encounter simulation (Section 2.2.1.4);
- *Outputs:* Process outputs from the simulations (Section 2.2.1.5).

The following five subsections describe each of these components, respectively. Figure 9 summarizes the overview.

Pseudocode for Proposed Risk Assessment Method #1: DAA Timing Approach to PRA

INPUTS

Input: Object detection algorithm (e.g., YOLO)

Input: System specification (e.g., camera resolution)

Input: Operating environment (e.g., fog, visual clutter)

Input: Encounter dataset (each encounter is a trajectory pair)

Input: System specification: DAA sampling rate

Input: NMAC definition

TOOL #1: Gazebo flight, environment, and detection simulation environment

Input: Object detection algorithm (e.g., YOLO)

Input: System specification (e.g., camera resolution)

Input: Operating environment (e.g., fog, visual clutter)

Input: Encounter snapshots (each snapshot an instance from a trajectory pair)

For each: encounter snapshot

    Compute: the operating environment at the snapshot instant

    Compute: the instantaneous separation distance

    Compute: the instantaneous detection outcome: either success or failure

Return: labeled (input, output) = (distance, outcome) pairs, one per snapshot

TOOL #2: Machine learning (logistic regression)

Input: Labeled (input, output) = (distance, outcome) pairs, one per snapshot

Compute: parameter estimates via logistic regression on the pairs

Return: instantaneous detection probability as function of separation distance and system and environment parameters

TOOL #3: Monte Carlo DAA Encounter Simulation

Input: Encounter trajectory pairs

Input: System specification: DAA sampling rate

Input: NMAC definition

Input: instantaneous detection probability as function of separation distance and system and environment parameters

For each: encounter trajectory pair

    Initialize: the encounter trajectory and the detection timer

    While: the encounter is not complete and there is not yet a detection:

        Compute: the separation distance at the current time instant

        Compute: the instantaneous detection probability using the separation distance

        Generate: a single random Bernoulli trial (success or failure) for the instantaneous detection

        Update: the detection timer by the detection delay

        If Bernoulli trial is a success **Then:**

            Stop: the detection timer and **Return:** the detection delay

    If: encounter is relevant and of type NMAC, **Then:**

        If: the detection delay is below the NMAC delay **Then: Return:** Encounter is a Success

        Else: Return: Encounter is a Failure

OUTPUTS

Return: relevant DAA risk assessment quantities, e.g., detection delay distribution, detection separation distance, probability of encounter success / failure

Figure 9. Pseudocode for PRA of DAA timing performance.

2.2.1.1 *Inputs: Parameters and Encounter Dataset*

This section briefly describes the inputs, including the encounter dataset.

- *Input: Object detection algorithm (YOLO):* this is the You Only Look Once algorithm used to process the camera sensor and determine whether or not the image contains an object of interest, *i.e.*, the intruder.
- *Input: System specification (camera resolution):* this is the dimensions (in pixels) of the camera image.
- *Input: Operating environment (fog, visual clutter):* this is the aspects of the simulated environment that will impact the operation of the object detection algorithm. In this report the two principal aspects of the simulated operating environment are fog and visual clutter.
- *Input: Encounter dataset (from MIT Lincoln Labs):* each encounter in the database is a trajectory pair. Each trajectory pair will have both an associated detection time/delay and NMAC time/delay corresponding to the encounter. Consider two aircraft (each one either crewed or uncrewed) operating in the same airspace at the same time, and suppose each aircraft has a trajectory in that space (*i.e.*, there is a pair of trajectories, or a trajectory pair). Several comments are pertinent:
  - *DAA system availability:* for the purpose of this discussion, assume exactly one of the two aircraft is equipped with a DAA system. The aircraft with the DAA system is termed the *ownship,* and the aircraft without the DAA system is termed the *intruder*.
  - *Minimum separation distance:* any encounter has an associated minimum separation distance, defined as the minimum of the instantaneous separation distance over all time instants of the encounter.
  - *Relevant encounters:* the relevant encounters are those where the associated minimum separation distance is smaller than the maximum detection distance. It is henceforth assumed that all encounters under discussion satisfy this property. Encounters that don't satisfy this property are, by definition, outside of the detection range of the DAA system, and as such any risk measure based upon DAA systems or operation is not relevant to them. See Figure 10.
  - Earliest detection time, actual detection time, and detection delay: there are three distinct aspects to detection time and delay:
    - *Earliest detection time:* the earliest detection time is the earliest time at which the separation distance of the encounter equals the minimum separation distance. This time is finite for all relevant encounters, by definition.
    - *Actual detection time:* the earliest time (if any) at which the DAA system detects the other aircraft. This is infinite if the DAA system does not detect the other aircraft.
    - *Detection delay:* the duration between the actual detection time (when finite) and the earliest detection time. This is infinite if the DAA system does not detect the other aircraft.
  - *Classification of relevant trajectories:* logically, there are two types of relevant encounters: non-NMAC and NMAC (see Figure 10):
    - *Non-NMAC type:* a relevant encounter is of type non-NMAC if the associated minimum separation distance is larger than the NMAC distance, *i.e.*, the encounter will not produce an NMAC.

        - *NMAC type:* a relevant encounter is of type NMAC if the associated minimum separation distance is smaller than the NMAC distance, *i.e.*, the encounter will produce one or more NMACs.
    - *Earliest NMAC time and NMAC delay:* there are two distinct aspects to NMAC time and delay, each one only defined for an encounter of NMAC type:
        - *Earliest NMAC time:* the first time that the separation distance of the encounter equals the NMAC distance.
        - *NMAC delay:* the duration between the earliest detection time (defined above) and the earliest NMAC time.
- *Input: System specification (DAA sampling rate):* the inverse of the minimum time between subsequent samples of the DAA system. It is assumed that the DAA system takes instantaneous samples and then processes them to detect if the sample indicates the presence of another aircraft. It is further assumed that the DAA system must complete this detection processing before the system can take a subsequent sample.
- *Input: NMAC distance:* the FAA's defined maximum distance such that any two aircraft, either crewed or uncrewed, separated by this distance (or less), are considered by the FAA to be at elevated risk of mid-air collision. It is henceforth assumed that the maximum detection distance exceeds the NMAC distance; if not, it would mean that the DAA system is underpowered relative to its requirement.

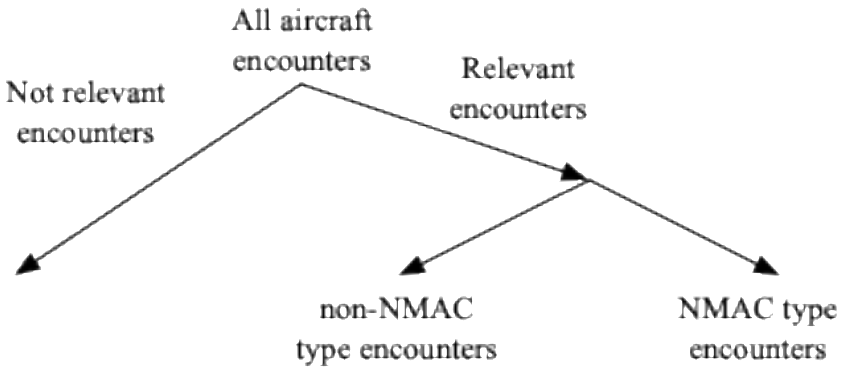

Figure 10. Encounter taxonomy: relevant and NMAC types.

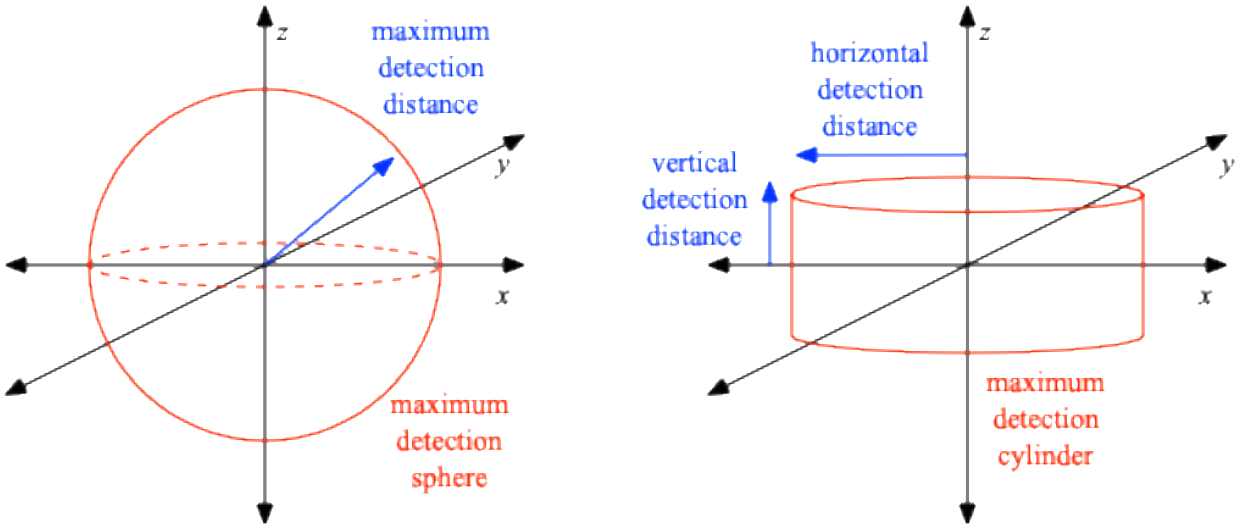

Figure 11. Maximum detection sphere (left) and cylinder (right).

Besides the above six inputs, it is also necessary to specify the following:

- *Maximum detection distance:* the detection possibility sphere is the three-dimensional sphere defined by its radius, termed the maximum detection distance (see left side of Figure 11). The maximum detection distance at which it is possible for the DAA system to detect an aircraft under ideal conditions. The governing assumption is that this distance constitutes a simple sufficient statistic for the positions of the two aircraft relative to the detection capability of the DAA sensor.
    - *Maximum detection cylinder:* While the Euclidean distance is considered here, it is recognized that a more accurate model might describe a maximum detection cylinder. This cylinder, centered at the aircraft with the DAA system, where the cylinder radius is the maximum horizontal separation distance, and the cylinder height is half the maximum vertical separation distance (see right side of Figure 11). The model must include these two component separation distances instead of the single Euclidean separation distance in cases where the DAA system's detection capability depends upon the component distances rather than the single distance.

2.2.1.2 *Tool #1: Gazebo Flight, Environment, and Detection Simulation Environment*

The first tool is the Gazebo software package, which is used to simulate flight, the environment, and the detection algorithm. The primary use of the software in this case is restricted to determining whether the detection algorithm succeeds or fails at a specific instance of a specific trajectory under specific operating conditions using specific DAA equipment.

The purpose of this use of the tool is to produce labeled (input, output) pairs where the key component of the input is the distance separating the two aircraft at the specified instance in the trajectory, and the output is either a Success or Failure, depending upon whether or not the detection algorithm does or does not detect the intruder. These (input, output) pairs, one for each of the specified encounter instants, is fed into Tool #2 to develop a model of the instantaneous detection probability that properly accounts for the separation distance, the operating environment, and the DAA equipment.

2.2.1.3 *Tool #2: Machine Learning (Logistic Regression)*

The second tool is machine learning, specifically logistic regression. The input of this tool is the (input, output) pairs for each of the encounter instants produced by Tool #1. These pairs are used to compute a parameterized model of the instantaneous detection probability, where the parameters include the separation distance, relevant system parameters, and relevant aspects of the operating environment. This instantaneous detection probability is used as an input in Tool #3. It is the probability that the DAA system will detect the other aircraft at a snapshot instance characterized by the separation distance between the two aircraft. This approach identifies the instantaneous detection event of a DAA system as a random variable drawn from a parameterized Bernoulli distribution, where the parameters are the separation distance, the relevant systems properties, and the relevant aspects of the operating environment. There are several components to this model:

- *Separation distance:* This is the Euclidean distance separating the aircraft in the encounter at the time instant at which the DAA sensor takes a reading. The governing assumption is that this distance constitutes a simple sufficient statistic for the positions of the two aircraft relative to the instantaneous detection success probability of the DAA sensor. While the Euclidean distance is considered here, it is recognized that a more accurate model will include either *i)* horizontal and vertical separation distances and/or *ii)* orientation and camera angles:
    - *Horizontal and vertical separation distances:* These are used to define a cylinder centered at the aircraft with the DAA system, where the cylinder radius is the horizontal separation distance and the cylinder height is twice the vertical separation distance. The model must include these two component separation distances instead of the single Euclidean separation distance in cases where the DAA system's instantaneous detection performance depends upon the component distances rather than the single distance. This consideration aligns with the related consideration of the maximum separation distance.
    - *Orientation and camera angles:* The orientation refers to the angle between the focal line of the camera and the line connecting the two aircraft. The focal line of the camera is defined for cases where the DAA sensor does not have a 360-degree lens (or an effective 360-degree lens through the combination of multiple cameras).
- *Relevant system properties:* the model should specify which properties of the DAA system will impact the detection probability and the detection delay, and an instance of the model should specify the values of those properties. Camera resolution is an example of a relevant system property used in this report.
- *Relevant aspects of the operating environment:* the model should specify which aspects of the operating environment will impact the detection probability and the detection delay, and an instance of the model should specify the values of those conditions. Fog and visual clutter are two examples of relevant aspects of the operating environment used in this report.

2.2.1.4 *Tool #3: Monte Carlo DAA Encounter Simulation*

The third tool is a Monte Carlo simulation of the operation of the DAA equipment for each encounter in the encounter database. The inputs to this tool are the encounter trajectory pairs, the specified DAA sampling rate, and the definition of an NMAC.

The tool works as follows for each encounter trajectory pair

- *Independent Bernoulli trials for detection delay:* an important component of the model specified above is the detection delay, which works as follows.
    - *Bernoulli trial for a sensor reading:* starting from the time the separation distance is below the maximum detection distance, and, continuing at any time for which this is the case, the (camera) sensor obtains a reading and this reading is processed by the object recognition algorithm of the DAA, which either detects or does not detect the other aircraft.
    - *Probability of success in the Bernoulli trial:* the probability of this detection depends upon the separation distance, as well as both the relevant system properties and the relevant aspects of the operating environment. As the outcome is either success (detection) or failure (no detection), this random experiment is a Bernoulli trial.
    - *Repeated independent trials as needed:* If the detection fails then there is another independent Bernoulli trial after the sensing delay has elapsed. At this point the probability of detection has changed due to the change in the separation distance. A new outcome is obtained, again either success or failure. This process repeats.
- *Stopping criteria for the Bernoulli trials:* there are three possible stopping criteria for this random process:
    - *Detection success:* the DAA system detects the other aircraft. In this case, the detection delay is the time elapsed since the earliest detection time until the time instant of the successful detection. Note, the detection delay is a function of random Bernoulli trials and is therefore a random variable. It is evident that the detection delay is a positive integer multiple of the sensing delay.
    - *Detection failure:* either *i)* the separation distance exceeds the maximum detection distance and never returns below it, or *ii)* the end of the trajectory sample is reached.
- *Connection with the geometric distribution:* the detection delay distribution is related to, but distinct from, a geometric distribution. The geometric distribution captures the total number of Bernoulli trials until the first success when the trials are independent and identically distributed. The first difference is that the detection delay is not the number of trials but rather the elapsed time between the first trial and the last trial, when that last trial is a success. The second difference is that the geometric distribution assumes the independent Bernoulli trials are identically distributed, whereas the probability of success of each trial in this setting will vary from instant to instant due to the different separation distances.

If the encounter is of NMAC type, then the encounter itself can be labeled as either a success or a failure:

- *Success:* The encounter is labeled as a success if the DAA system successfully detected the other vehicle before the NMAC; specifically, if the detection delay is less than the NMAC delay.
- *Failure:* The encounter is labeled as a failure if the DAA system failed to detect the other vehicle before the NMAC; specifically, if the detection delay exceeds the NMAC delay.

2.2.1.5 ***Outputs: Process Outputs from the Simulations***

Finally, the raw outputs from Tool #3 are processed to yield useful risk measures. The raw outputs are, for each encounter:

- The encounter statistics (*e.g.*, the first time the separation distance is below the maximum detection distance, the first time the separation constitutes an NMAC);
- The detection time and delay, and the separation distance at that time;
- Whether or not the encounter is a success or failure, as defined above.

These raw outputs may be processed to produce the following useful risk assessment measures:

- The distribution of the detection delay;
- The distribution of the distance at the detection instant;
- The probability of the encounter being a success or failure.

2.2.2 Review of the ASTM DAA Timing Standard

This subsection provides a structured review of the ASTM DAA Timing Standard and outlines the key timing components that govern detection, alert, and avoidance processes.

The ASTM DAA Timing Standard is a critical component of Beyond Visual Line of Sight (BVLOS) operations, ensuring safe and efficient airspace integration for UAS [ASTM, 2023]. The DAA system consists of multiple timing functions that govern the detection, classification, alerting, and avoidance of potential conflicts. These functions define the timing constraints under which a UAS must operate to avoid mid-air collisions effectively. Figure 12 is a visual summary of the standard from [ASTM, 2023].

The ASTM timing standard outlines how each function within the DAA system must work cohesively to minimize response delays while maintaining high detection accuracy. Factors such as sensor latency, processing speed, and communication delays all contribute to the overall system efficiency. The DAA timing framework ensures that all these elements align to provide rapid and reliable DAA capabilities, even in dynamic and high-traffic environments.

While the ASTM DAA Timing Standard presents a complete set of timing functions for detect-and-avoid operations, our current implementation focuses specifically on the detection function and its timing characteristics. Other timing functions – including those related to alerting and avoidance – are reviewed here to provide a comprehensive understanding of the standard, but are not yet part of this working model. These components represent potential future enhancements to the timing model framework.

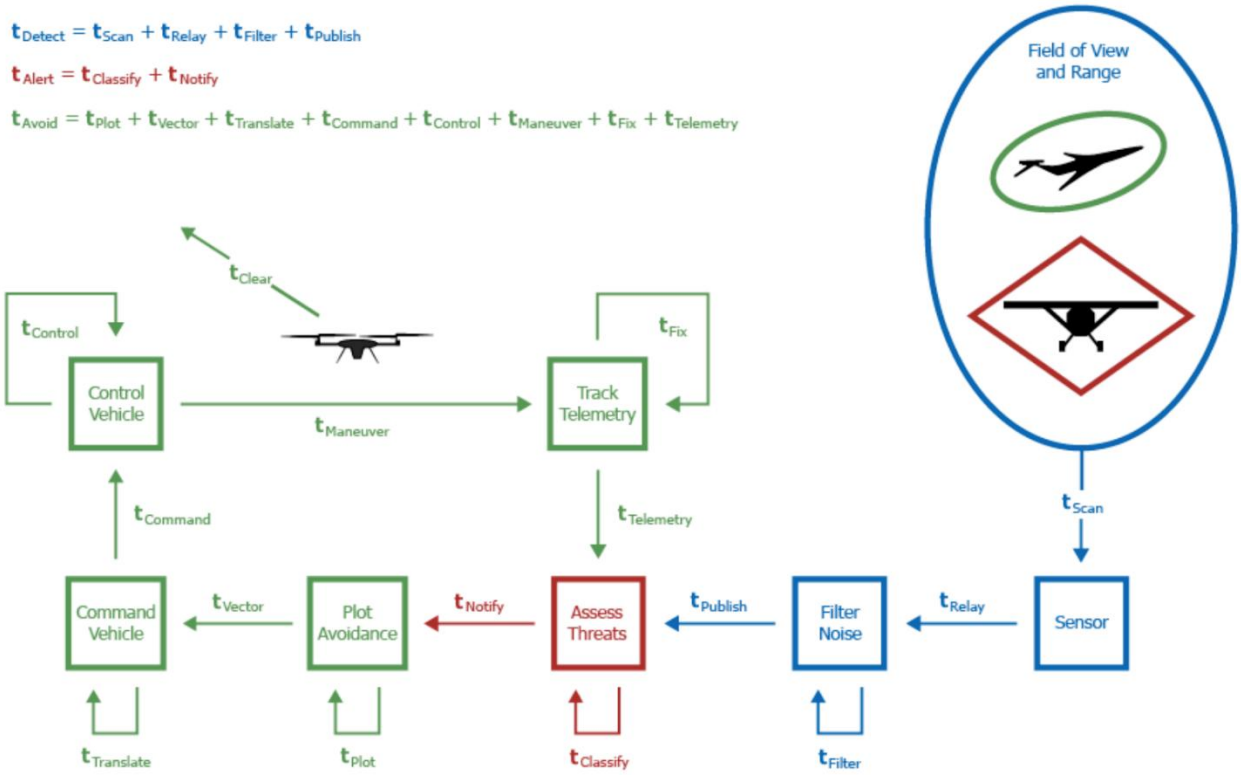

Figure 12. System Timing Model [ASTM, 2023].

This section provides an in-depth examination of the 14 timing functions within the ASTM DAA standard, focusing on detection, alert, and avoidance functions. Each function is defined by specific parameters and equations that contribute to the overall response time of the system. The standard outlines key performance criteria for detecting cooperative and non-cooperative intruders, issuing timely alerts, and ensuring that avoidance maneuvers are executed within required timeframes. Additionally, external factors such as environmental conditions, aircraft dynamics, and the complexity of encounter scenarios can impact timing performance. Ensuring precise synchronization across all functions is essential for maintaining operational integrity and compliance with safety standards.

Understanding these timing aspects is crucial for meeting safety and operational performance requirements in the national airspace. As UAS operations continue to expand, refining these timing constraints will play an essential role in ensuring reliable autonomous and remotely piloted flight operations. The integration of advanced technologies, such as machine learning-based predictive analysis and sensor fusion techniques, may further enhance the responsiveness and effectiveness of DAA systems in the future.

2.2.2.1 *Detection Function (DF) Timing*

The Detection Function (DF) is responsible for detecting intruders and providing necessary data to the alert function. The timing constraints associated with this function include:

- t_{scan}: Maximum time between sensor updates, determining the minimum detection precision.

- t_{Relay}: Maximum latency from the sensor to processing/fusion, which includes transmission and reception time.
- t_{Filter}: Time required for pre-processing sensor data, such as filtering, fusion, and tracking, before passing it to the alert function.
- $t_{Publish}$: Latency from filter processing to alert function presentation.

Then $t_{DF} = t_{Scan} + t_{Relay} + t_{Filter} + t_{Publish}$.

DF timing plays a crucial role in ensuring that the intruder aircraft's position and trajectory are accurately identified within the allocated time budget. The effectiveness of DF timing depends on the update rate of sensors, the computational efficiency of tracking algorithms, and environmental conditions affecting sensor performance. For example, sensor performance may be influenced by ambient noise and clutter, such as echoes from radar, bright sunlight affecting optical sensors, or platform vibrations interfering with acoustic sensors.

2.2.2.2 *Alert Function (A1F) Timing*

The Alert Function (A1F) processes detection data and determines when to issue alerts to the avoidance system. Timing components include:

- $t_{Classify}$: Maximum time required to assess and classify a potential threat.
- t_{notify}: Maximum time to present hazard information to the avoidance function.

Then $t_{Alert} = t_{Classify} + t_{notify}$.

This function ensures that the alert reaches the pilot or automation system within a safe response window. If alerts are delayed, the avoidance function may not have enough time to react appropriately, leading to increased risk. The prioritization and classification of hazards are crucial in maintaining effective separation standards. For instance, alert displays may use color coding and aural indications to differentiate between high-priority threats and minor intrusions.

2.2.2.3 *Avoid Function (A2F) Timing*

The Avoid Function (A2F) calculates and executes necessary maneuvers to maintain safe separation. The timing parameters include:

- t_{Plot}: Time required to compute an avoidance trajectory.
- t_{Vector}: Latency in transferring the computed trajectory to vehicle control.
- $t_{Translate}$: Time required to convert the trajectory into actionable vehicle commands.
- $t_{Command}$: Latency in transmitting vehicle commands to the flight controller.
- $t_{Control}$: Time taken for the flight control system to interpret and initiate the command.
- $t_{Maneuver}$: Duration of the avoidance maneuver from initiation to completion.
- t_{Fix}: Time required to update ownship state and confirm maneuver effectiveness.
- $t_{Telemetry}$: Latency in transmitting updated position and orientation data to the A1F.

Then $t_{Avoid} = t_{Plot} + t_{Vector} + t_{Translate} + t_{Command} + t_{Control} + t_{Maneuver} + t_{Fix} + t_{Telemetry}$.

The effectiveness of the A2F depends on real-time computational efficiency, vehicle response dynamics, and environmental factors such as wind conditions. Minimizing latency in A2F timing enhances the probability of a successful avoidance maneuver. For example, small UAS operating at low altitudes may execute avoidance maneuvers by rapidly descending to avoid an overhead aircraft, while larger UAS may require more complex trajectory planning.

In summary, the ASTM DAA Timing Standard provides a structured framework for ensuring a timely and effective response in BVLOS operations. Each function plays a vital role in enabling UAS to detect, classify, alert, and avoid conflicts efficiently. The DF ensures that intruders are identified within an appropriate time frame, while the A1F processes and prioritizes potential threats. The A2F then executes necessary maneuvers to prevent conflicts, adhering to strict timing constraints.

By adhering to these timing constraints, operators can achieve high safety and compliance levels within regulated airspace. Additionally, the integration of advanced sensor fusion, optimized computational processing, and low-latency communication channels further enhances the system's capability to meet operational safety requirements. Ensuring a seamless and synchronized timing workflow across all functions is essential for mitigating risks and maintaining well-clear distances.

Possible future direction: Integration of Full Timing Chain
While the current study concentrates on the detection timing component of the ASTM DAA framework, with more time, future efforts may extend the Monte Carlo simulation environment to include additional timing functions, such as alert generation and avoidance maneuver execution.

Integrating the full ASTM timing architecture would enable a more detailed assessment of DAA system responsiveness, allowing for a complete end-to-end timing analysis under varied environmental and operational conditions.

2.2.3 Review of Risk Assessment Frameworks

Traditional and alternative risk assessment approaches will be reviewed to determine their applicability to DAA systems in the following sections.

2.2.3.1 *Traditional Risk Assessment Approaches*

This section reviews traditional risk assessment approaches.

2.2.3.1.1 Qualitative Risk Matrices

Qualitative risk matrices have long served as a foundational tool in aviation SRM. In the case of UAS, risk assessment involves using descriptive or categorical assessments instead of numerical values to evaluate risks. It focuses on likelihood, impact, and potential consequences. These matrices help to prioritize risks for mitigation efforts.

In traditional aviation safety frameworks, such as those outlined in FAA Order 8040.4C and 8040.6A, qualitative matrices guide hazard assessments and inform decisions on mitigation strategies [FAA 8040.4C, 2023], [FAA 8040.6A, 2023]. However, their use in UAS - especially those incorporating DAA systems – introduces notable limitations that compromise both

repeatability and relevance. For example, the likelihood of a mid-air collision or Loss of Well Clear (LoWC) is inherently probabilistic and often poorly captured by fixed, ordinal categories.

One prominent and widely adopted example of a qualitative framework is the Specific Operations Risk Assessments (SORA), issued by the Joint Authorities for Rulemaking on Unmanned Systems (JARUS) [JARUS, 2019]. SORA employs structured decision-making matrices to assign operational risk levels based on Ground Risk Class and Air Risk Class (ARC). These classifications feed into a mitigation hierarchy to determine the Specific Assurance and Integrity Levels required for a given operation. While SORA has become a cornerstone of risk assessments in European UAS regulation and provides standardized workflows, it retains many limitations typical of matrix-based approaches.

For instance, in SORA, ARC classifications are based on qualitative judgements about airspace complexity and the likelihood of encountering manned aircraft, rather than empirical encounter rate models. These classifications are primarily designed for operations in international contexts and may not translate well to U.S. airspace, which includes vast regions where non-cooperative aircraft frequently operate. One limitation is that ARCs do not adequately distinguish between cooperative and non-cooperative intruders, which can lead to counterintuitive outcomes – for example, low-risk airspace as defined by ARC may, in reality, present greater collision risk than medium- or high-risk airspace due to the presence of non-cooperative traffic. Moreover, the naming conventions used (e.g. "low risk") may suggest a level of potentially misleading assumptions.

Depending on the specific airspace controls – such as mandatory equipage or surveillance infrastructure – the technical challenge of developing an effective DAA system may be greater in ARC-designated low-risk areas than in others. The mitigation effectiveness levels, while defined procedurally, still rely heavily on expert opinion and categorical ratings (*e.g.,* low/medium/high effectiveness). As pointed out by [Du, 2024], SORA's qualitative structure makes it difficult to model operational uncertainties and failure propagation chains and lacks the granularity needed for data-driven validation of UAS safety performance.

These limitations are particularly critical in the context of DAA-enabled operations, where performance is defined by a series of time-dependent processes such as *T_scan*, *T_filter*, and *T_publish*. A static matrix may not accurately reflect the impact of detection delays, sensor performance variability, or environmental influences on collision risk.

In the context of this project's focus on quantitative timing standards (*e.g.*, ASTM F3442/F3442M) and detection delay modeling, the limitations of qualitative metrics are particularly constraining [ASTM, 2023]. For example, a DAA system with a 2-second median detection delay may be significantly safer than one with a 5-second delay, yet both could fall under the same "likely-severe' category in a traditional qualitative matrix. On the other hand, a quantitative delay-distribution-based risk assessment model provides more precise insights into collision risk under various system architectures and environmental conditions.

However, it is also important to note that earlier detection is not universally better. A shorter detection delay may result in the system passing more unfiltered or uncertain data to the avoidance

logic and pilot interface, potentially increasing cognitive load or leading to false maneuvers. Some of this signal refinement occurs during the track initiation phase, before more advanced classification or filtering algorithms are applied. Thus, quantitative timing models should ideally be integrated with system-level considerations such as filtering latency, tracking quality, and display logic to fully assess risk.

2.2.3.1.2 Bowtie Analysis

Bowtie analysis is a visual risk assessment method used to depict how safety events may unfold by mapping causes on one side and consequences on the other, centered around a single critical event. It offers a holistic view of risk scenarios by identifying threats that could trigger a hazard and the potential outcomes if those threats are not managed. Between these, the model places barriers – preventive barriers to avoid the event and mitigation barriers to reduce its impact – thereby clarifying where safety controls are or should be placed within a system [Aust, 2020]. Technically, bowtie models define several key components:

- *Threats:* Initiating events or conditions that could lead to the top event.
- *Preventive Barriers:* Controls designed to prevent the top event from occurring.
- *Top event:* The moment when control over a hazard is lost.
- *Consequences:* Potential outcomes following the top event.
- *Mitigative barriers:* Controls intended to reduce the severity or likelihood of those consequences.
- *Escalation factors:* Conditions that could reduce the effectiveness of barriers.
- *Degradation controls:* Safeguards that protect the barriers themselves.

This barrier-based framework allows safety professionals to systematically trace where controls exist, where they may fail, and who is responsible for each layer of defense. However, bowtie models typically treat barriers as binary (effective or failed), which limits their ability to account for partial effectiveness, interdependencies, or probabilistic behavior.

A recent and sophisticated application of bowtie analysis is found in the FAA-sponsored MITRE study on pilot mental health risk [Campion, 2024]. It used a bowtie framework that explicitly categorized barriers by effectiveness, which are “very effective,” “somewhat effective,” “less effective,” and discussed their evidence base and vulnerability to escalation factors [Campion, 2024]. For instance, neurocognitive testing was rated as highly effective in managing executive dysfunction, but only if implemented early in the pilot certification process. [Faturachman, 2023], in their bowtie model for sUAS operations, followed a similar logic by integrating a qualitative risk matrix to evaluate combinations of severity and likelihood across threat-consequence pathways. Their model, however, lacked dynamic control evaluation or feedback loops, illustrating a common limitation of traditional bowtie applications.

To improve consistency in bowtie development, [Aust, 2020] proposed incorporating the Ishikawa 6M framework –Man, Machine, Method, Material, Milieu, and Management – as a systematic way to identify threats, barriers, and escalation factors. Their work focused on aviation maintenance risk, where they demonstrated that categorizing threats according to the 6M dimensions reduced subjectivity and improved cross-team alignment for risk reviews.

However, the technical limitations of bowtie analysis become pronounced in systems such as DAA. DAA safety depends on variables such as detection delay distributions, intruder encounter geometry, false alarm rates, and environmental variability – none of which are naturally supported in static bowtie models. Bowtie does not model conditional probabilities, time-resolved behavior, or feedback loops, which are critical for evaluating the real-time performance of autonomous systems under uncertainty. Therefore, in this work, the assessment relies on probabilistic methods, including Bayesian inference, Monte Carlo simulations, and low-altitude encounter modeling, to evaluate detection system performance.

2.2.3.1.3 Fault Tree Analysis (FTA)

FTA is a well-established top-down approach used to identify combinations of failures that can lead to a predefined undesired event or the top event. It uses Boolean logic gates (AND, OR) to model how basic events (*e.g.*, sensor faults, loss of signal) propagate through intermediate conditions to result in system-level hazards. In aviation system safety assessments, FTA has been applied to structure failure pathways and ensures that critical risks remain within acceptable thresholds, as defined by severity-based probability limits, *e.g.*, 10^{-9} for catastrophic outcomes [Leung, 2017].

FTA is traditionally static and binary in nature: it models whether a failure occurs or not, and what consequences that leads to. This structure makes it suitable for design-time assessments – evaluating system architecture and identifying single points of failure or key risk contributors. For instance, a DAA system might use FTA to examine how sensor fusion errors, communication losses, or algorithmic faults could independently or jointly lead to a failure to detect an intruder.

FTA offers transparent logic for tracing fault paths, which aids in system certification planning and early-stage hazard decomposition. This is evident in frameworks like Consequence Severity Level modeling, which adapts FTA logic to aviation-specific severity classifications, supporting compliance with FAA-defined thresholds [Leung, 2017]. FTA can be utilized to verify that all critical hazards have at least one prevention or mitigation path. In UAS safety studies, such as [Xiao, 2023], FTA has been used to identify root-level contributors to crash events or flight disruptions, enabling targeted safety measures. Its mathematical structure allows top event probabilities to be approximated as:

$$Q_i = \frac{N_i}{N_T \,.\, T}$$

where Q_i represents the probability of occurrence for an event i , N_i represents the number of occurrences of a basic event, N_T represents the total number of accidents, T indicates the time period of the dataset in years [Xiao, 2023].

While FTA can be utilized for both qualitative and quantitative analysis [Xiao, 2023], and is useful for deterministic fault logic, it lacks the capacity to represent time-dependent risk, probabilistic sensor performance, or dynamic intruder behavior - all of which are essential for a realistic DAA system. DAA risk evolves with encounter geometry, delay distributions, and system response timing – none of which can be captured in a binary fault tree without extensive transformation. That's why in the context of Task 2, the team evaluates risk using probabilistic, time-resolved

models that more appropriately capture the detection timing, false alarm tradeoffs, and encounter variability that define DAA system performance.

2.2.3.1.4 Event Tree Analysis (ETA)

ETA is a forward, scenario-based risk modeling technique used to evaluate the range of possible outcomes following an initiating hazardous event. ETA structures sequential system responses into branches, each representing success or failure of safety functions, allowing analysis to quantify the probability of different end states. The conduct of a risk assessment is the process of generating the risk triplet set:

$$R = RISK = \{< S_i, p_i, C_i >\}$$

where S_i is the i^{th} scenario, p_i is the probability or likelihood of the i^{th} scenario, and C_i is the consequences associated with the i^{th} scenario [Prassinos, 2011]. PRA is the formal methodology used to derive and quantify the risk triplet for the derived scenarios of the system, process, or activity being analyzed in an integrated manner.

This approach is formally described in [Prassinos, 2011] as part of FAA-aligned system safety methodology, and was used by [Pascarella, 2022] to evaluate drone intrusions near airports by modeling detection, threat assessment, and mitigation steps as branches in the event tree.

ETA assumes discrete, binary outcomes and fixed branching probabilities. It lacks time-resolved modeling, continuous probabilistic variables such as range, velocity, etc., and feedback mechanisms. Despite limitations, ETA can support early-stage DAA system architecture evaluation. For example, modeling what-if failure combinations, visualizing the impact of detection barrier reliability, quantifying residual risk for certification purposes if detection success probabilities are known. However, for operational DAA risk assessment, more dynamic models like Bayesian networks, Monte Carlo encounter simulations are more suitable.

Possible future direction: Integration of Traditional Risk Frameworks

While traditional approaches such as qualitative matrices, Bowtie analysis, FTA, and ETA are not implemented in this study, they provide valuable reference points for structuring risk logic and informing certification pathways. In future work, these models could support early-phase system design reviews or regulatory compliance assessments. Although these methods lack the time-resolved and probabilistic fidelity required for operational risk modeling, they may complement dynamic simulations by offering structured overviews of threats, mitigations, and escalation paths in DAA system design. Future extensions could incorporate detection performance outcomes – including true positives, false positives, true negatives, false negatives – into Bowtie or Event-Tree frameworks. This would enable tracing how detection errors propagate through the system and impact mitigation actions.

2.2.3.2 ***Alternative Risk Assessment Approaches for DAA Systems***

Traditional qualitative methods for assessing safety risks in aviation, such as fault trees and event trees analysis, while useful, often fall short of accurately capturing the intricate interactions and probabilistic nature of risks associated with DAA systems in unmanned aircraft operations. Given

the complexity, variability, and uncertainties inherent in these systems, a shift toward more quantitative, adaptive, and data-driven methodologies is essential.

In contrast to the traditional approaches, the alternative methods described in this section form the foundation of this project's current implementation. Specifically, the MIT Lincoln Laboratory (MIT LL) Dynamic Bayesian Network model is used to generate realistic intruder encounter scenarios, which are then integrated into out Monte Carlo simulation framework. Alongside this, a machine learning-based detection model supports the probabilistic estimation of detection success based on separation distance and environmental conditions.

Alternative risk assessment approaches, including Bayesian Networks, Monte Carlo Simulations, and Machine Learning-Based Risk Prediction, offer promising frameworks to address the challenges posed by DAA-enabled UAS operations. These approaches leverage statistical inference, computational simulations, and historical data analysis to provide more comprehensive, accurate, and dynamic risk evaluations that significantly enhance safety decision-making and system reliability assessments.

2.2.3.2.1 Bayesian Networks

Bayesian networks provide a powerful, structural framework for modeling the dynamic, uncertain, and highly coupled risk factors that characterize DAA operations. The Bayesian modeling developed by MIT LL for aircraft encounter modeling serves as a strong foundation for extending these methods to assess risks in DAA systems (MIT LL, 2021).

The core content of Bayesian reasoning is conditional probability [Wang, 2024]. The probability of event A given event B is expressed as:

$$P(A|B) = \frac{P(A \cap B)}{P(B)}$$

However, in practical risk analysis, we are often more interested in $P(B|A)$ which is the probability of an underlying condition given an observed event, which is harder to calculate directly. Bayes' theorem enables this reverse inference:

$$P(B|A) = \frac{P(A|B) \times P(B)}{P(A)}$$

Bayesian networks are an extension of Bayes' theorem, Bayesian networks are mathematical models based on probabilistic reasoning, usually presented as a graphical network. A Bayesian network takes the form of a directed acyclic graph, where the nodes in the graph represent different random variables, and the links between the nodes represent the correlations between the variables. Each node's state is determined based on the states of its parent nodes through conditional probability distributions. Bayesian networks thus allow both forward prediction and backward inference, essential for dynamic and evolving risk scenarios. A critical principle is that the network must remain acyclic, meaning no loops are allowed between nodes.

The manned Bayesian Encounter Model developed at MIT Lincoln Lab constructed encounter models using radar-based historical track data by probabilistically relating aircraft states such as

altitude, heading, vertical rate, and turn rate [MIT Lincoln Labs, 2021]. This model, released via the em-model-manned-bayes GitHub repository [MIT Lincoln Labs, 2021], forms the core of the encounter generation process in the Task 2 simulations. The model leverages a Dynamic Bayesian Network structure to represent dependencies among aircraft state variables across time, capturing how aircraft behave in realistic operational environments. The initial state includes variables such as:

- G: Geographic location
- A: Airspace class
- L: Altitude layer
- v: Airspeed
- $\dot{v}$: Acceleration
- $\dot{h}$: Vertical rate
- $\dot{\psi}$: Turn rate

Each of these variables is probabilistically dependent on others, forming the joint distribution of aircraft states from which realistic encounters can be sampled. The graphical structure of the initial state Bayesian network, shown in Figure 13, represents the conditional relationships between aircraft state variables used to simulate close encounters.

This structure enables efficient sampling of encounter scenarios. For instance, given a sampled airspace class and altitude layer, the network determines likely vertical rates and speeds based on learned distributions, improving fidelity in encounter geometry and maneuver realism.

In Task 2, the MIT Bayesian encounter model is integrated directly into the DAA risk simulation framework. It serves as the primary encounter generator, providing realistic intruder state trajectories under a variety of low-altitude operational contexts. These are essential for evaluating how DAA systems detect, classify, and respond to intruders.

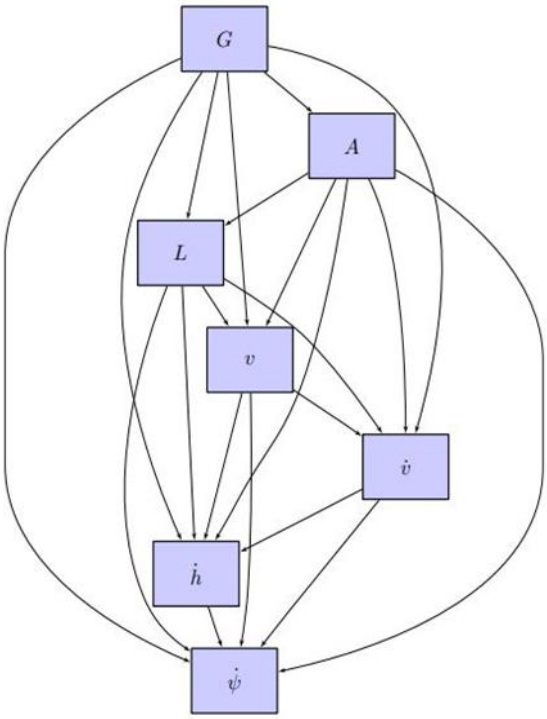

Figure 13. Bayesian network in MIT Lincoln Labs encounter model [MIT Lincoln Labs, 2021].

This model supports:

- *Realistic intruder generation:* Aircraft trajectories are sampled based on actual statistical distributions observed in radar surveillance data, ensuring realism in terms of speed, vertical rates, and maneuver patterns, especially in low-altitude Class G airspace.
- *Integration with detection delay models:* Sampled encounter states are input into DAA system simulations, where probabilistic detection delays (*e.g.*, from sensor lag, classification uncertainty, or algorithm latency) are modeled in conjunction with aircraft motion.
- *Evaluation of performance metrics through conditional analysis, such as:* $P(Detect \mid Separation < d), P(Avoid \mid Alert)$.
  These conditional probabilities help estimate false alarm rates, missed detections, and risk ratios that form the basis for DAA performance evaluation.
- *Monte Carlo simulations:* The Bayesian network-based encounter model is also used to drive large-scale Monte Carlo simulations, in which the stochastic nature of intruder trajectories, detection timing, and system response is fully captured [Kochenderfer, 2008].

This model supports both correlated and uncorrelated encounters – the latter being particularly important for non-cooperative traffic, such as general aviation aircraft not following standard rules of flying under visual flight rules. By capturing the variability and uncertainty of these behaviors, the Bayesian network ensures that DAA systems are evaluated against challenging, real-world scenarios.

Possible Future Direction: Incorporating Clutter and False Tracks into Encounter Modeling
The MIT Lincoln Labs Bayesian Encounter Model is a strong foundation for simulating realistic aircraft trajectories. However, it does not include false tracks caused by clutter – such as birds, cars, or ground reflections – because it was originally developed for cooperative systems like TCAS, which use transponders and are not affected by such clutter. For vision-based or non-cooperative DAA systems, false tracks can be a challenge. In future work, we plan to add clutter models that simulate these false intruders. This also allows us to study how detection thresholds affect false alarms and missed detections under more realistic conditions.

2.2.3.2.2 Monte Carlo Simulations

Monte Carlo simulations are widely recognized in aviation safety research for their ability to evaluate system-level risk under uncertainty. In collision risk modeling, they allow for the approximation of complex, multi-dimensional outcome distributions where analytical solutions are intractable.

Monte Carlo simulations form the quantitative backbone of the risk modeling approach in ASSURE A71 Task 2. By repeatedly simulating randomized aircraft encounters with varying input parameters, this method allows for probabilistic evaluation of DAA system detection timing, risk of NMAC, and environmental sensitivity in operational settings.

The simulation framework integrates:

- Realistic encounter trajectories generated using the MIT LL Bayesian Encounter Model [MIT Lincoln Labs, 2021].
- Sigmoid-based probabilistic detection models fitted from empirical Gazebo simulation data under various environmental conditions.
- Bernoulli trials at each time step, where detection is a stochastic process driven by modeled probability curves and the instantaneous separation distance between ownship and intruder aircraft.

Each Monte Carlo trial simulates the evolution of a unique encounter by:

- A joint distribution of intruder aircraft states (altitude, speed, vertical rate, etc.) is sampled using the MIT LL Dynamic Bayesian Network model [MIT Lincoln Labs, 2021].
- A detection probability curve – a sigmoid function of distance is applied at each time step.
- A Bernoulli trial is performed at each time step using the probability to determine detection status.
- The time of detection t_{detect} is compared to t_{NMAC} to determine if detection occurs before a potential collision.

This yields an empirical estimate of a successful detection rate:

$$P_{success} = \frac{N(t_{detect} < t_{NMAC})}{N_{total}}$$

which quantifies the proportion of encounters where detection occurs early enough to allow avoidance. Here,

- $P_{success}$ is the empirical probability of successful detection, *i.e.*, the proportion of simulated encounters where detection occurs early enough to allow for collision avoidance.
- $N(t_{detect} < t_{NMAC})$ is the number of Monte Carlo simulation trials where the detection time occurs before the time of NMAC.
- N_{total} is the total number of Monte Carlo trials run in the simulation.

These simulations allow one to extract distributions of detection delays, separation distances at detection, and probabilities of well-clear violations.

It is important to note that while $P_{success}$ captures whether detection occurred before the first NMAC, this does not necessarily imply that the ownship could execute a successful avoidance maneuver. At high closure rates, even brief delays from system or pilot response may leave too little time to maneuver. Additional factors such as system latency, pilot or automation response time, and required maneuver distance can impact whether the detected threat can be avoided in practice.

2.2.3.2.3 Machine Learning-Based Risk Prediction

Machine learning models have emerged as critical tools in risk assessment frameworks for UAS, especially when tasked with predicting safety violations or failure points in complex and uncertain operational environments. For instance, [Truong, 2020] applied classification regression, decision trees, neural networks, gradient boosting, random forests, Bayesian networks, and memory-based reasoning to FAA UAS incident reports to predict risk-related violations such as flying beyond regulated altitude or entering restricted airspace.

In the DAA system within Task 2 of the ASSURE A71 framework, it enables the estimation of detection delays and potential failure points. In the current implementation, a regression-based detection timing model was developed using simulation data from Gazebo-based environments. The model fits sigmoid-shaped probabilistic detection curves to the observed detection outcomes across various encounter geometries and environmental conditions. These functions capture the likelihood of timely detection as a function of the separation distance and visibility levels. The predictive detection timing model enables one to simulate a variety of operational scenarios, quantify detection failure risk, and assess how detection timing shifts under varying visibility and geometry. These outcomes directly feed into risk metrics.

2.2.4 Review of DAA System Performance Metrics

DAA systems must be evaluated using performance metrics that reflect their effectiveness in detecting intruders, generating alerts, and supporting avoidance maneuvers, particularly in BVLOS operations. This section reviews several key performance metrics referenced in the ASTM F3442/F3442M standard and broader literature.

2.2.4.1 *Risk Ratios*

The risk ratio is a fundamental performance parameter for DAA systems, representing the relative effectiveness of a system in reducing the risk of mid-air collisions. Risk ratio is calculated as the probability of mid-air collision with a DAA system divided by the probability of mid-air collision

without a DAA system [Johnson, 2015]. Recent simulations by Mississippi State University researchers, incorporating data from 137 general aviation pilots, have led to updated Risk Ratio tables that account for variables like beta value, intruder aircraft type, turn rate, and delay time. These simulations reinforce that the industry-accepted baseline values for risk ratios under ASTM F3442/F3442M-23 are LoWC risk ratio of 0.5 and NMAC risk ratio of 0.3 [Amerson, 2024]. Although risk ratios are not directly computed in this study, they are reviewed here to contextualize performance thresholds used in industry.

2.2.4.2 *Conditional Probabilities*

Conditional probabilities reflect the likelihood of achieving a desired outcome, such as issuing an alert or executing a successful avoidance maneuver, given that a preceding event, such as detection, has already occurred. These metrics form the backbone of PRAs used to validate DAA system performance across a range of operational scenarios. In the context of DAA systems, some of the most relevant conditional probabilities include:

- *P(Alert | Detect)*: The probability that an alert is generated after a threat has been successfully detected.
- *P(Avoid | Alert)*: The probability that an effective avoidance maneuver is executed following an issued alert.
- *P(Avoid | Detect)*: A more direct conditional metric that assesses the likelihood of avoiding a mid-air collision or a LoWC event given successful detection.

Rather than assessing DAA system functions in isolation, conditional probabilities allow for a more transparent evaluation of DAA system-level performance, as shown through Bayesian network modeling [Weinert, 2018]. Conditional probabilities have also been utilized to model conflict detection, showing how factors like latency and separation affect detection outcomes [ASTM, 2023]. It is a powerful tool for modeling DAA system logic and may be integrated in future extensions using dynamic Bayesian modeling framework.

2.2.4.3 *Detection Time Distributions*

In this study, detection timing is modeled as a probabilistic distribution derived from Monte Carlo simulations using realistic encounter trajectories and sigmoid-based detection models. These detection delay distributions serve as the core of our quantitative risk assessment.

The detection time distribution represents the statistical distribution of times from when an intruder aircraft first enters the detection range of the DAA sensors to when the DAA system successfully registers the presence of that intruder. Shorter and consistent detection times are necessary to enable timely alerts and effective avoidance maneuvers.

Characterizing detection time as a probability distribution rather than a single deterministic value is important since it accounts for uncertainties in sensor performance, environmental variability, and operational scenarios. ASTM F3442/F3442M-23 specifically emphasizes detection timing requirements within its DAA performance criteria, noting the importance of consistent and prompt detection to achieve safe BVLOS operations in complex airspace environments [ASTM, 2023]. NASA's fast-time simulation studies have demonstrated that different encounter geometries and intruder velocities significantly influence detection latency. Consequently, detection times can be better represented using statistical distributions. It allows robust probabilistic assessments of system reliability across diverse operational scenarios [Cone, 2019].

2.2.4.4 *False Positive/Negative Rates*

False positive and false negative rates quantify the accuracy of threat detection in a DAA system.

- *False Positives:* It occurs when the DAA system incorrectly identifies a safe aircraft or non-threatening situation as hazardous.
- *False Negatives:* It occurs when the system fails to detect an actual threat, increasing the risk of collision or loss of safe separation.

High false-positive rates can lead to unnecessary interruptions in flight operations and reduce overall mission efficiency. In addition to reducing mission efficiency through unnecessary avoidance maneuvers, false positives can also introduce safety risks. These may include increased pilot workload, confusion, alert fatigue, repeated automation responses, and interference with critical flight phases such as approach and landing.

Conversely, high false-negative rates pose a direct safety risk by leaving genuine threats undetected [Costley, 2022]. A balance between these two error types is crucial for DAA systems, maintaining both safety and operational effectiveness. In this study, false positives and false negatives are estimated using probabilistic detection outcomes derived from YOLO-based object detection under varying environmental conditions in the Gazebo simulation framework.

Factors such as sensor accuracy, tracking algorithms, environmental conditions, and intruder dynamics significantly influence these error rates. For instance, radar-based DAA systems are sensitive to uncertainties in intruder aircraft positioning, orientation, and velocity, affecting detection accuracy and subsequently impacting false positive and false negative performance [Costley, 2022].

2.2.4.5 *Response Time Metrics*

Response time metrics quantify the total time taken by a DAA system to notify the operator or automated control system and subsequently execute avoidance maneuvers after a threat is detected. Quick and consistent response times are crucial to ensure effective avoidance and maintain safety margins. The response process can be segmented into three intervals: detection time, alerting time, and avoidance maneuver execution time.

The design and complexity of pilot interfaces significantly influence these intervals. Specifically, pilot response times-including time to detect, decide upon, and execute maneuvers-vary with the information level presented in DAA displays. In [Fern, 2015], the experimental results show that advanced information displays led to approximately 33% faster total response times than basic displays. Although response time matrices are not modeled in this current system, which focuses on autonomous detection timing, these matrices can be considered important for future implementation that incorporates human-in-the-loop modeling or full ASTM timing chains.

Possible future direction: Expanded performance evaluation. In this study, detection time distributions and false positive/negative rates were directly assessed through Monte Carlo simulations and YOLO-based object detection in Gazebo. However, other metrics—including risk ratios, conditional probabilities, and response time metrics—were not implemented. These are reviewed for completeness and alignment with ASTM standards. Future implementations may

incorporate these metrics using Bayesian inference, pilot response modeling, and full-system timing analysis to enable a more comprehensive, end-to-end evaluation of DAA system effectiveness under real-world operational conditions. In future iterations of this work, we also aim to model operational consequences of high false positive rates.

2.2.5 System, Environmental, and Human Factors Affecting Detection Time

Factors that impact DAA detection time may be divided into the three categories of system-related, environmental, and human factors. Examples in each category include:

- *System-related factors:* Sensor performance, processing time, communication delays.
- *Environmental factors:* Weather conditions, electromagnetic interference, terrain obstructions.
- *Human factors:* Operator response time, decision-making processes.

The category names indicate the intended definition in each category:

- *System-related factors* are tied to system design and implementation and are independent of the operating environment or the behavior of a human;
- *Environmental factors* are connected with the operational environment rather than the system design or the behavior of a human;
- *Human factors* are connected directly to human behavior (including cognition).

This section reviews both implemented and aspirational components affecting detection time. In the current work, selected system and environmental factors - such as sensor resolution, fog conditions, and object detection accuracy, etc.– are incorporated into simulations using YOLO-based models in Gazebo. Other aspects, such as human factors, radar clutter, and pose uncertainty, are reviewed for context but not included in the current implementation. Future implementations may incorporate additional system uncertainties, navigation degradation, and pilot-in-the-loop delays.

While consideration of human factors is outside the scope of this report, the rest of this section addresses the first two categories.

2.2.5.1 ***System-Related Factors***

There are many different types of system-related factors that impact DAA system performance; eleven of the most important are listed in the following subsections.

2.2.5.1.1 Sensor Type and Capabilities

DAA systems employ two main sensor categories: cooperative sensors that receive information directly transmitted from other aircraft, and non-cooperative sensors that obtain information indirectly through passive or active detection techniques [Legowo, 2017].

2.2.5.1.2 Electronic Conspicuity (EC) equipment

For safe integration of drones and crewed aircraft in shared airspace, some form of EC is essential. Many experts particularly support Automatic Dependent Surveillance-Broadcast (ADS-B) systems, which broadcast critical information including aircraft position, identification, altitude, and velocity [Grote, 2021].

2.2.5.1.3 ADS-B Limitations

While ADS-B is widely used, it has notable disadvantages, including security vulnerabilities and the fact that not all aircraft are required to have ADS-B transponders. This makes it less than 100% reliable as a standalone DAA system, particularly in Very Low Level flights [Mariscal-Harana, 2020], [Kim, 2017].

2.2.5.1.4 Radar System Parameters

The effectiveness of radar-based detection is determined by specific system parameters that must be optimized for reliable performance. These parameters significantly influence detection probability and range [Costley, 2022].

2.2.5.1.5 Aircraft Physical Characteristics

The Radar Cross-Section (RCS) of aircraft being detected plays a crucial role in detection capability. Smaller UAS with reduced RCS present greater detection challenges than larger aircraft [Costley, 2022].

2.2.5.1.6 Sensor Size and Weight Constraints

sUAS face significant limitations in sensor selection due to weight and size restrictions. For example, while terrestrial acoustic sensor arrays might provide 360° detection up to 5 nautical miles away, they are often too large and heavy for sUAS applications [Lai, 2024].

2.2.5.1.7 Detection Timing Requirements

For Unmanned Traffic Management (UTM) applications, DAA systems must provide alerts at least 10 seconds before a potential collision to ensure minimum safety separation, requiring sensors with sufficient range and processing speed [Lai, 2024].

2.2.5.1.8 Encounter Geometry and Speed

The relative positioning and velocity of aircraft significantly impact detection capability. Detection systems must account for various approach angles and speeds to ensure reliable threat identification [Omeri, 2022].

2.2.5.1.9 Communication, Navigation, and Surveillance (CNS) Uncertainties

Errors and limitations in CNS systems directly affect detection reliability. These uncertainties must be carefully considered when establishing separation criteria [Omeri, 2022].

2.2.5.1.10 Sensor Resolution and Response Time

Critical performance parameters include sensor resolution (ability to distinguish between closely-spaced objects) and speed of object capture, which directly impact the system's ability to provide timely alerts [Fitrikananda, 2023].

2.2.5.1.11 Optoelectronic System Limitations

Camera and optical sensor-based systems offer precise detection but are heavily dependent on lighting conditions, limiting their reliability across varying operational scenarios. [Semenyuk, 2024].

Possible future direction: Expanded System Factor Analysis. In the current implementation, certain system-related factors—such as detection timing requirements, encounter geometry, and relative speed—are directly incorporated into the detection modeling framework. Additionally, sensor resolution and response time are reflected using fixed-resolution YOLO-based object detection in the Gazebo simulation environment. However, other key system elements discussed above, including radar characteristics, EC variations, and communication uncertainties, are not yet explicitly varied or modeled. These factors represent important components of the broader DAA architecture and may be integrated into future system simulations to assess their influence on detection performance and system reliability.

2.2.5.2 *Environmental Factors*

There are many different types of environmental factors that impact DAA system performance; eight of the most important are listed in the following subsections.

2.2.5.2.1 Weather Conditions

Various atmospheric conditions can substantially impair detection capabilities. Rain, fog, snow, and other precipitation can reduce visibility and interfere with sensor performance for DAA systems [Khan, 2022], [Seidaliyeva, 2023]. These conditions can lead to false positives or false negatives in UAS identification, creating significant challenges for reliable detection [Seidaliyeva, 2023].

2.2.5.2.2 Lighting Conditions

Outdoor operations face unique challenges from variable lighting, including sun interference during daytime operations and reduced visibility in low-light conditions [Sumi, 2024]. Optoelectronic recognition systems that utilize cameras and optical sensors are particularly affected by lighting variations, with performance directly dependent on adequate illumination [Semenyuk, 2024].

2.2.5.2.3 Terrain and Urban Features

Physical elements such as buildings, trees, and varying terrain can obstruct sensors and create detection blind spots [Seidaliyeva, 2023]. These obstructions are especially problematic in urban environments where complex infrastructure can limit line-of-sight for sensors.

2.2.5.2.4 Background Noise

Environmental noise can interfere with acoustic-based detection systems and create challenges for accurate identification [Seidaliyeva, 2023].

2.2.5.2.5 Aircraft Pose Uncertainties

Environmental factors like wind gusts create disturbances that affect aircraft positioning and orientation, which in turn impact detection probability [Costley, 2022].

2.2.5.2.6 Reflective Objects

Surrounding reflective objects in the environment can create radar clutter, potentially leading to false detections or masking actual threats [Semenyuk, 2024].

2.2.5.2.7 Detection Range Limitations

While current detection ranges show good performance in ideal conditions, environmental factors can significantly reduce effective detection distances, requiring optimization for real-world collision avoidance applications [Singh, 2024].

2.2.5.2.8 Navigation Challenges

In environments where global positioning measurements are contested, degraded, or denied, navigation errors from inertial systems using noisy sensors further complicate accurate detection [Costley, 2022].

Possible future direction: Expanded Environmental Condition Modeling. In this project's current implementation, fog conditions were varied in simulation and incorporated in the detection probability modeling. Other environmental conditions, such as lighting, terrain, background noise, etc., are not explicitly swept in current simulations. These factors represent realistic operational challenges that may significantly influence detection reliability. In future validation efforts, these conditions could be systematically varied to better evaluate system robustness under diverse and degraded environmental scenarios.

2.2.6 Sensor Resolution and Detection Time Budget

Sensor resolution plays a critical role in the performance of DAA systems, particularly in terms of the time required to detect potential collision threats and the accuracy of the response. A higher-resolution sensor generally provides more precise obstacle localization and faster threat recognition, but often at the cost of increased computational demands, energy consumption, and system complexity.

The current model uses a fixed-resolution camera configuration (8.9 MP GigE units) in the Gazebo-YOLO simulation environment. Sensor resolution is held constant in this study and is not explored as a variable affecting detection time. The reviewed literature highlights key insights and trade-offs associated with sensor resolution and detection time across various DAA architectures.

Reference [Tirri, 2014] demonstrated that advanced filtering methods, such as particle filters, significantly enhance obstacle tracking accuracy compared to extended Kalman filters, particularly under non-linear dynamics typical of UAS environments. The improved tracking precision, driven by better resolution radar data and higher-fidelity state estimation, leads to more accurate predictions of Distance at Closest Point of Approach (DCPA) and consequently shorter detection-to-decision cycles. However, this comes with increased computational requirements, suggesting a trade-off between resolution and real-time processing feasibility. In a complementary approach, [Bigazzi, 2022] explored a hybrid sensor suite combining a 77 GHz radar and a stereoscopic camera, showing that the fusion of low-resolution long-range radar with high-resolution short-range stereo vision enables both early detection and fine obstacle localization. This architecture exploits the strengths of each modality—radar's robustness under adverse conditions and vision's spatial precision—while mitigating their individual weaknesses. Yet, integrating multi-modal data requires efficient synchronization and processing pipelines, highlighting the trade-off between sensor diversity and system complexity. [Fasano, 2023] provided an analytical framework linking sensor accuracy to conflict detection performance through mathematical models. They show that

sensing uncertainty directly affects the estimation of the time to CPA and DCPA, both of which are essential for early conflict resolution. Importantly, they advocate for an adaptive sensing approach where sensor resources are dynamically allocated based on the geometry and urgency of the encounter, thereby balancing resolution and update rate across the field of view. In scenarios involving small UAS operating at low altitudes, [Omeri, 2022] emphasized that rapid detect-and-avoid decisions are particularly sensitive to uncertainties from both sensor noise and system latencies. Their work supports using performance-based well-clear thresholds and time-based separation logic to compensate for varying sensor resolutions. Simulations confirm that insufficient sensor resolution, especially in dynamic environments with tight reaction times, leads to late alerts or unnecessary evasive maneuvers, underlining the importance of resolution-aware conflict modeling. Finally, [Kuru, 2023] proposed the Drone Aware Collision Management system, which relies on EC data rather than high-resolution sensors alone. They argue that real-time low-latency positional feeds from EC devices can enable effective conflict resolution even without sophisticated high-resolution sensors. This shifts the trade-off from sensor resolution to network reliability and positional update frequency, particularly for scalable multi-agent UAS operations.

In summary, higher sensor resolution generally leads to improved detection times and tracking precision, enhancing the effectiveness of DAA systems. However, this comes with trade-offs in computational burden, power consumption, and sensor integration complexity. Hybrid sensing systems, adaptive resource allocation, and real-time data fusion frameworks present promising paths to manage these trade-offs effectively.

Possible future direction: Additional Camera Resolution. Although this project's current implementation uses a fixed-resolution camera model—specifically, five 8.9-megapixel GigE cameras, future work could explore how varying resolution levels affect detection performance. This setup, modeled after the uAvionix Casia X system, reflects a high-end commercial off-the-shelf configuration. In a full implementation, the resolution could be systematically swept, for example, by simulating lower-resolution sensors (*e.g.*, 2 MP or 4 MP), to evaluate the trade-off between detection delay, false detection rates, and computational burden. This approach—mirroring fog sensitivity analysis—would help quantify how sensor resolution impacts success measures under diverse environmental and encounter conditions.

2.2.7 Review of Bayesian FA/MD Estimation Approach

Bayesian models have become fundamental to improving detection systems in UAS operations, where the tradeoff between false alarms (Type I errors) and missed detections (Type II errors) is critical. Whether in communication, safety, mission planning, or network security, UAS systems operate under uncertainty and often limited resources, making probabilistic and adaptive methods essential.

A particularly effective application of Bayesian modeling is in sequential detection problems, where decisions must be made quickly as data arrives. Traditional fixed-sample-size detectors require collecting all observations before making a decision, which can delay responses or overwhelm UAS computational resources. To address this, Bayesian Quickest Detection (BQD) frameworks were developed. These models continuously update the likelihood of competing hypotheses, such as the presence or absence of a primary user in a spectrum band, and determine

the optimal stopping time for making a decision. By balancing false alarm probability (P_f) and detection delay, BQD improves spectrum sensing efficiency, which is crucial in cognitive UAS networks.

Mathematically, the BQD framework minimizes the combined cost of false alarms and delay using:

$$\inf_{T_s \in T} P(T_s < t) + c\, E[(T_s - t + 1)^+],$$

where T_s is the stopping time, t is the unknown change point, and c is a cost-weighting parameter [Wu, 2023]. By sequentially evaluating the likelihood ratio:

$$\Lambda_{\text{quick}} = \prod_{i=1}^{s} \frac{P(r_i|\mathcal{H}1)}{P(r_i|\mathcal{H}0)},$$

where r_i is the observation at time i, BQD ensures that decisions can be made with minimal delay while maintaining acceptable false alarm rates. Simulation studies have demonstrated that, especially under tight time constraints, BQD outperforms conventional Bayesian detection, achieving much lower false alarm probabilities without sacrificing detection performance.

Beyond sensing, Bayesian modeling also plays a key role in mission planning, where UAS must balance the accuracy of tasks (like damage inspection) with limited flight time and energy. Bayes risk-based planning integrates not only the probability of detection but also the costs associated with correct and incorrect decisions. The total mission cost is expressed as:

$$\begin{aligned}\text{Cost} = {} & C_{00}\, P(\mathcal{H}0|\mathcal{H}0)P(\mathcal{H}0) + C_{01}\, P(\mathcal{H}0|\mathcal{H}1)P(\mathcal{H}1) + C\_10\, P(\mathcal{H}1|\mathcal{H}0)P(\mathcal{H}0) \\ & + C\_11\, P(\mathcal{H}1|\mathcal{H}1)P(\mathcal{H}1),\end{aligned}$$

where the C_{ij} terms represent the costs of true negatives, false negatives, false positives, and true positives, respectively. This framework allows UAS to adapt their flight paths dynamically to areas of higher risk or uncertainty, optimizing overlap ratios in sensor coverage and tuning flight parameters to minimize total cost.

In the domain of UAS network security, Bayesian models also play a central role through Bayesian game theory, where the interaction between a defender (Intrusion Detection System [IDS]) and an attacker is formulated as a strategic game with incomplete information. The IDS agent and attacker each aim to maximize their respective payoffs, adjusting their strategies based on observed behavior. Bayesian Nash equilibrium is used to find an optimal balance, allowing the IDS to maintain a high detection rate while minimizing resource consumption [Sun, 2018].

Finally, Bayesian networks have been widely used for accident risk assessment, where multiple uncertain factors interact. Using a tree-augmented naïve Bayesian network, UAS accident data can be analyzed to model the interdependencies between environmental, technical, and human factors, providing probabilistic estimates of accident severity [Sun, 2024]. This approach improves accident prediction and guides proactive interventions.

Across these applications, Bayesian models provide a cohesive, mathematically grounded framework that allows UAS systems to balance performance, safety, and efficiency under uncertainty.

Possible future direction: In future extensions, cost-based Bayes risk models can be integrated to enable real-time updating of detection likelihoods and dynamic tuning of detection thresholds. This could improve the simulation's ability to capture uncertainty in system behavior, especially under time-critical or resource-constrained scenarios.

2.2.8 Review of the Detection Delay Distribution in DAA Systems

The detection delay probability distribution in a DAA system requires several distinct but interdependent analyses and models, which are reviewed in the following sections.

2.2.8.1 *Component-Based Delay Analysis*

The total detection time in a DAA system is the sum of sequential delays from its core components: Scan, Relay, Filter, and Publish, as defined in Equation (1) of the Appendix and outlined in the ASTM DAA Timing Standard [ASTM, 2023]. Each component represents a necessary step from initial sensor scanning to making detection information available for threat assessment. The nominal values for these, or related delay types (*e.g.*, ADS-B, Tracker, C2 Link delays), are specified in standards like RTCA DO-365B [Serres, 2022], providing benchmarks for system evaluation (see Appendix, Table 1). Understanding the contribution of each component is vital, as delays in any stage directly impact the overall time available for the system to respond to potential conflicts.

2.2.8.2 *Statistical Probability Distribution Models*

In practice, component delays (Scan, Relay, Filter, Publish) vary and are better represented as random variables than fixed values. Each component's delay can be characterized by an appropriate probability distribution (*e.g.*, normal, exponential) to capture its inherent variability. The overall detection time distribution is then derived by combining the distributions of these individual components, often through convolution (for independent, sequential processes) or Monte Carlo simulation.

2.2.8.3 *System-Level Delay Analysis*

The DAA system architecture fundamentally shapes the detection time distribution. The arrangement of processing steps (serial vs. parallel) dictates how individual component delays aggregate, impacting the overall latency. Furthermore, there exists a trade-off between the complexity of algorithms (*e.g.*, for filtering or tracking) and timing performance; more sophisticated algorithms may improve accuracy but increase processing delay. Analyzing these architectural aspects is crucial for optimizing system responsiveness.

2.2.8.4 *Environmental Factor Integration*

Environmental conditions significantly influence DAA system performance and modify the delay distributions of its components. Factors such as adverse weather (fog, rain), poor lighting, visual clutter, and the distance to an intruder can degrade detection performance and increase processing time. A mathematical framework, as outlined in the Appendix (Sections 4.3-5.3), is needed to

incorporate these effects. This typically involves modeling the instantaneous detection probability *p(detect|Env)* to be dependent on factors like distance (x) and environment (Env). For instance, visibility effects can be modeled using functions like the logistic function presented in Equation (13), which adjusts detection probability based on visibility conditions. Simulation results consistently show that degraded environmental conditions (*e.g.*, increased fog) lead to longer detection times and reduced detection ranges.

2.2.8.5 *Detection Delay Probability Distribution Derivation*

For discrete-time analysis with detection attempts every δ seconds, the *c(PMF)* for the detection time can be derived based on the sequence of instantaneous detection probabilities *(pl).* The probability of detection occurring exactly at time step a is given by Equation (7) in the Appendix. This PMF(Probability Mass Function) explicitly links the time-varying detection probability sequence to the overall distribution of detection times. The analysis considers a maximum time step $a\_max = \lceil T/\Delta t \rceil$, representing the simulation or encounter horizon. The probability calculated for this final step, *P(a),* using Equation (8), encompasses the possibility of detection failure within the timeframe T. This PMF derivation is fundamental for quantifying the likelihood of timely versus missed detections in risk assessments.

2.2.9 Review of DAA Requirements in Different Operating Environments

Different types of DAA operations require specialized risk assessment methodologies, which are discussed in the following sections.

DAA systems are critical enablers for safe UAS operations across a wide range of applications. The effectiveness and design of DAA systems must be tailored to the specific characteristics of each operational domain. This section reviews how DAA is applied across various categories, emphasizing technical challenges, risk factors, and relevant research findings.

2.2.9.1 *Airborne DAA systems: Evaluating Sensor Effectiveness in Real-Time Detection*

Airborne DAA systems are essential for ensuring UAS safety by detecting and tracking cooperative and non-cooperative aircraft in real time. These systems typically integrate sensors such as radar, LiDAR, electro-optical/infrared cameras, and ADS-B receivers. Their effectiveness hinges on the ability to deliver timely and accurate detection across a range of operational environments—including cluttered urban settings, low-light conditions, and high relative speeds.

Recent advances in vision-based DAA systems have enhanced the ability of sUAS to operate safely under Size, Weight, and Power (SWaP) constraints. A notable example is the AirTrack framework, a deep learning–driven system developed for long-range aircraft detection and tracking onboard sUAS. AirTrack employs deep neural networks to process high-resolution visual data while compensating for ego-motion (movement of the host UAS), achieving real-time detection and tracking with superior accuracy over previous methods, as validated on the Amazon Airborne Object Tracking dataset [Ghosh, 2023].

Complementing this, [Fang, 2024] introduced SEB-YOLOv8s, a lightweight detection model designed specifically to improve sUAS detection in complex backgrounds, such as forests, cities, and mountainous regions, where traditional models struggle with high false positive rates. SEB-

YOLOv8s incorporates attention mechanisms and a boundary-aware backbone to enhance both accuracy and robustness. Experimental results showed that SEB-YOLOv8s outperformed baseline YOLO models in detection precision and recall while reducing model parameters and computational load, making it particularly suitable for deployment on SWaP-constrained platforms. This work addresses key DAA challenges, including small target detection, background interference, and real-time inference.

Ongoing research continues to focus on reducing false alarms, improving detection ranges, integrating multi-sensor fusion, and aligning airborne DAA systems with regulatory standards such as ASTM F3442 for BVLOS operations.

2.2.9.2 *Ground-Based DAA Systems: Assessing Surveillance Networks and Communication Relays*

Ground-based DAA systems are critical for ensuring UAS operational safety, particularly when onboard sensing is limited by weight, power, or payload constraints. These systems rely on ground surveillance networks composed of radar installations, ADS-B receivers, acoustic sensors, and multilateration systems to monitor both manned and unmanned aircraft. The gathered data is transmitted to UAS operators or autonomous systems through communication relays, enabling real-time conflict detection and avoidance.

One of the key lessons from the FAA ASSURE program is the importance of ground-based surveillance systems in supporting BVLOS and complex operations. The ASSURE First Annual Report highlights that ground-based radar networks, in combination with UAS Service Suppliers (USS), can provide a layered DAA architecture that significantly reduces collision risk in controlled and uncontrolled airspace. These systems, when paired with reliable communication links, ensure that UAS can comply with separation minima, even in areas with dense air traffic or limited line-of-sight visibility [ASSURE, 2021]. A second layer of research focuses on Flying Ad Hoc Networks (FANETs), where UAS themselves serve as dynamic communication relays between ground stations and other UAS. [Bekmezci, 2013] provided one of the seminal surveys on FANETs, describing how UAS nodes form mobile ad hoc networks with rapid topology changes and challenging propagation environments. In this framework, UAS not only act as sensors but also as airborne network nodes that enhance the range, redundancy, and robustness of the ground-based DAA network.

Challenges for ground-based DAA include maintaining low-latency communication, ensuring resilient data links under interference or adverse weather, integrating heterogeneous sensor types, and ensuring scalability to handle high-density UAS operations. As ground-based DAA evolves, combining fixed ground infrastructure with flexible UAS relays and mesh networks will play an increasing role in expanding coverage and improving detection reliability.

2.2.9.3 *UTM-Supported DAA Systems: Integration Into UTM Frameworks*

The integration of DAA systems into UTM frameworks is critical for scaling safe and efficient UAS operations, especially for BVLOS flights and high-density airspace. UTM provides the digital infrastructure to handle flight planning, authorization, strategic deconfliction, tactical conflict resolution, and real-time rerouting.

The FAA emphasizes that DAA is a core component of UTM operations, particularly to enable BVLOS missions without visual observers. Operators are required to implement DAA either through technical solutions (such as airborne or ground-based sensors) or procedural means, depending on the operational risk profile and airspace type [FAA, 2023]. Ongoing FAA UTM Pilot Programs are evaluating DAA performance under live operational conditions, contributing to future regulatory standards. Internationally, the International Civil Aviation Organization (ICAO) has published a UTM framework outlining the integration of DAA within critical airspace management functions such as conflict detection, conformance monitoring, and contingency planning [ICAO, 2020]. The ICAO framework highlights interoperability between UTM and traditional air traffic management systems, which is essential for mixed-use airspace safety. A seminal contribution to the UTM concept came from [Kopardekar, 2016], who proposed a federated architecture for UAS traffic management in low-altitude airspace. Their work introduced the concept of USS exchanging flight intent, geofencing, weather, and DAA-related data to facilitate collaborative airspace management. This framework established foundational principles such as distributed decision-making, cooperative separation, and scalable traffic coordination—principles that continue to shape UTM research today.

Key ongoing challenges in UTM-supported DAA include scaling to dense traffic environments, securing communication channels, developing predictive conflict resolution models, and ensuring international regulatory harmonization. The future of UTM will rely heavily on seamless DAA integration to guarantee safety and operational efficiency.

2.2.9.4 *Large UAS Operations: Risk Models for High-Altitude, Long-Range Operations*

Large UAS, particularly those operating at high altitudes and over long ranges, pose unique challenges for risk assessment and management. These aircraft typically operate under Instrument Flight Rules, often in controlled airspace alongside crewed aviation, where the consequences of failure can be severe. Risk models for large UAS must address not only mechanical and operational failures but also complex interactions with air traffic control, other aircraft, and environmental factors.

One promising approach is the unified airspace risk management framework proposed by [Bijjahalli, 2022], which integrates the performance of CNS systems into collision risk modeling. By analyzing CNS error characteristics, the framework translates them into spatial domains, enabling the creation of protection volumes around aircraft. This allows both strategic and tactical risk assessment and enhances safety in mixed-use airspace, making it particularly suitable for large UAS engaged in BVLOS and long-endurance missions. The European Union Aviation Safety Agency (EASA) has also conducted extensive risk portfolio analyses for UAS operations. Their safety portfolio identifies major risk areas such as airborne conflicts, ground impacts, and third-party injuries. EASA emphasizes the need for robust risk models capable of accounting for emerging hazards, system redundancies, and evolving regulatory frameworks [EASA, 2016].

Overall, incorporating advanced risk modeling techniques is essential to ensure the safe integration of large UAS into the national airspace system. These models support better decision-making, improved system design, and harmonized operational procedures across civil aviation authorities.

2.2.9.5 *sUAS Operations: Risk Assessment in Low-Altitude, High-Density Urban Environments*

sUAS operating in urban environments face unique challenges due to low-altitude flight paths, high population densities, and complex infrastructures. These factors necessitate comprehensive risk assessment models to ensure safety and compliance with regulatory standards.

[Li, 2023] introduced a methodology focusing on ground risk assessment for unmanned aircraft in urban settings. Their approach quantifies flying risk by evaluating potential ground fatalities resulting from various risk sources. By analyzing UAS specifications and ground environment characteristics, they developed safety level maps that assist in decision-making for safe UAS operations in urban areas. [Primatesta, 2019] proposed a two-dimensional location-based risk map to quantify the risk to the ground population from UAS operations over specific urban areas. Their probabilistic approach combines layers such as population density, sheltering factors, and obstacles to assign risk values to different locations, facilitating the identification of high and low-risk zones. [Zhang, 2023] developed a path-planning algorithm for UAS in urban environments that incorporates ground risk maps. Their strategy aims to generate UAS paths that minimize ground risk and flying costs, enhancing safety and efficiency over inhabited areas.

These studies collectively contribute to the development of robust risk assessment frameworks for sUAS operations in urban settings, emphasizing the importance of integrating environmental data, population dynamics, and advanced modeling techniques to ensure safe and efficient UAS deployments.

2.2.9.6 *Multi-Vehicle Operations: Collision Avoidance and Risk Modeling for Swarms of Drones*

Coordinated operations involving multiple UAS, commonly referred to as drone swarms, present unique challenges in collision avoidance and risk management. The dynamic nature of swarm environments necessitates advanced algorithms that can ensure safe and efficient navigation.

One notable approach is the integration of Proximal Policy Optimization with a Generalized Integral Compensator and a CNN–LSTM fusion network. This method enables UAS to learn effective collision avoidance strategies through deep reinforcement learning, allowing for real-time decision-making in complex environments [Liang, 2023]. Additionally, the Vector Field Histogram algorithm has been enhanced with Apollonius circle concepts and information-sharing strategies to improve obstacle avoidance in UAS swarms. This approach allows for better navigation in environments with dynamic obstacles, ensuring that UAS can adapt their paths collaboratively [Fu, 2023]. For cooperative trajectory planning, a bilevel model has been proposed, addressing both task allocation and conflict avoidance. The upper level focuses on task sequencing, while the lower level assigns holding times to prevent potential conflicts, ensuring smooth operations in complex urban environments [Wang, 2021].

These advancements highlight the importance of integrating learning-based algorithms with cooperative strategies to manage the risks associated with multi-UAS operations. As drone swarms become more prevalent in various applications, such as surveillance, delivery, and environmental monitoring, robust collision avoidance and risk modeling techniques will be crucial for their safe and efficient deployment.

Possible future direction: Expansion to Other Operating Contexts
This section reviews DAA requirements across diverse operational environments to contextualize how detection timing models may eventually be applied. While the current study focuses on airborne detection timing for single sUAS in urban-like environments, future work could extend to ground-based DAA systems, UTM-integrated operations, large UAS with CNS risk modeling, and multi-vehicle swarm scenarios. These additions would broaden the applicability of the model to more complex and diverse operational settings.

2.2.10 Review of the MIT Lincoln Labs Encounter Simulation Software and Dataset

The MIT LL Terminal Airspace Encounter provides a robust foundation for validating the probabilistic detection delay model proposed in earlier sections. This section presents simulation results based on Monte Carlo analysis using these encounter trajectories, demonstrating how the abstract mathematical framework translates into practical risk assessment.

2.2.10.1 *Dataset and Simulation Overview*

The MIT-LL dataset contains one million encounter scenarios between two aircraft, where trajectory data includes position points, velocity, and orientation information sampled at regular intervals. Each encounter represents a potentially hazardous situation where aircraft come within close proximity. For this project's simulation purposes, researchers focused specifically on encounters with minimum separation distances below the maximum detection threshold but varying in terms of geometry, approach angles, and environmental conditions.

The simulation used a subset of these encounters, applying the detection delay distribution model to analyze when and if the DAA system would successfully detect an intruder aircraft. Rather than using deterministic detection times, the team modeled detection as a series of Bernoulli trials at each time step, where the probability of successful detection varies based on separation distance and environmental factors.

2.2.10.2 *Detection Probability Modeling*

For each encounter, the team implemented the detection probability function that incorporates the environmental factors outlined in detail in previous sections and the Appendix. This probability function determines the likelihood of detection at each time step based on the instantaneous separation distance between aircraft and the simulated environmental conditions.

The detection probability at any given time step is modeled as a function of the separation distance and relevant environmental factors. This function captures the fact that detection becomes less likely as the separation distance increases or as environmental conditions degrade.

2.2.10.3 *Implementation of Bernoulli Trials for Instantaneous Detection*

At each time step in the simulation, a Bernoulli trial determined whether detection occurred. This approach accurately represents the stochastic nature of real-world detection systems. The simulation recorded:

- The time step at which detection first occurred (if any);
- Whether detection happened before the NMAC threshold was reached;

- The separation distance at the time of detection.

For scenarios where detection never occurred during the trajectory, the outcome was recorded as a missed detection. The implementation included careful handling of the conditional probabilities, each trial being conditionally independent given the specific geometry and environmental conditions at that time step.

Figure 14 presents visualizations of four distinct aircraft encounter scenarios from the simulation. The trajectories show the ownship (blue) and intruder (red) paths in 3D space. Each plot illustrates different outcome types analyzed: successful detection without collision (top left), non-detection without collision (top right and bottom left), and non-detection resulting in collision (bottom right). Detection points are marked with a star, while collision points are marked with a cross.

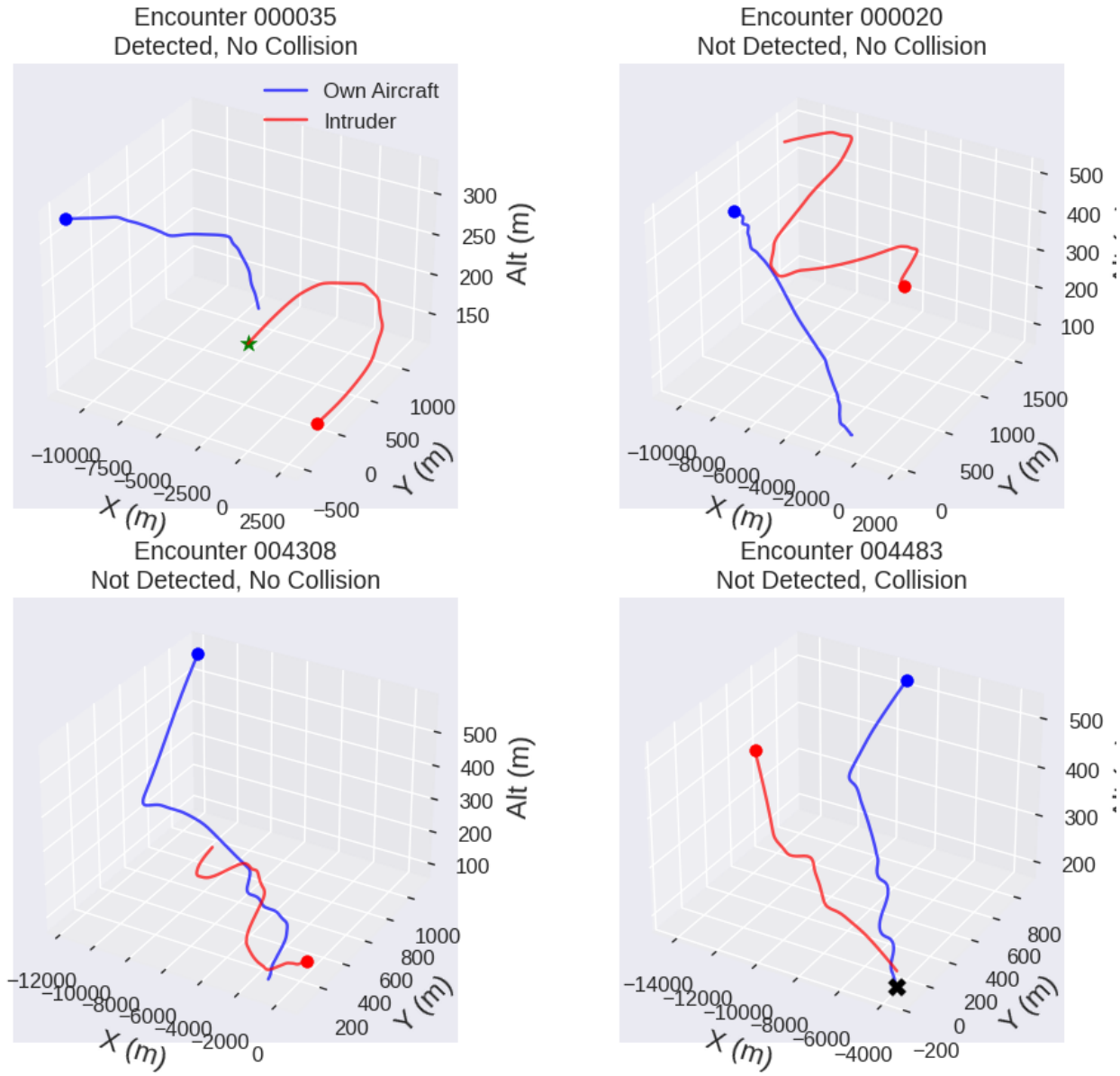

Figure 14. Visualization of four distinct aircraft encounter scenarios from simulation.

2.2.10.4 ***Detection Delay Distribution Analysis***

The analysis using the MIT-LL dataset revealed several important patterns regarding detection timing:

- *Detection Time Distributions:* The simulations generated empirical distributions of detection times based on the probabilistic model. These empirical distributions aligned with the characteristics predicted by the theoretical framework developed in Section 2.2.8, validating the PMF's applicability to realistic encounter scenarios.
- *Environmental Impact Quantification:* By running simulation sets with varying environmental parameters (*e.g.*, visibility levels), the analysis quantified the impact of these factors. As expected, adverse conditions like reduced visibility shifted the detection time distributions, indicating longer average detection delays and increased variance.
- *Geometry-Specific Effects:* The simulations analyzed how different encounter geometries (*e.g.*, head-on vs. overtaking) affected detection timing. Certain geometries correlated with significantly different detection time distributions, even for similar minimum separation distances, underscoring the need for geometry-aware risk assessment in DAA systems.

2.2.10.5 ***Probability of Detection before NMAC***

A crucial goal of the simulation effort was to investigate the relationship between the modeled detection time distribution and the probability of a NMAC. By analyzing whether the simulated DAA system detected the intruder before an NMAC occurred across numerous encounters, the study showed that:

- The likelihood of an NMAC is related to the parameters of the detection time distribution (*e.g.*, mean and variance). Shorter and more consistent detection times correlated with lower NMAC probabilities. That is, earlier average detection increases the likelihood that the intruder is identified before the ownship reaches the NMAC boundary, providing more opportunities for successful avoidance.
- Environmental factors influence NMAC probability indirectly through their impact on detection times. Degraded environmental conditions led to longer detection delays and consequently higher NMAC probabilities.

2.2.10.6 ***Anticipated Model Validation***

The simulation results derived from the MIT-LL dataset are intended to validate key theoretical aspects of the probabilistic detection model:

- *PMF Accuracy:* The analysis will compare the empirical distribution of detection times obtained from the simulations against the theoretical PMF derived in Section 2.2.8 (based on Appendix Equations 7-8). Statistical tests will be used to assess the goodness of fit and confirm the PMF's ability to represent detection timing.
- *Independence Assumption Validity:* While the theoretical model often assumes conditionally independent detection attempts between time steps, the simulations using realistic aircraft dynamics will help assess the practical validity of this approximation.

- *Environmental Factor Sensitivity:* The simulations are designed to quantify how modeled environmental factors influence the entire shape and key parameters (mean, variance) of the detection time distribution, going beyond simple mean-time effects.

Detailed quantitative results and specific findings from these simulations will be presented in subsequent sections, including the Gazebo simulation analysis (Section 2.2.12.1.1).

2.2.10.7 *Implications for Risk Assessment*

These simulation results translate directly to practical risk assessment approaches:

- *Risk quantification:* By simulating thousands of potential encounters under varying conditions, we can derive statistical measures of risk specific to operation types, environments, and DAA sensor configurations.
- *System requirements validation:* The results provide concrete data to validate whether a particular DAA system meets the timing requirements specified in standards like ASTM F3442/F3442M.
- *Operation-specific analysis:* Different operation types (BVLOS, urban air mobility, etc.) can be assessed by focusing on encounter geometry and environmental conditions most relevant to those operations.

The simulation results demonstrate that the probabilistic detection time approach offers significant advantages over deterministic models, particularly in capturing the inherent uncertainty in real-world detection scenarios and providing a more nuanced understanding of collision risk.

2.2.11 Gazebo Simulation Environment

To evaluate the practical implementation and performance of DAA timing distribution models in simulated environments, the research team transitioned from theoretical frameworks and datasets to simulation platforms that can replicate realistic conditions. This section highlights the tools and environments used to test DAA detection under variable conditions, with an emphasis on visual perception and environmental complexity.

2.2.11.1 *Simulation Setup*

This subsection outlines the simulation setup used to model and evaluate the DAA system. It describes the architecture, key software and hardware components, and the various modules integrated within the closed-loop environment.

The architecture of the simulation environment is a modular, closed-loop framework in which DAA algorithms are developed and integrated. It is flexible enough to support the investigation in various DAA scenarios, including the definition of the ownship type and mission, the flight conditions of one or more non-cooperative intruders, and environmental conditions, such as foggy or cloudy weather.

The main functional blocks of the environment and their interconnections are presented in Figure 15. The tool uses Matlab and Simulink, interfaced with Gazebo via Robot Operating System (ROS), to ensure maximum portability and flexibility. The simulation environment consists of the following main components:

- Graphical-interface Gazebo

- Communication module ROS
- Ownship/Intruder vehicle module
- DAA Control system module
- Guidance and navigation module
- Intruder GNSS module
- YOLO detection system

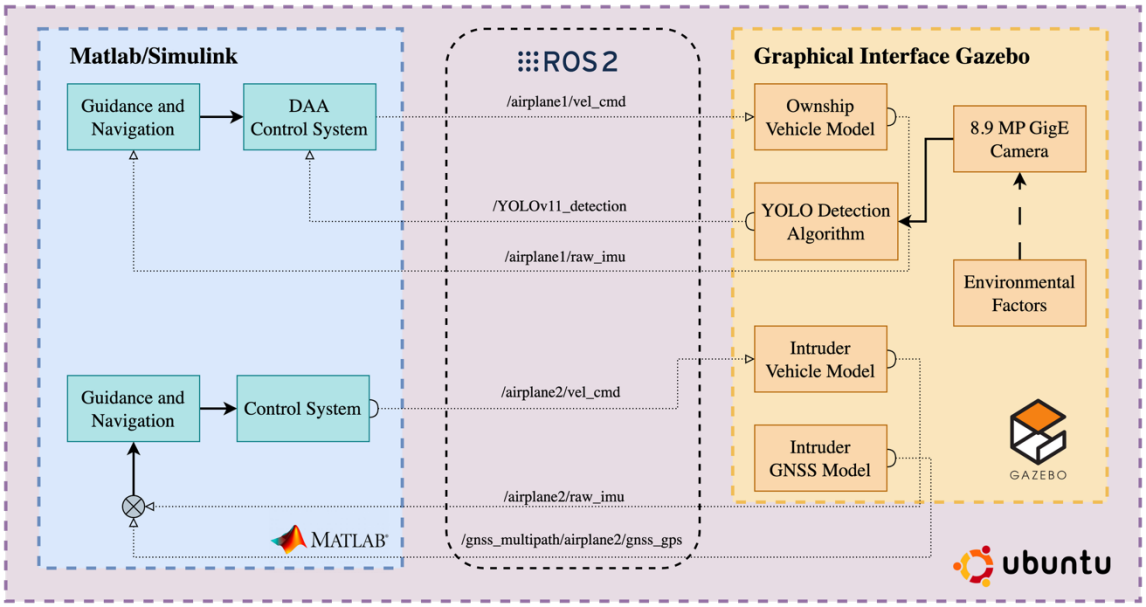

Figure 15. Simulation architecture.

2.2.11.1.1 Graphical-Interface Gazebo

The simulation environment includes the physical characteristics of the world and its interactions with the ownship and intruder aircraft. The default physics engine used by the Gazebo platform is Open Dynamic Engine and uses the rendering library Object-Oriented Graphics Rendering Engine for a 3D visualization of objects and scenes. An example of a map visualized in Gazebo is presented in Figure 16. The map recreates a 1.8 km x 2.6 km area around the Hanscom Air Force Base and includes different types of obstacles such as buildings, roads, vegetation, and disturbances such as different weather conditions.

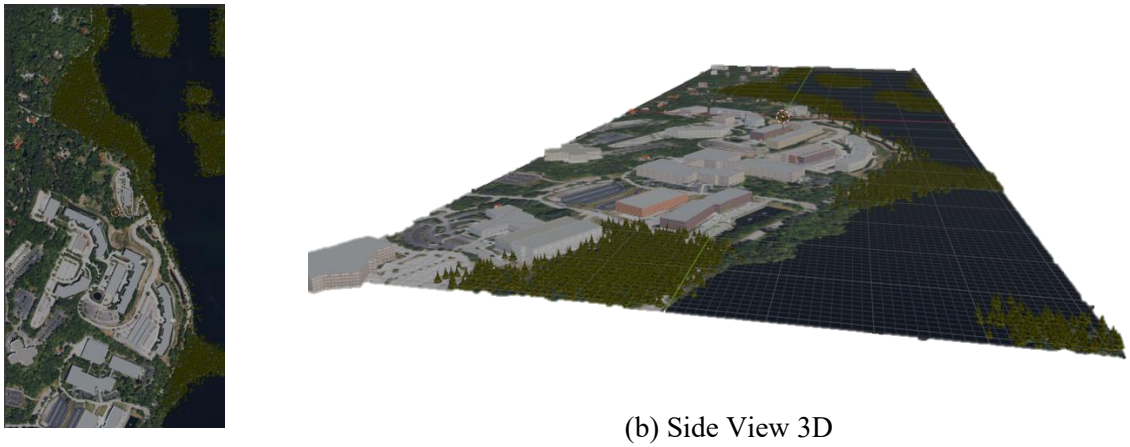

a) Top View

(b) Side View 3D

Figure 16. Simulation environment. example world.

2.2.11.1.2 Communication Module ROS

The ROS computation graph (seen in Figure 17) illustrates a closed-loop simulation of the ownship and the intruder operating within the Gazebo environment described in Figure 15. Sensor data, including IMU outputs, GNSS positions, velocities, and camera images, are published to various topics. A centralized path-following controller node (/One_Airplane_Path_Follower_81473) receives IMU outputs from the intruder (/imu_2/out), camera images (/camera_combination), GNSS position and velocity from the intruder (/gnss_multipath/airplane2/gnss_gps, /gnss_multipath/airplane2/gps_vel) and odometry data from the ownship (/airplane_1/odom, /airplane_2/odom) to the Matlab/Simulink controllers to compute velocity commands for both airplanes. These commands are then sent back through the /cmd_vel topics, completing the control loop. Each airplane publishes its odometry, which are used both for navigation and to broadcast transforms (/tf), allowing all nodes to maintain a coherent understanding of spatial positions and orientations.

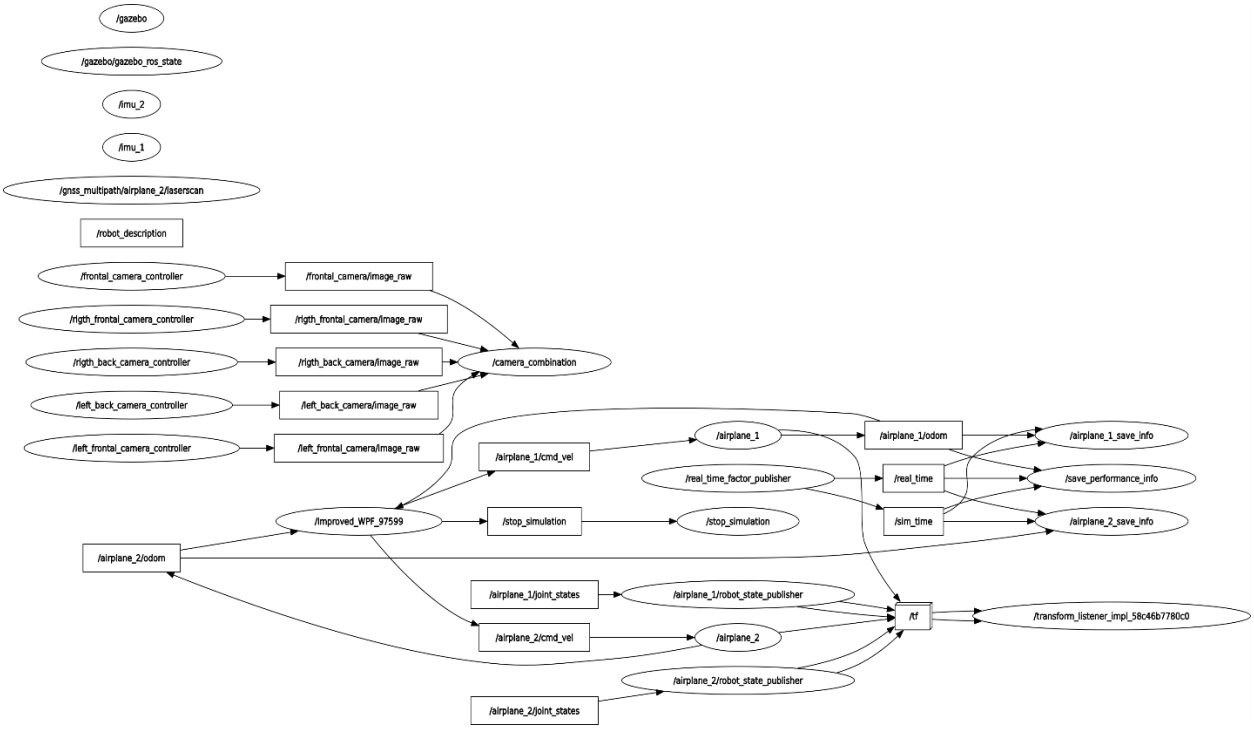

Figure 17. Simulation environment ROS network.

2.2.11.1.3 Ownship/Intruder Vehicle Modules

Both aircraft models are implemented in Matlab/Simulink. At this stage, they are represented using an autopilot-based kinematic guidance framework within Simulink, which provides the commanded airspeed and velocity commands (cmd_vel) to the Gazebo simulation environment. This approach reduces the model complexity by eliminating the force and moment equations, focusing only on the kinematic behavior of the aircraft. This model assumes a coordinated turn with zero sideslip, where the states of the UAS are: UAS ground speed V_g, roll ϕ, flight path angle γ, course χ, airspeed V_a, altitude h, north position p_n, East position p_e, and roll speed $\dot{\phi}$. Wind effects are added in a simplified version inside the position kinematics using its velocity components: North wind speed w_n, East wind speed w_e , and Down wind speed w_d. Finally, the autopilot responsible for coordinated turns regulates the UAS's airspeed, altitude, and heading using commanded inputs: airspeed V_{a_c} , course χ_c, and roll ϕ.

$$\dot{\vec{x}} = \begin{bmatrix} \dot{p}_n \\ \dot{p}_e \\ \dot{h} \\ \dot{\chi} \\ \dot{\gamma} \\ \dot{V}_a \\ \dot{\phi} \\ \ddot{\phi} \end{bmatrix} = \begin{bmatrix} V_g \cos\chi \cos\gamma + w_n \\ V_g \sin\chi \cos\gamma + w_e \\ V_g \sin\gamma - w_d \\ \frac{g\cos(\chi-\psi)}{V_g} \tan\phi \\ k_\gamma(\gamma_c - \gamma) \\ k_{V_a}(V_{a_c} - V_a) \\ k_{p_\phi}(\phi_c - \phi) \\ k_{p_\phi}(\phi_c - \phi) - k_{d_\phi}(-\dot{\phi}) \end{bmatrix}$$

The commands of the model are calculated using the Fixed-wing Waypoint Follower from Matlab UAS Toolbox. It computes the commanded heading and altitude using a reference point located at a user fixed distance (L), from the UAS's current position to the Path defined by the set of waypoints.

Within Gazebo, the aircraft is modeled as a Cessna 172 (see Figure 18) equipped with an integrated IMU sensor that supplies raw inertial data (raw_imu) to the guidance and navigation system. The objective is to simulate any vehicle model within Simulink and transmit the resulting force vectors and velocity components to Gazebo. This approach allows leveraging Gazebo's realistic sensor models, environmental dynamics, interactions with external objects, visual detection, and configurable disturbances.

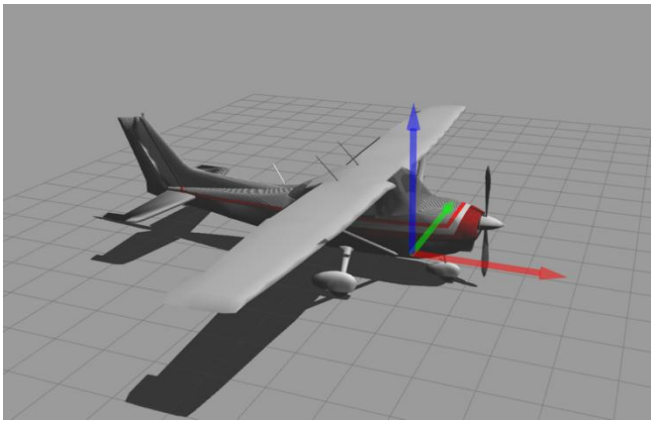

Figure 18. Gazebo Cessna 172 Physical Model.

2.2.11.1.4 DAA Control System Module

The DAA control system is a geometric avoidance algorithm that classifies obstacles and performs small avoidance maneuvers to reduce the deviation from the original course. The algorithm works by deciding if an obstacle is a threat using the airplane collision cones. The airplane speed needs to be constant to make the controller work [Lin, 2018].

First, the smallest safe radius (d_m) needs to be defined for each obstacle, that is, an area where the UAS cannot enter. This value is affected by the obstacle velocity (d_{mv}), vehicle velocity (d_{mi}), vehicle dimensions (d_{ma}), and airspace limitation (d_{lim}). The constants are decided by mission constraints:

$$d_m = k_1 d_{mv} + k_2 d_{mu} + k_3 d_{ma} + k_4 d_{lim}$$

Then, the minimum future distance is calculated using the relative velocity($\overrightarrow{v_{rel}}$), relative position ($\overrightarrow{r_{rel}}$) between the vehicle and all the obstacles, and the angle between the relative components(θ_{to}). In case the distance is lower than the safe radius, the obstacle is defined as a threat.

$$r_{min} = |\overrightarrow{r_{rel}}| \sin(\theta_{to})$$

If there are multiple obstacles, the algorithm checks if any of the other obstacles overlap inside the collision vehicle cone. If there is at least one, it would combine the minimum distance of all the

implicated obstacles, generating a new collision cone with its own relative distance, minimum safe distance, and relative velocity [Lin, 2018].

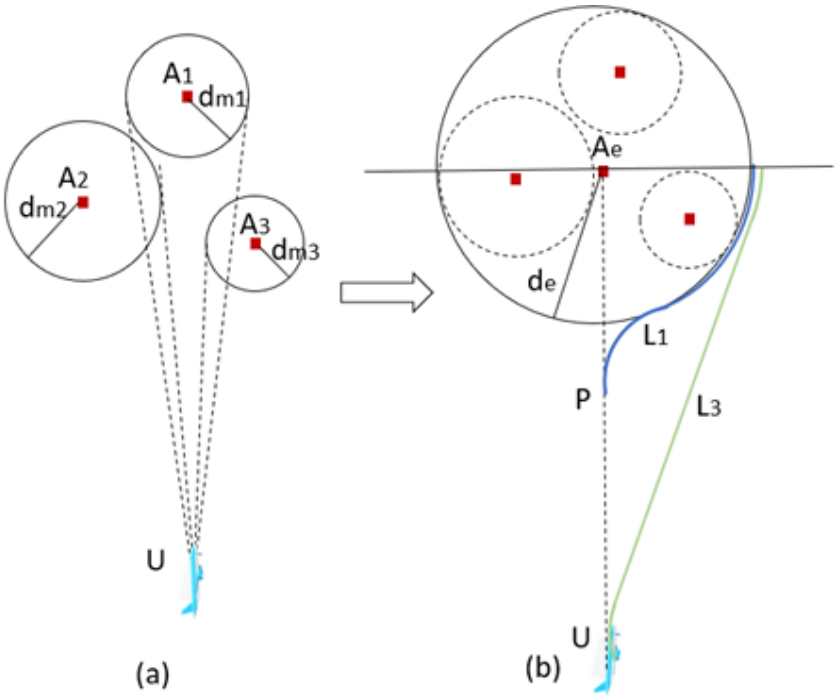

Figure 19. Multiple obstacle avoidance in case of overlap [Pant, 2022].

The avoidance maneuver starts when the critical time (t_c) is lower than a specified limit. The critical time is the remaining time the vehicle must avoid the obstacle, considering its minimum turn radius (ρ_{min}), and the obstacle safe radius.

$$t_c = \frac{|\overrightarrow{r_{rel}}| \cos(\theta_{to}) - \rho_{min} - (d_m - |\overrightarrow{r_{rel}}| \sin(\theta_{to}))}{|\overrightarrow{v_{rel}}|}$$

The minimum cost obtained stands for the best track, and the cost coefficients (η_1 and η_2) can change depending on the vehicle position, velocity or trajectory.

$$cost = \eta_1 |\psi_{com} - \psi_o| + \eta_2 |\gamma_{com} - \gamma_o|$$

The weights (η_1 and η_2) in the cost function in case there are moving obstacles are going to change, so the trajectory is generated in the sphere region that is opposite to the obstacle movement. The weights are calculated with an inverse equation proportional to the angle between the velocity of the obstacle and the position of the evection points on the sphere, α. Therefore, the trajectory with the lowest cost will be at a higher angle with respect to the obstacle's future position. Additionally, the constant k_1 is increased in case of altitude avoidance since it is not the most suitable option.

$$\eta_1 = \frac{1}{\alpha + 0.5}$$

$$\eta_2 = \frac{1}{\alpha + 0.5} + k_1$$

Finally, the return to the principal course is done by calculating the nearest waypoint after the avoidance and continuing the track from that point.

2.2.11.1.5 Intruder GNSS Module

An GNSS model is also implemented in Gazebo using an open-source GNSS multipath emulation plugin presented in [Pant, 2022]. The plugin simulates the multipath signal reflections using two lidar-based sensor rays generated from the UAS, one ray connects the UAS with the satellite, while the other is launched in the perpendicular opposite direction to check for reflection surfaces.

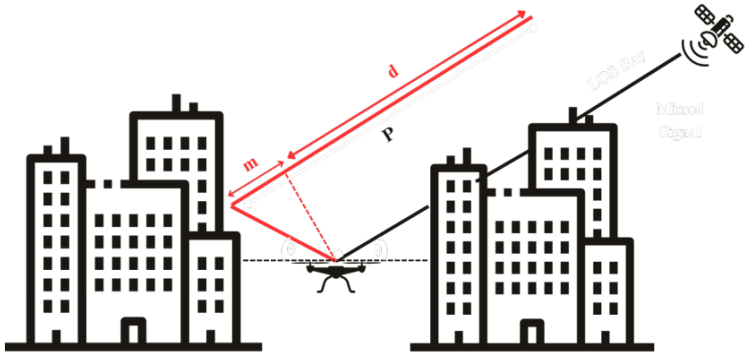

Figure 20. Multipath reflection in urban zones [Pant, 2022].

If the second deployed ray detects a reflection, the satellite is considered to have an obstruction of the line of sight, and a multipath offset (m) is added to the pseudorange (P) between the UAS and the satellite. The multipath offset is the added distance when the GPS signals are reflected by nearby surfaces before the receiver detects the satellite signal. The modeled plugin uses only single reflection, as additional reflections have a negligible impact on the multipath offset [Ray, 1999]. It also reduces the complexity of the Gazebo buildings, assuming a normal 900 reflection with the structure. These assumptions did not affect the performance of the detection, as the plugin showed a similar estimation to the one from real GPS data. The plugin estimates the receiver's position using the Least Squares method over all the pseudoranges equation of the visible satellites. Since the plugin models a precise GPS in the urban area, a satellite is considered visible by the plugin if its multipath offset is less than 100 (m). The pseudoranges for each visible satellite Pi where i represents the number of the satellite is composed by: actual range (ρ_i), the multipath offset (m_i), a time offset ($c_0\Delta t$), and a white noise (e_i) with a standard deviation of 10.

$$P_i = \rho_i + m_i + c_0\Delta t + e_i$$

The pseudorange values are related to the pseudoranges equation where the visible satellite position is defined as $\vec{x}_i = [x_i, y_i, z_i]$, the receiver's states are $\vec{x} = [x, y, z, c_0\Delta t]$, and n is the number of visible satellites.

$$\begin{bmatrix} P_1 \\ P_2 \\ P_3 \\ \vdots \\ P_n \end{bmatrix} = \begin{bmatrix} \sqrt{(x_1 - x)^2 + (y_1 - y)^2 + (z_1 - z)^2} + c_0\Delta t \\ \sqrt{(x_2 - x)^2 + (y_2 - y)^2 + (z_2 - z)^2} + c_0\Delta t \\ \sqrt{(x_3 - x)^2 + (y_3 - y)^2 + (z_3 - z)^2} + c_0\Delta t \\ \vdots \\ \sqrt{(x_n - x)^2 + (y_n - y)^2 + (z_n - z)^2} + c_0\Delta t \end{bmatrix}$$

Then, the least squares method is used to estimate the receiver's position by reducing $\Delta\vec{x}$ from the equation:

$$\Delta\vec{P} = H\Delta\vec{x} + \vec{e}$$

Where $H \in R^{n\times 4}$ is the negative Jacobian obtained from the pseudorange equations. Then, the receiver's position $\hat{x}$ is estimated using the least squares method. This iterative process will stop when convergence is achieved or when the number of iterations reaches a predefined maximum.

$$\Delta\vec{x} = (A^T A)^{-1} A^T \Delta\vec{P}$$

2.2.11.1.6 YOLO Intruder Detection Algorithm

The YOLO vision-based detection algorithm, originally introduced by Joseph Redmon et al. [Redmon, 2016], enables real-time object detection by predicting bounding boxes and class probabilities directly from full images in one evaluation using a single neural network, drastically reducing the computation time. The detection network combines convolutional and connected layers, converting a high-resolution image into a series of feature maps that capture edges, patterns, shapes, etc., at multiple scales. The final layer predicts both class probabilities and bounding box coordinates (x,y,w,h, and confidence). This work uses the newer YOLOv11 model and its versions, since they are the most enhanced ones.

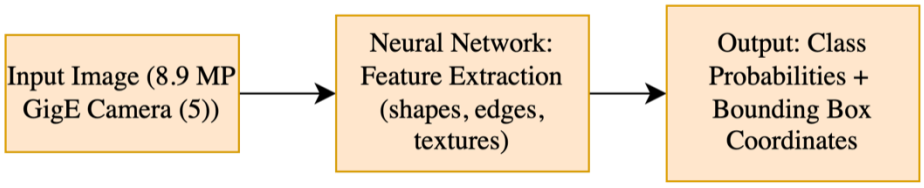

Figure 21. YOLO schematic architecture.

The five cameras used in the Gazebo simulation for the YOLO detection algorithm are modeled after the 8.9 MP GigE cameras used in the uAvionix's Casia X collision avoidance system. They are placed around the aircraft as follows: front, front-right, front-left, rear-right, rear-left. Each camera provides an 80-degree horizontal field of regard, resulting in a combined 360-degree horizontal coverage with an overlap of 40 degrees between adjacent cameras. The vertical field of view is 50 degrees. These cameras operate in Visual Meteorological Conditions, from 30 minutes after sunrise to 30 minutes before sunset, regardless of cloud coverage. Detailed camera specifications are shown in Table 3.

Table 3. 8.9 MP GigE camera specifications.

Input Voltage	Power	Mass	External Dimensions	Operating Temperature
802.3at PoE	2.5W Nominal 3W Peak	Camera ~180g Camera Cambles (1m) ~60g	60mm (W) x 60mm (L) x 105mm (D)	0ºC to 60ºC

2.2.11.2 ***Simulation Scenarios***

This subsection outlines the simulation scenarios used to evaluate DAA system performance under realistic operating conditions. Key elements include the selection and filtering of trajectory data and the implementation of varied environmental conditions such as clutter, fog, and image noise.

Testing DAA systems in realistic scenarios could represent a problem, as there are an infinite number of scenarios that two or more UAS can generate. Therefore, real trajectory data needs to be collected to realistically represent the collision risk involved in the DAA maneuvers done in terminal airspace. The Unmanned Aircraft Terminal Area Encounters dataset developed by MIT Lincon Labs provides up to one million simulated encounters designed specifically for safety assessments of DAA systems. Their main objective is to evaluate the effectiveness of the avoidance system under critical phases of the flight, such as the ones in Class D airspace (takeoff and landing) [MIT Lincoln Laboratory, 2025].

Gazebo is a simulation software with the capabilities to simulate environmental conditions (fog, clouds, and light sources), sensors (IMU, GNSS, Cameras, Lidar, or others), and their interaction between 3D models (forces, ray reflections, and collision). One of the main limitations of realistic simulations as those done in Gazebo, is the computational time, which most of the time matches the real-time durations. Simulating the one million encounters from MIT is not optimal, as it would take a computer approximately four years to finish all the trajectories once. Additionally, using a vision-based detection system like YOLO to generate detection data throughout the complete trajectory is inefficient, too, given that an intruder is outside the field of view of the camera over most of the trajectory. Consequently, CPA zones inside the encounters are the perfect place to generate detection data. Inside these zones, YOLO constantly generates detection data, the critical segments of each trajectory are represented, and the computational time is reduced, enabling the production of more simulations under a variety of visual conditions.

Still, not all the CPA zones are equally effective at applying the YOLO detection system and generating detection data. In past simulations, YOLO models showed limitations in how far they can reliably detect an intruder with a minimum detection threshold. This threshold can be modified depending on the situation, but for zones with large amounts of clutter (cities), it is preferable to increase the minimal threshold (≥ 0.55), reducing the false positive percentage. On the other hand, range limitations constrain the CPA zones to fall within the model's effective detection range. The following table summarizes the average maximum distance with processing time each YOLO model can reliably detect the intruder.

Table 4. Maximum intruder detection distance for YOLO models with average processing time for visual ideal conditions.

YOLO Model	Yolo11n	Yolo11s	Yolo11m	Yolo11l	Yolo11x
Ave. Maximum Distance (ft)	919	1300	1360	1364	1374
Ave. Preprocessing time (ms)	2.4	3.75	5.91	6.4	10.5
Ave. Inference time (ms)	5.51	7.76	16.08	21.21	36.72
Ave. Postprocessing time (ms)	1.3	1.18	1.23	0.78	0.83

The results show that higher detection models than the simplest *Yolo11n* converge to a maximum detection distance of approximately 1360 ft under ideal conditions (without fog, empty world, and a clear camera image). However, the average processing time for all the models increases significantly without a proportional increase in the detection range. Therefore, for simulation purposes, *Yolo11m* is shown to be the ideal model that balances high detection speeds, maintaining the limit in the detection range.

Based on the results, the MIT encounters need to be filtered to identify those with a CPA inside the recognition limits of Yolo11m. To summarize all the CPA zones inside the encounters, MIT *Unmanned Aircraft Terminal Area Encounters* dataset includes an encounter information file ("terminal_encounter_info_20200630.csv"), that summarizes the CPA flighting condition of each encounter, including the time, position, orientation, and flight phase of both the own-ship and the intruder [MIT Lincoln Laboratory, 2025]. This is the main file used to filter and select encounters with a suitable CPA of 1500 ft or less. Although the threshold value is higher than the average maximum detection range of *Yolo11m*, it increases the number of filtered tracks from 69801 to 78404 and generates a margin that accounts for the variability in the field of view without being too far from the detection limits.

As an open-source multi-robot simulator that uses ROS, Gazebo benefits from having a growing community that is constantly developing and updating plugins. Consequently, the simulation realism is improved every year, by updating the modeling of sensors, environmental conditions, robot actuators, external disturbances, and complex mechanisms presented in dynamical systems [Koeing, 2004]. Specifically, Gazebo can modify the vision characteristics like visual clutter, fog, and noise in the images to see the effect during the detection.

2.2.11.2.1 Clutter Scenarios

To begin with the visual characteristics, since the encounters are performed at low altitudes within Class D airspace, visual clutter in Gazebo is applied by changing the simulation environment. This characteristic affects the background complexity by obstructing and increasing the number of objects YOLO must process to identify the intruder. Inside the simulation, Gazebo supports any environment type if it contains at least a 3D model that represents it in a STL or COLLADA format. An easy way to obtain background information of locations from the real-world is to use the OpenStreetMap (OSM) database. It provides a compilation of geographical and location features

including buildings, roads, rivers, parks, vegetation and terrain [OpenStreetMap, 2017]. The BLOSM plugin in Blender is then used to generate a detailed 3D model of the environment, that presents all the characteristics specified on the OSM file [vvoovv, 2025]. For the simulations of DAA scenarios, different environments have been integrating into the Gazebo simulator. These environments include deserts, mountainous terrain, major cities (New York), forests, and the surroundings of Hanscom Air Force Base used for the MIT encounters set.

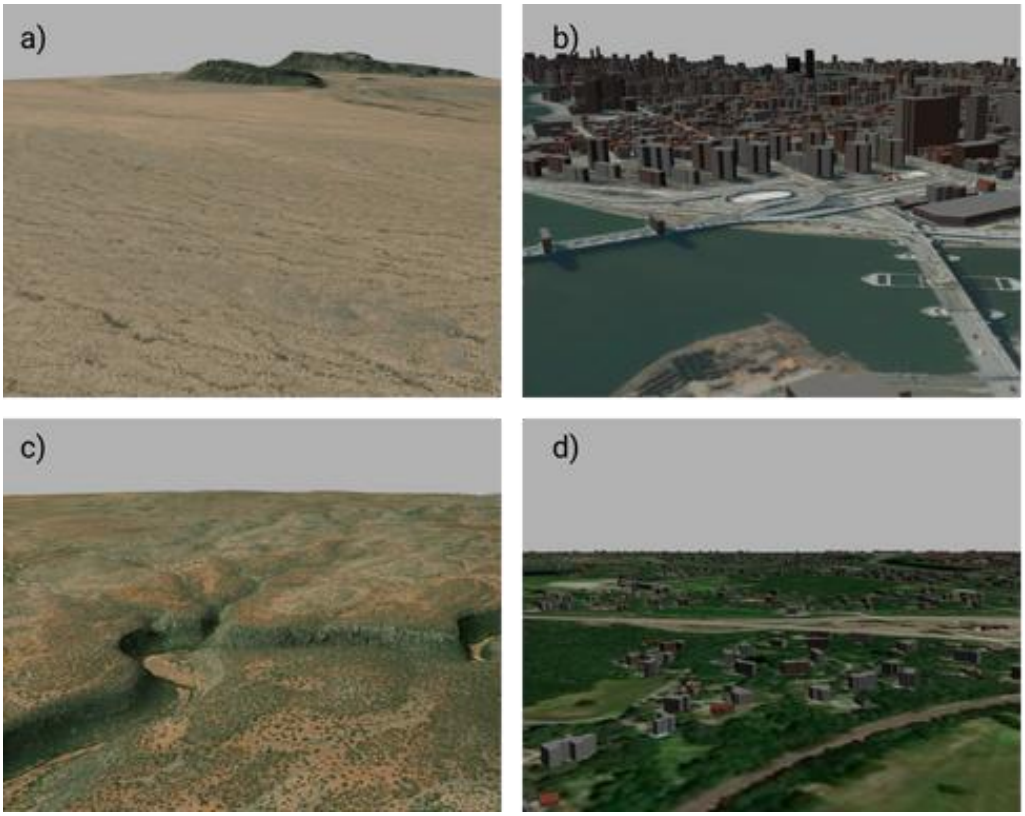

Figure 22. Real-world environments simulated in Gazebo.

The simulated environments are: (a) Sonoran Desert, (b) Times Square, (c) Rocky Mountains, and (d) Hanscom Air Force Base.

2.2.11.2.2 Environmental Conditions Simulation: Fog Scenarios

Secondly, fog is another characteristic in Gazebo that directly affects intruder detection by reducing the visibility coefficient (α) of objects inside the field of view depending on the distance (z) from the staring viewpoint. Gazebo already has installed two attenuation models that simulate fog. The first is a linear model, where visibility decreases between an initial distance (start) and a final distance (end), after which all the objects inside the simulation are completely covered by fog [OGRE Team, 2025].

$$Linear\ Fog\colon \alpha(z) = \frac{(z - start)}{(end - start)}$$

On the other hand, exponential fog is the second model, a more realistic representation of real fog in Gazebo. It exponentially decreases α depending on the distance and density (ρ) responsible for controlling how the fog intensifies [OGRE Team, 2025].

$$Exponential\ Fog\colon \alpha(z) = e^{-\rho z}$$

During the detection simulations, three levels of exponential fog were analyzed and compared against the no-fog ideal condition using the filtered CPA MIT encounters with the Hanscom Air Force Base as environment. The three levels of fog are characterized by a density being minimum fog (ρ =0.001), medium fog (ρ =0.005), and high fog (ρ =0.01).

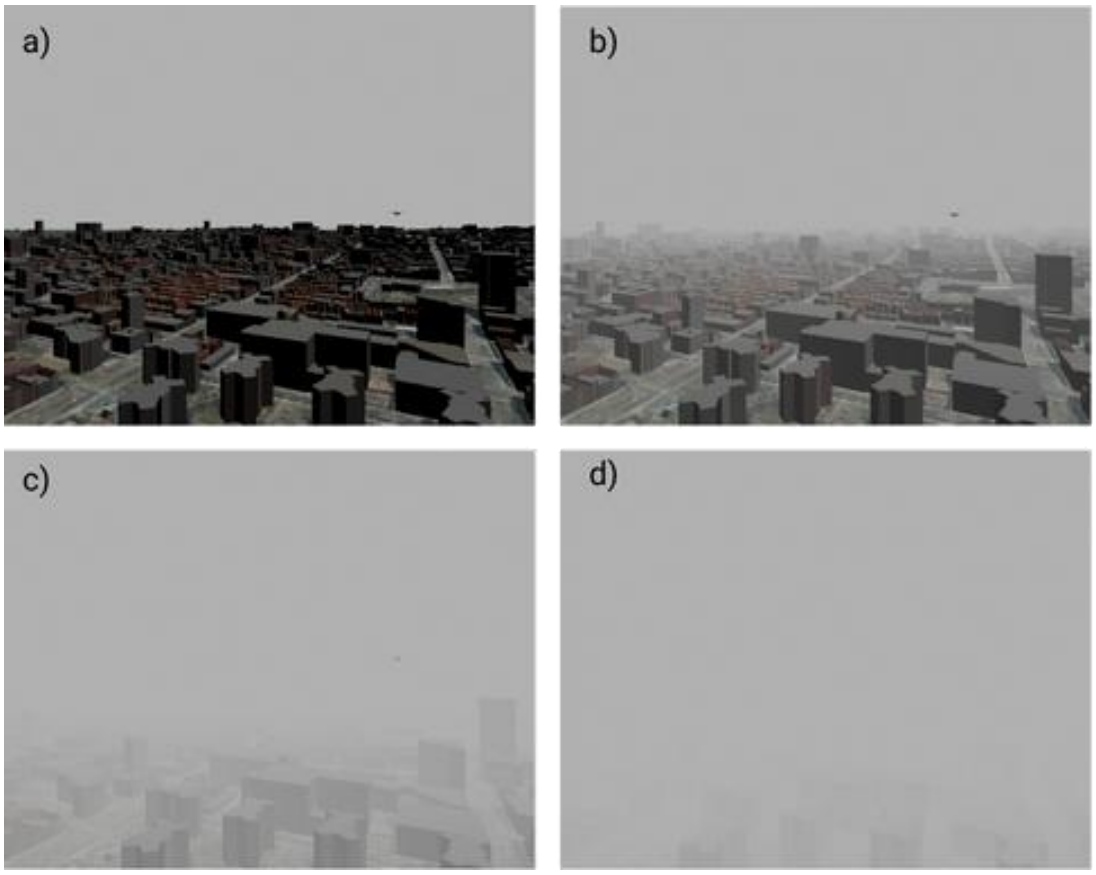

Figure 23. Fog levels applied in a New York City environment in Gazebo.

In Figure 23, (a) No fog, (b) Minimum fog, (c) Medium fog, and (d) High fog illustrate the progressive reduction in visibility used during detection simulations.

2.2.11.2.3 Camera Noise

Lastly, camera noise is another visual characteristic in the simulations, which focuses on simulating real camera noise, temperature image distortions, low-light graininess, and communication errors. The main purpose of this distribution is to test the robustness of detection algorithms like YOLO, under abrupt and random frame modifications that lead to a higher false detection rate and loss of sight of the intruder trajectory. For Gazebo, the noise is presented as a normalized Gaussian distribution added to each color channel (Red, Green, and Blue) of every

pixel of the image. This value needs to be translated to the 8-bit intensity representation range from 0 to 255 to move inside the Gazebo nodes [Open Source Robotics Foundation, 2025]. Figure 24 presents some examples of how noise affects image resolution at different levels.

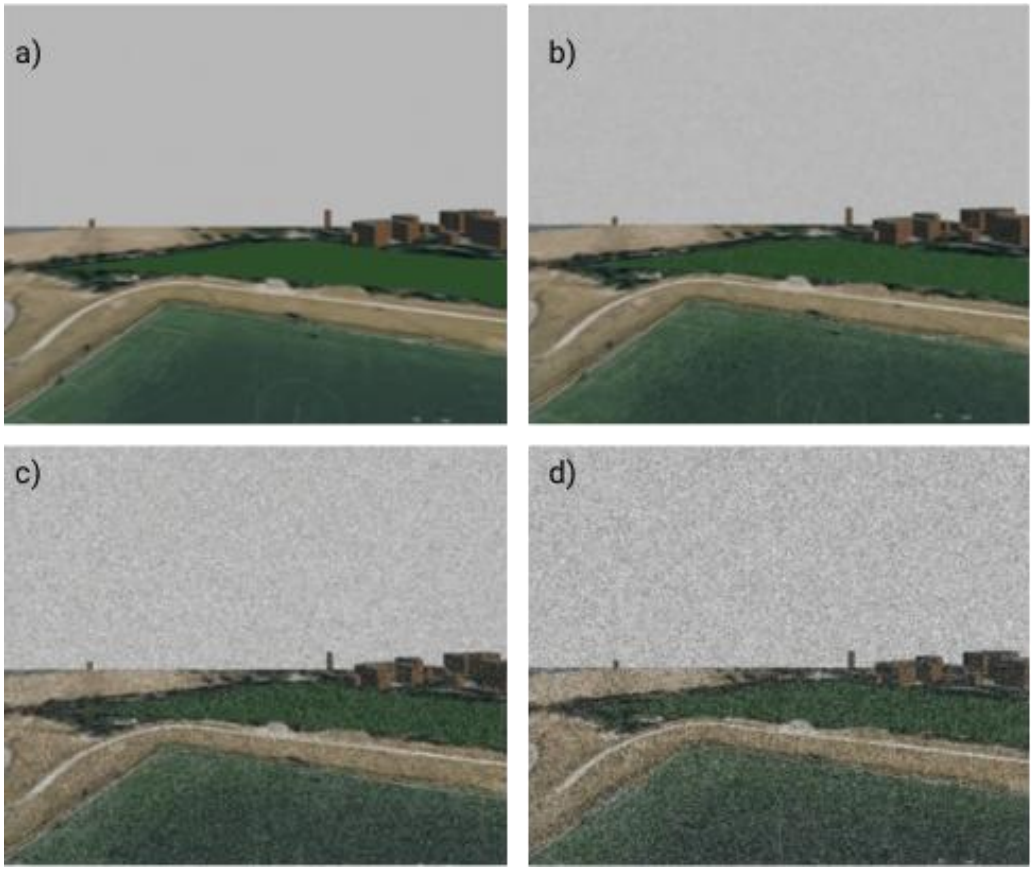

Figure 24. Levels of noise in images.

In Figure 24, (a) No noise, (b) Low noise (std = 0.005), (c) Medium noise (std = 0.05), and (d) High noise (std = 0.1) show the visual impact of increasing image noise on detection performance.

2.2.11.3 ***Detection Time Distribution Results***

YOLO's computational efficiency is commonly measured using the execution time of its three phases: preprocessing, inference, and postprocessing. Preprocessing time refers to the time it takes to resize the image, normalize the pixels, and augment the data, so it is ready to be processed. Inference time relates to the velocity of the system to process the data and determine the predictions; it is determinant in real-life applications as it is the longest and most important step during the detection. Postprocessing time corresponds to the refinement of the detection by applying a non-maximum suppression to reduce redundant solutions, and detection thresholds that eliminate lower confidence predictions [Redmon, 2018]. During the MIT CPA simulations, the detection process is affected due to the diverse environmental disturbances. Consequently, analyzing the detection time is important to evaluate the performance of YOLO during an avoidance maneuver. The actual analysis is done using the preliminary results that detected the intruder from the 7500 CPA tracks in the Hanscom Air Force Base at different levels of fog.

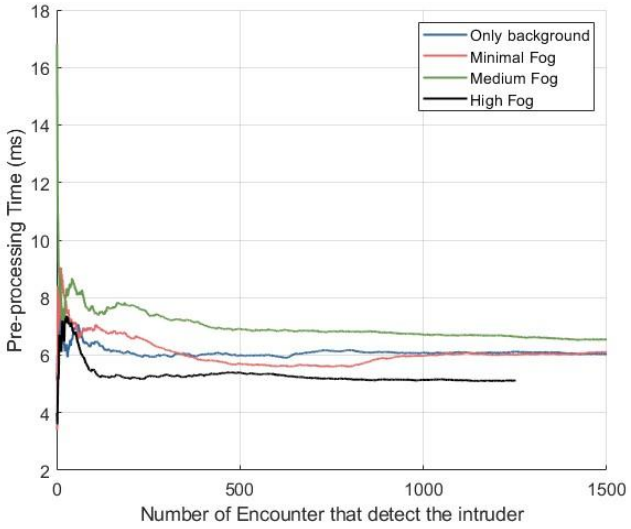

Figure 25. Average preprocessing time of MIT CPA filtered encounters detecting the intruder.

The average preprocessing time shows that at higher fog levels of fog the process to prepare the image is faster as majority of the objects are completely covered by fog. Therefore, high levels of fog make a fast-preprocessing process.

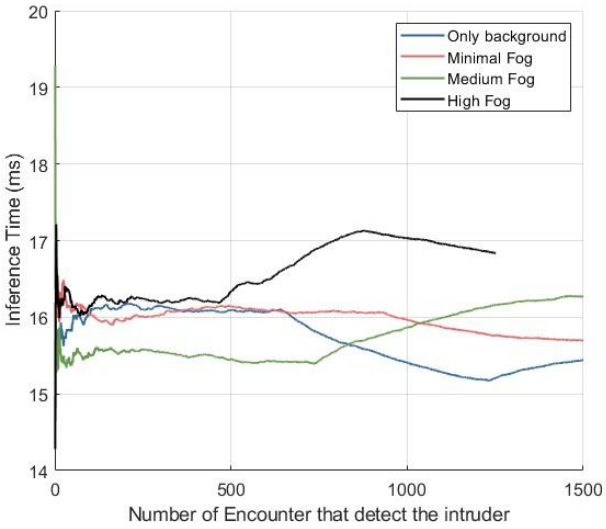

Figure 26. Average inference time of the MIT CPA filtered encounters detecting the intruder.

For the inference time, this trend is reversed, as the inference is slower when images are not sufficiently prepared.

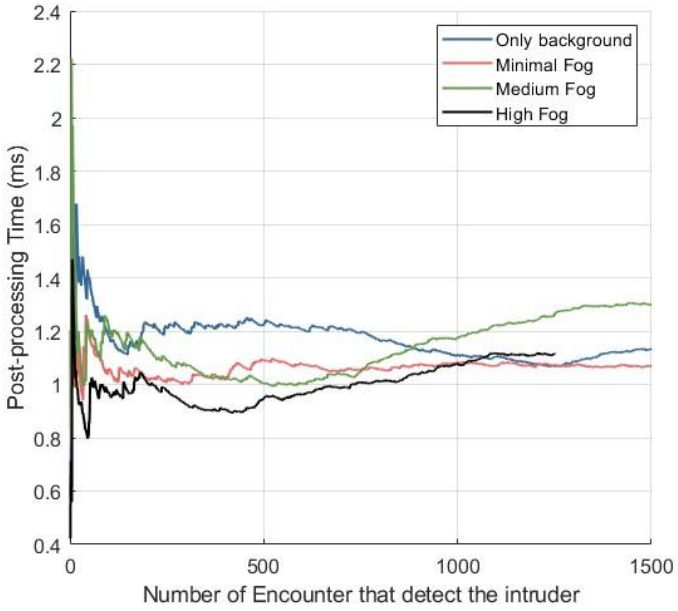

Figure 27. Average postprocessing time of MIT CPA filtered encounters detecting the intruder.

Finally, post-processing time is related to the number of objects the detection algorithm detects in the image, so having medium to lower levels of fog increases the time YOLO needs to eliminate possible false positives coming from the image. A summary of the detection times is presented in Table 5.

Table 5. Average processing times of YOLO over the CPA MIT filtered encounters at different levels of fog.

Fog Level	**Average Preprocessing time (ms)**	**Average Inference time (ms)**	**Average Postprocessing time (ms)**
Only Background	6.04	15.43	1.13
Minimal Fog	6.02	15.7	1.07
Medium Fog	6.54	16.27	1.03
High Fog	5.12	16.84	1.11

Overall, the complete detection of intruder with YOLO at different fog levels is around 22.79 (ms) using the intermediate detection model *Yolo*. This small value occurs as YOLO is constrained to only search for shapes like the intruder, so other shapes defined in the memory in the algorithm are excluded, improving the detection rate and making possible the real-world implementation of the algorithm in DAA strategies.

2.2.11.4 ***Environmental Factor Validation***

First, each environmental factor is being tested by itself to see the direct effects on the YOLO detection system. Consequently, a small batch composed of the first 100 MIT encounters is tested

in an empty Gazebo world (no visual clutter) with different visibility conditions. These conditions range from changing the environment, levels of fog, and camera noise. Clutter is the first environmental factor to be tested alone.

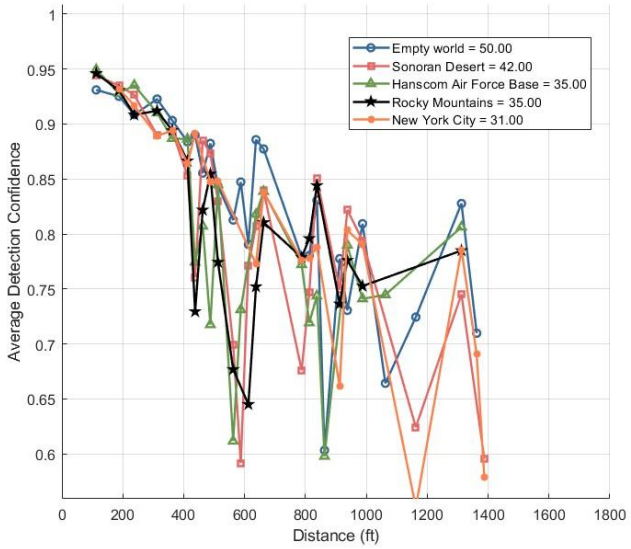

Figure 28. Average detection confidence of the first 100 filtered encounters over different clutter conditions.

The detections made in different clutter conditions show how intruder detection is easier at low clutter conditions like desert or the empty world, but harder in urban areas (Hanscom Air Force Base and New York), where the number of visible disturbances like buildings, roads, or vegetation increases. On the other hand, lower detection in the Rocky Mountains is caused by the unaltered encounters, which can make the intruder hide or crash against a mountain. Overall, the detection trend seems to be similar for all the different clutters, as their effect is to distract the detection system without modifying the image clarity. Next, fog is the only factor analyzed.

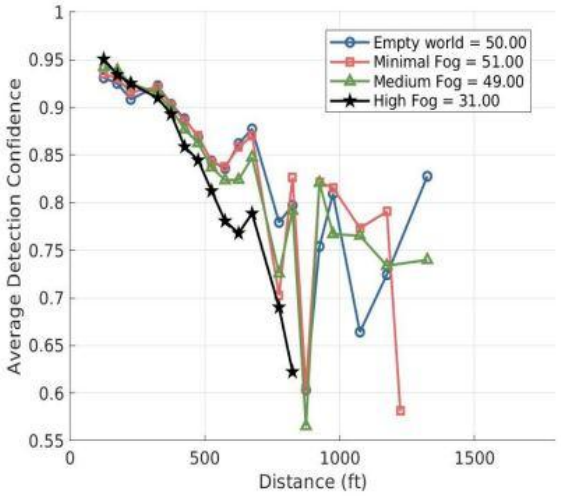

Figure 29. Average detection confidence of the first 100 filtered encounters over different fog conditions.

The fog trend mainly illustrates that, in case fog is the only environmental factor added, the average detection confidence would decrease as the fog density increases. At a low or medium level of fog the detection of the intruder is still possible, but this is not guaranteed under the influence of a heavier fog. The last environmental factor to be tested alone is the camera noise.

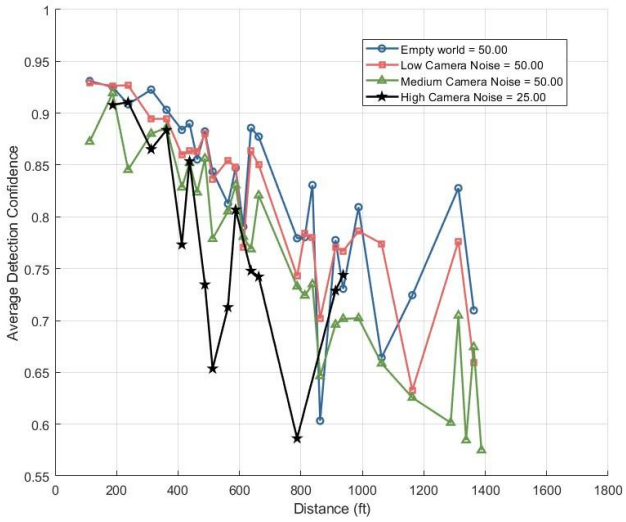

Figure 30. Average detection confidence of the first 100 filtered encounters over different camera noise levels.

The camera noise has a random effect on the detection of the intruder, as with low and medium noise, the number of detections is stable, but the detection confidence itself has a disturbance. This effect is amplified for high levels of noise, where the detection is not assured even at low separation. When combined with other environmental disturbances principally clutter, camera noise becomes critical, as it affects the performance of the DAA controller by increasing the number of false positives and randomly missing the intruder position.

Now, 7500 filtered CPA MIT encounters have been processed as preliminary results to show how combining two or more environmental factors affects the detection precision. These initial results focus on the addition of three levels of fog (minimal, medium, and high) in a fixed Hanscom Air Force Base clutter. The combination of clutter with other visual disturbances can increase the number of false positives to the point that the defined minimal threshold is insufficient to eliminate them all. Therefore, the preliminary results must be filtered to generate a proper analysis and comparison of false positives across different environmental factors. The filter identifies if the intruder position vector comes from the intruder passing through the field of view of the ownship cameras. In case the intruder passes, it also checks whether the intruder is detected by the field of view of the respective camera. Consequently, a false detection is identified if either the position vector avoids the field of view of all the cameras or the specific camera that should have detected. A quick example of how the filter works is presented in Figure 31.

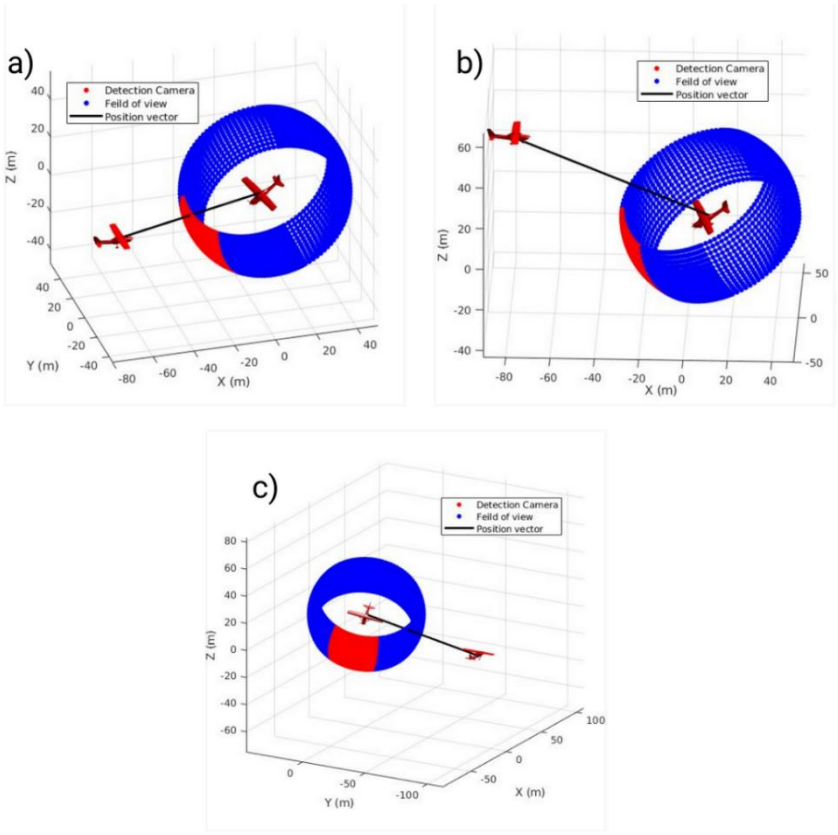

Figure 31. False positive detection using the filter in the three different scenarios.

In (a), the detection is real as the position vector passes through the corresponding detection camera. In (b), the filter finds a false positive as the position vector does not pass through the field of view of the camera. In (c), the filter identifies a false positive because the detection camera does not match with the camera defined from the coordinates of the airplanes.

The principal characteristic that affects intruder detection is the distance between the own ship and the intruder, as it affects the size of the intruder in the image. Figure 32 shows the detection

confidence distribution of the preliminary simulations where only the background of the Hanscom Air Force Base is added.

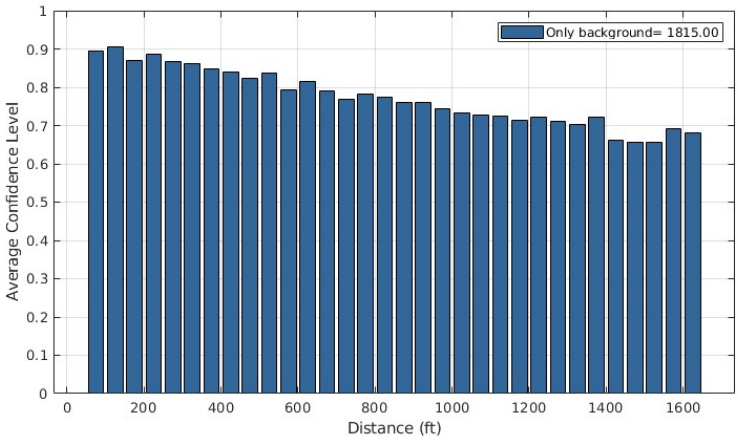

Figure 32. Preliminary results of the detection confidence distribution over the range only with the Hanscom Air Force Base.

The figure demonstrates that from the filtered 7500 CPA encounters, the detection model only detected the intruder successfully in 1815 encounters, in addition to 222 detections that resulted to be a false detection. This low number of detections resulted from intruders not lying inside the field of view of the cameras, as well as the presence of background clutter that interferes and complicates the proper detection made by YOLO. The number of false detections is related to the clutter, too, as some figures in the scene could be confused with the shape of the intruder. The graph shows that confidence tends to decrease when distance increases. However, spikes appear throughout the distribution, principally generated by the relative intruder's orientation based on how much of the airplane geometry is presented on the image. Next, different levels of fog are added to see the effect on the average confidence level.

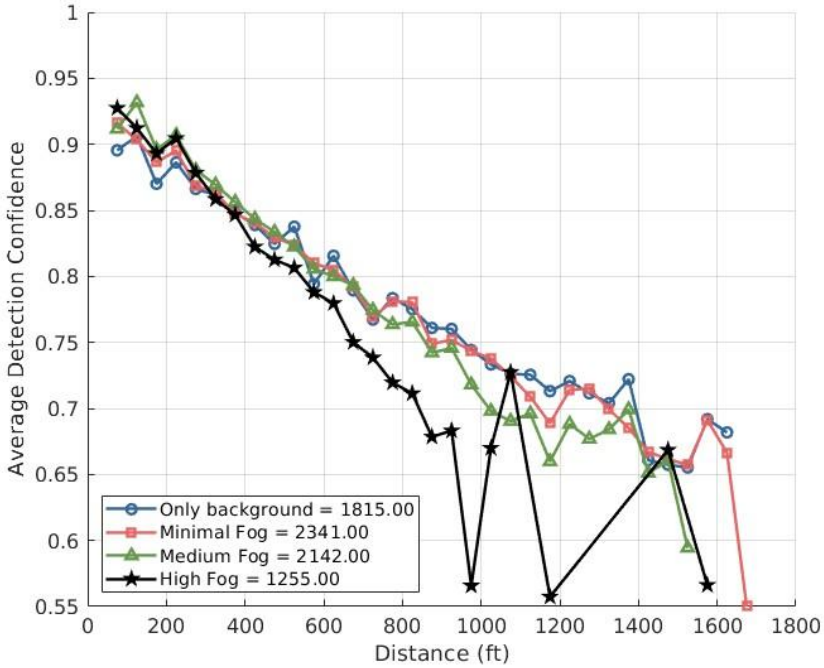

Figure 33. Average detection confidence made by YOLO in the preliminary encounters set at different levels of fog.

The graph reveals two outcomes, there is a higher detection rate at minimal or medium fog, and there are spikes in the fog conditions after 800 ft. The increasing detection rate at fog conditions is caused because the fog at small distances reduces the background clutter, so the shape of the intruder is more defined, and the detection system has a better detection. Some examples of this effect are presented in the next figures.

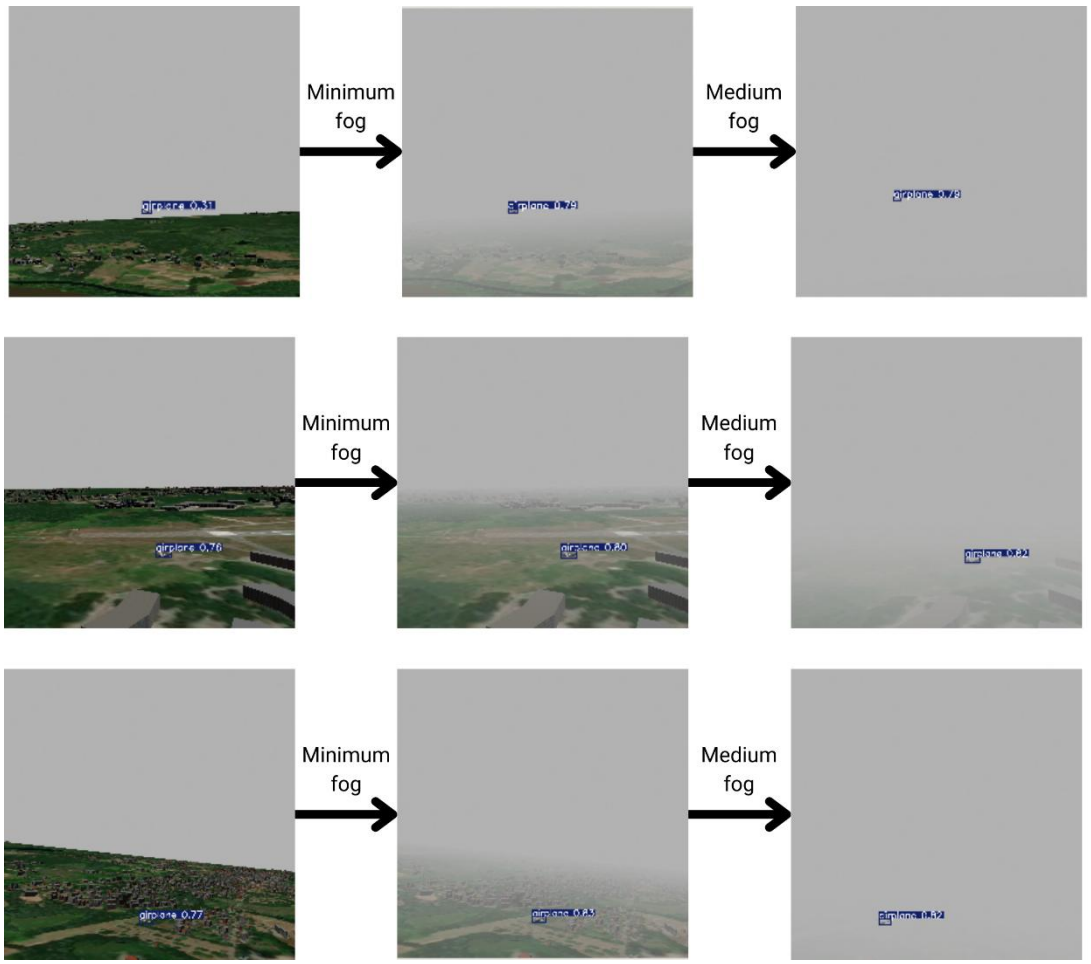

Figure 34. Examples of how fog increases the detection confidence due to a reduction of clutter in CPA encounters 79, 57, and 46.

On the other hand, the spikes at the end of the high fog detection occur due to false positives detection. As environmental factors affect the view of the cameras, YOLO has a higher likelihood of detecting false positives in the same zone as the intruder, making it invisible to the filter. An example of this type of detection is presented in the detection of encounter 61175.

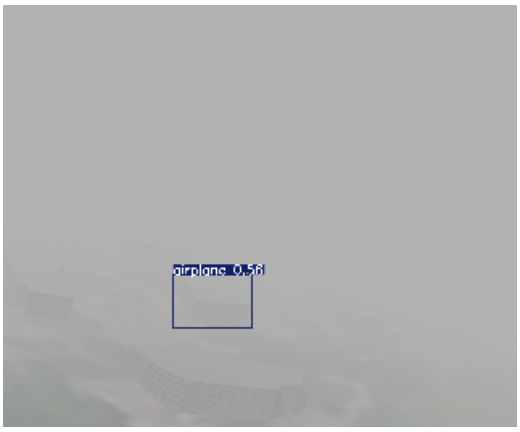

Figure 35. False detection at high fog.

Therefore, the minimal detection threshold increases to 0.7 to reduce the maximum number of false positives coming from the combination of environmental conditions. After the new threshold is applied, the average confidence changes to:

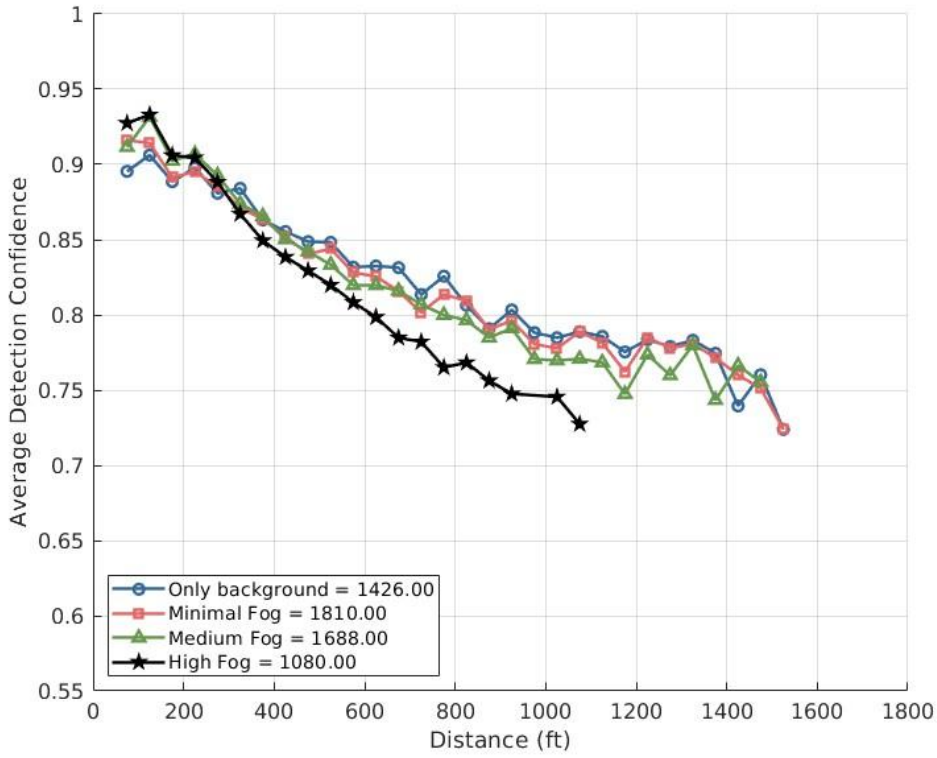

Figure 36. Average detection confidence made by YOLO in the preliminary encounters set at different levels of fog and using an increased detection threshold of 0.7.

After increasing the detection threshold, Figure 36 still shows a higher detection rate and confidence levels in the presence of minimal and medium fog at small distances. However, the clear-sky condition slightly outperforms the others as the distance increases. The geometric filter was applied again to detect how the new detection threshold affects the false positive detection due to clutter.

Table 6. Comparison between false positives filtered after the minimal detection threshold increase of 0.7.

Fog Level	False positives >0.55	False positives >0.7	% Decrease in False positives
Only Background	222	157	-29.28%
Minimal Fog	296	202	-31.76%
Medium Fog	245	181	-26.12%
High Fog	124	96	-22.58%

Overall, incrementing the detection threshold is good to reduce the number of false positives at detection. Even so, depending on the environment, a higher increase could interfere with the position estimation of the intruder in the DAA control. Therefore, a specific threshold needs to be identified for specific environmental conditions to ensure a reliable avoidance maneuver of the UAS. For these preliminary results, only the fog levels were fully applied to the 7,500 CPA-filtered tracks using the Hanscom Air Force Base clutter environment. However, additional simulations are done daily, where the clutter, camera noise, and fog levels vary iteratively to generate a big enough dataset.

2.2.12 Simulation Results

The Gazebo simulation environment was employed for realistic DAA system performance testing. The discussion of its use and its integration into the overall methodology is divided into the following subsections.

2.2.12.1 *Mathematical Modeling of the Detection Probability*

The mathematical modeling of the detection probability includes several modeling decisions and methodologies; these are reviewed in the following subsections.

2.2.12.1.1 Distance Binning and Detection Probability Distribution Calculation

To develop a meaningful statistical representation of detection capabilities, the research team first organized the range data into discrete bins. The team created 17 range bins from 0 to 3000 feet (with varying bin widths to ensure sufficient data points in each bin). For each range bin, researchers calculated the detection probability as the ratio of successful detections in the bin to the total encounters in the bin. This binning approach allowed the team to observe how detection probability changes with range while managing statistical noise in the data.

Figure 37. Distribution of detection ranges by visibility condition.

Figure 37 presents probability density distributions of detection ranges (in feet) across four visibility conditions: Clear, Light Fog, Moderate Fog, and Heavy Fog. The density plots illustrate how the distribution of detection ranges shifts and narrows as visibility deteriorates. Under Clear conditions (purple), detections occur at greater distances with a wide distribution extending beyond 1500 feet. In contrast, Heavy Fog conditions (light green) compress the detection range distribution significantly, with the peak density occurring around 400-500 feet and very few detections beyond 1000 feet. Light and Moderate Fog conditions (blue and teal) show intermediate distributions, demonstrating the progressive degradation of detection capability with increasing fog density.

2.2.12.1.2 Sigmoid Model of Parameter Dependence

After establishing the empirical detection probabilities for each range bin, the research team needed a continuous mathematical model to describe this relationship. The researchers selected a sigmoid function due to its ability to capture the characteristic "S-shaped" curve typically observed in detection probability versus range relationships:

$$P(\text{detection}|\text{range}) = L/\left(1 + \exp\left(-k * (\text{range} - x_0)\right)\right)$$

Where:

- L represents the maximum detection probability (typically 1.0)
- x_0 represents the inflection point (the range at which detection probability equals 0.5L)
- k controls the steepness of the probability curve (how quickly probability drops with increasing range)

The sigmoid function was chosen specifically because it possesses several important mathematical properties that align well with the physical properties of detection probability. First, it is monotonic and non-decreasing, which is essential for modeling a cumulative distribution function of detection probability. This monotonicity reflects the real-world characteristic that detection probability cannot decrease as objects move closer. Second, the sigmoid function naturally bounds the probability between 0 and L (typically 1.0), ensuring that this model respects the fundamental constraints of probability theory. Finally, the sigmoid offers a smooth transition between asymptotic behavior at extreme ranges, which matches the physical reality of detection systems that approach certain limiting probabilities as range becomes very small or very large.

2.2.12.1.3 Parameter Estimation via Nonlinear Regression

The research team used nonlinear least squares fitting, via SciPy's *curve_fit* function, to estimate the optimal parameters for each environmental condition. The fitting procedure:

- Used the midpoints of each range bin as the independent variable;
- Used the calculated detection probabilities as the dependent variable;
- Started with initial parameter estimates (L=1.0, x_0=1000, k=0.01);
- Iteratively refined these parameters to minimize the sum of squared errors between the model and observed data.

For each environmental condition, this process yielded a unique set of parameters that best described the detection probability as a function of range.

2.2.12.1.4 Results and Model Validation

The fitted models demonstrated clear differences in detection capabilities across the four environmental conditions. As expected, detection probability decreased with increasing range, but the rate of decrease was significantly affected by fog density:

- *Clear:* Maintained relatively high detection probabilities (>0.3) out to approximately 1400 feet, with gradual degradation beyond that range.
- *Light:* Showed slightly reduced detection probabilities compared to ideal conditions, with the steeper drop-off occurring around 1300 feet.
- *Moderate:* Exhibited substantially degraded detection capabilities, with detection probability dropping below 0.3 at approximately 1000 feet.
- *Heavy:* Demonstrated severely limited detection range, with probability dropping below 0.1 beyond just 800 feet.

The confidence in this model fit was assessed through the parameter error estimates obtained from the covariance matrix produced by the curve fitting process. Lower parameter errors indicated stronger confidence in the model fit.

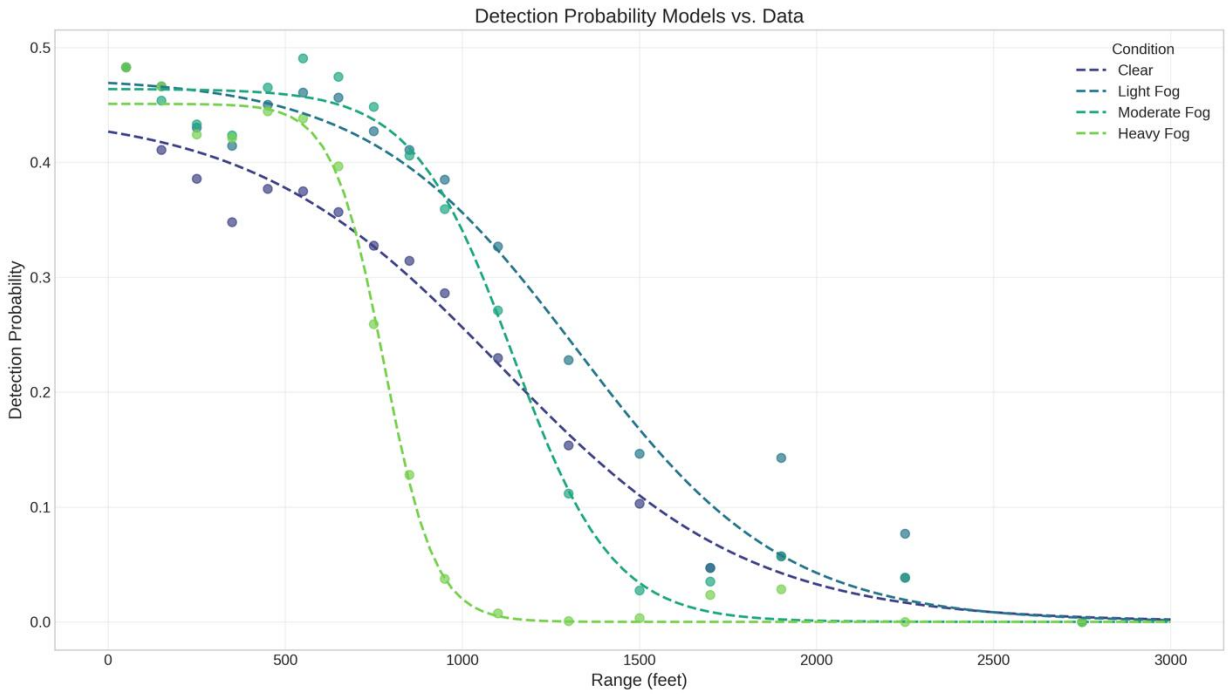

Figure 38. Detection probability models vs. empirical data for various visibility conditions.

Figure 38 illustrates the relationship between detection probability and range (in feet) under four different visibility conditions: Clear, Light Fog, Moderate Fog, and Heavy Fog. The dotted lines represent fitted sigmoid models for each condition, while the scattered points show the empirical detection probabilities calculated from Gazebo simulation data. The figure demonstrates the significant impact of adverse weather conditions on detection capabilities, with detection probability decreasing as range increases, and this degradation accelerating dramatically in heavier fog conditions. Note how Heavy Fog (green) shows near-zero detection probability beyond 1000 feet, while Clear conditions (navy) maintain meaningful detection probabilities beyond 1500 feet.

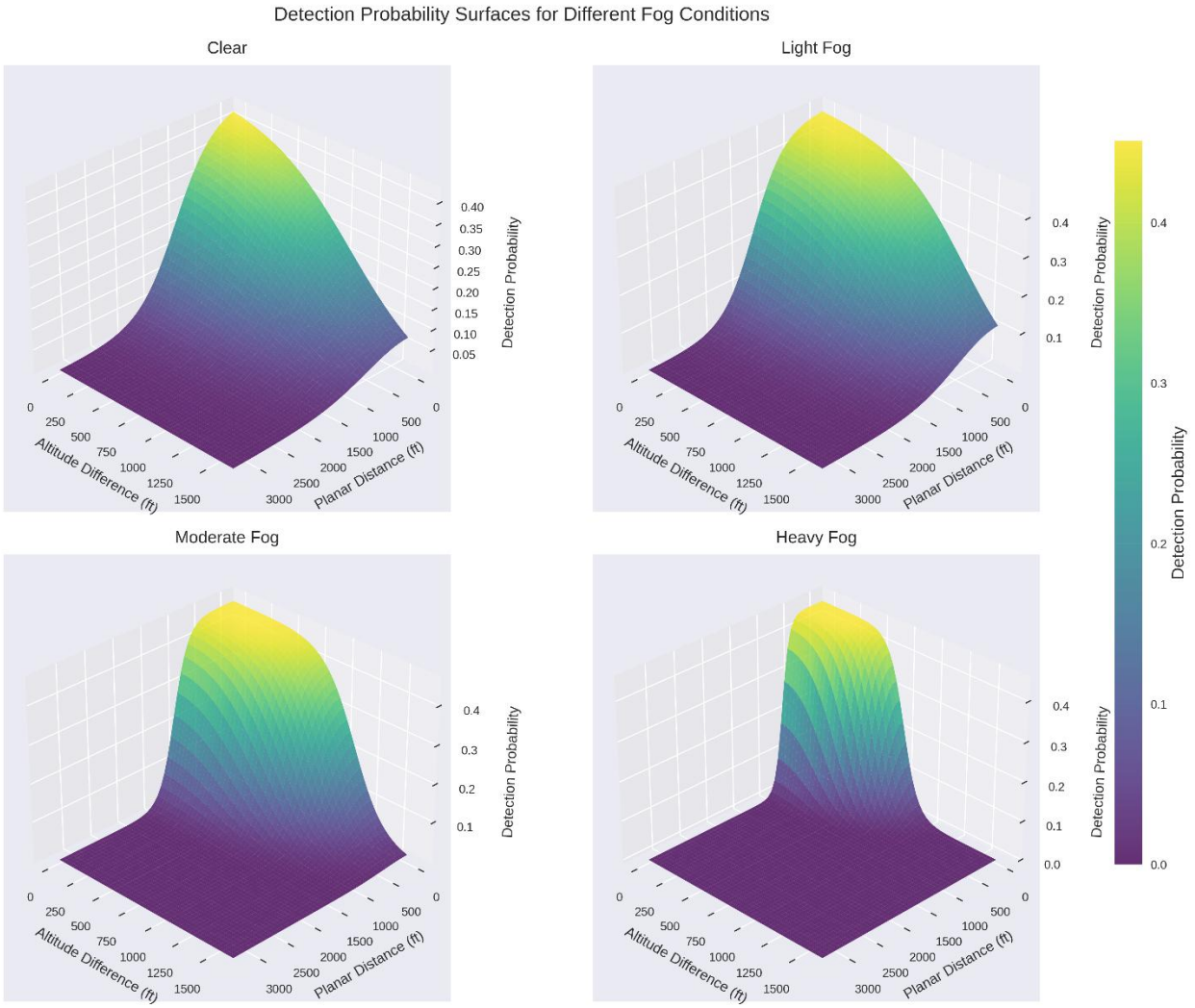

Figure 39. Detection probability surfaces for different fog conditions.

Figure 39 presents 3D visualizations of detection probability as a function of both planar distance (horizontal separation) and altitude difference between aircraft across four visibility conditions. Each surface plot illustrates how detection probability varies based on the three-dimensional positioning of aircraft. As fog density increases from Clear to Heavy Fog, the detection probability surface compresses significantly in the planar distance dimension, with Heavy Fog showing a much narrower effective detection range regardless of altitude separation. The surfaces also demonstrate how detection probability decreases with increasing altitude difference, creating a dome-like probability surface that peaks at close horizontal ranges with minimal vertical separation. These 3D models were incorporated into the Monte Carlo simulations to provide a more realistic representation of detection capabilities in three-dimensional airspace.

2.2.12.1.5 Application to Monte Carlo Simulations

These fitted detection probability models serve as a foundation for subsequent Monte Carlo simulations of DAA system performance. By incorporating these models, one can:

- Simulate realistic detection behavior under various environmental conditions.

- Generate detection time distributions that account for environmental factors.
- Calculate NMAC probabilities under different operational scenarios.
- Assess the sensitivity of DAA system performance to environmental conditions.

For each simulated encounter in the Monte Carlo analysis, the detection probability at a given range can be determined using the appropriate model based on the specified environmental condition. This probability then drives a Bernoulli trial determining whether detection occurs at that time step.

2.2.12.2 ***Integration of Detection Probability Models into Monte Carlo Simulations***

The detection probability models derived from Gazebo simulation data provided a robust foundation for implementing more realistic Monte Carlo simulations of DAA system performance. Rather than relying on simplistic deterministic models, the research team integrated the empirically derived sigmoid probability functions to simulate detection events in various environmental conditions. This approach enabled a more accurate assessment of how DAA systems would perform in real-world scenarios with varying visibility conditions. This integration is best explained through several distinct steps that are described in the following subsections.

2.2.12.2.1 Implementation Methodology

The integration process involved several key steps:

- *Model Parameter Extraction:* For each visibility condition (Clear, Light Fog, Moderate Fog, and Heavy Fog), the team extracted the fitted sigmoid model parameters (L, x_0, k) from the earlier Gazebo simulation analysis.
- *Trajectory Sampling:* Using the MIT LL Terminal Airspace Encounter Set, the team sampled encounter trajectories to create a diverse set of potential aircraft interaction scenarios.
- *Probabilistic Detection Implementation:* At each time step in the simulation, the team:
    - Calculated the instantaneous separation distance between aircraft;
    - Applied the appropriate sigmoid model based on the specified environmental condition;
    - Generated a random number and compared it with the calculated detection probability;
    - Registered a detection event if the random number was less than the calculated probability.
- *Performance Metric Collection:* For each simulated encounter, the team recorded:
    - *Detection rate:* whether detection occurred at all;
    - *Detection distance:* the range at which detection first occurred;
    - *Detection latency:* the time from encounter start to first detection;
    - *NMAC rate:* whether an NMAC event occurred;
    - *NMAC detection rate:* whether detection occurred before an NMAC.

2.2.12.2.2 Simulation Results

The Monte Carlo simulations yielded comprehensive insights into how DAA system performance varies across different visibility conditions. As shown in Table 7 the detection

performance metrics reveal a clear correlation between visibility degradation and reduced system effectiveness:

- *Detection Rate:* The overall probability of detecting an intruder aircraft decreased substantially as visibility worsened, with a dramatic drop from 93.33% in Light Fog to just 46.43% in Heavy Fog conditions.
- *Detection Distance:* The average distance at which detection first occurred decreased from 416.22 meters in Light Fog to only 192.82 meters in Heavy Fog, representing a 54% reduction in average detection range.
- *Detection Latency:* As visibility decreased, the average time required to detect an intruder increased from 100.03 seconds in Light Fog to 107.46 seconds in Heavy Fog conditions.
- *NMAC Rate:* The probability of an NMAC event increased more than fourfold from 0.49% in Light Fog to 2.17% in Heavy Fog, highlighting the significant safety implications of operating in degraded visibility.
- *NMAC Detection Rate:* Notably, the detection rate before NMAC remained at 0% across all conditions, indicating that when NMACs occurred, they did so without prior detection by the DAA system.

Table 7. Summary of detection performance metrics across visibility conditions.

	Detection rate	Avg detection distance (ft)	Avg latency	NMAC rate
Clear	89.51%	1298	101.16 s	0.56%
Light Fog	93.33%	1366	100.03 s	0.49%
Moderate Fog	80.97%	1035	103.94 s	0.63%
Heavy Fog	46.43%	633	107.46 s	2.17%

2.2.12.2.3 Detection Range and Latency Distribution Analyses

Beyond the aggregate metrics, the distribution analysis provided further insights into the stochastic nature of detection performance:

- *Detection Latency Distributions* (Figure 40): The probability density functions for detection latency showed a rightward shift as visibility degraded, with mean latency increasing and distribution shapes changing. Interestingly, the standard deviation decreased in Heavy Fog (21.88s) compared to Clear conditions (26.17s), suggesting less variability but consistently poorer performance in degraded visibility.

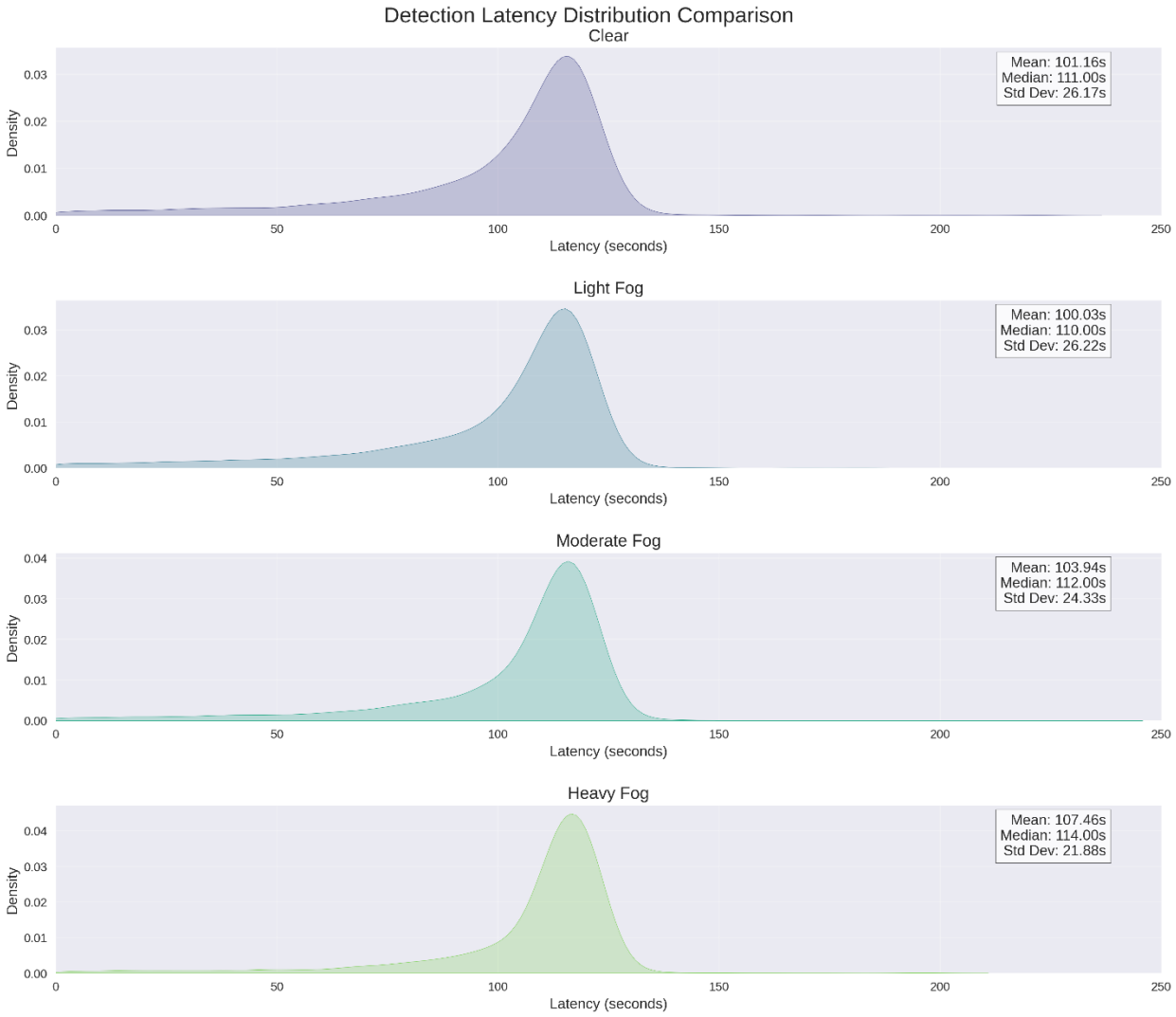

Figure 40. Detection latency distribution comparison across visibility conditions.

- *Detection Range Distributions* (Figure 41): The range distributions clearly demonstrated the dramatic impact of visibility on detection capability. The mean detection range decreased from 1363.0 ft in Clear conditions to just 711.8 ft in Heavy Fog. Additionally, the standard deviation narrowed significantly from 492.9 ft to 180.0 ft, indicating a much more constrained operational envelope in poor visibility.

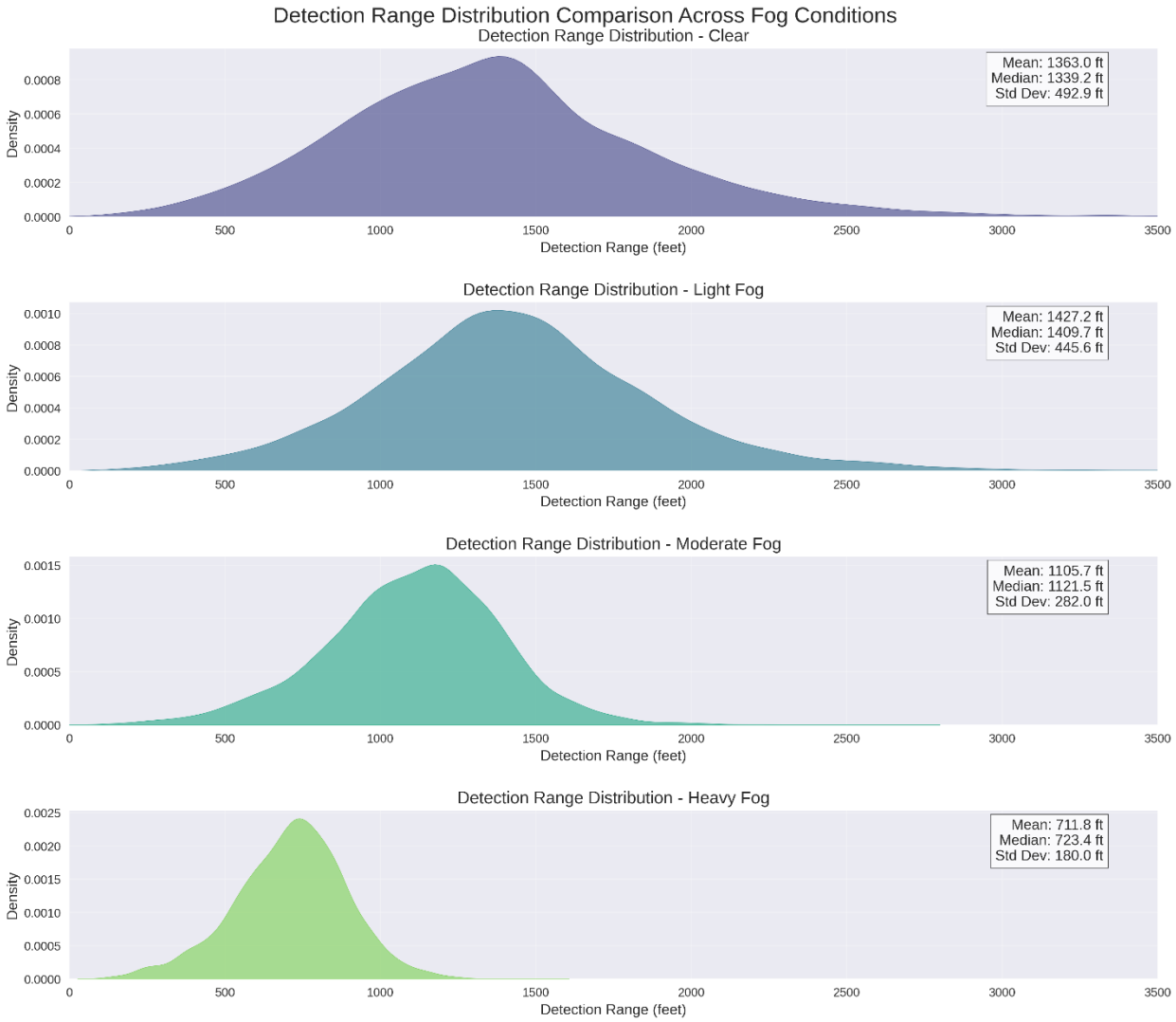

Figure 41. Detection range distribution comparison across fog conditions.

2.2.12.2.4 Operational Implications

These simulation results have several important implications for DAA system requirements and operational risk assessment:

- *Environmental Adaptivity:* DAA system requirements should account for environmental conditions, potentially implementing adaptive thresholds based on visibility conditions.
- *Risk Mitigation Strategies:* In degraded visibility, additional risk mitigation measures may be necessary, such as reduced operational speeds, increased separation requirements, or operational limitations.
- *System Design Considerations:* The significant performance degradation in poor visibility suggests that multi-modal sensing approaches might be necessary for robust DAA performance across all environmental conditions.
- *Safety Margins:* The substantial increase in NMAC rates under Heavy Fog conditions indicates that larger safety margins should be incorporated when operating in degraded visibility environments.

Figure 42 presents a comparison of detection outcomes for a single encounter (048072) simulated under four different fog conditions (Clear, Light, Moderate, Heavy) using the empirically derived sigmoid probability model. The trajectories show Ownship (blue) and Intruder (red) aircraft paths. The visualization demonstrates that while detection (marked with a green star) succeeded in Clear and Light Fog conditions, it failed under Moderate and Heavy Fog conditions for the identical encounter geometry. This illustrates the sensitivity of the detection model to simulated visibility and highlights the critical role environmental factors play in DAA system performance.

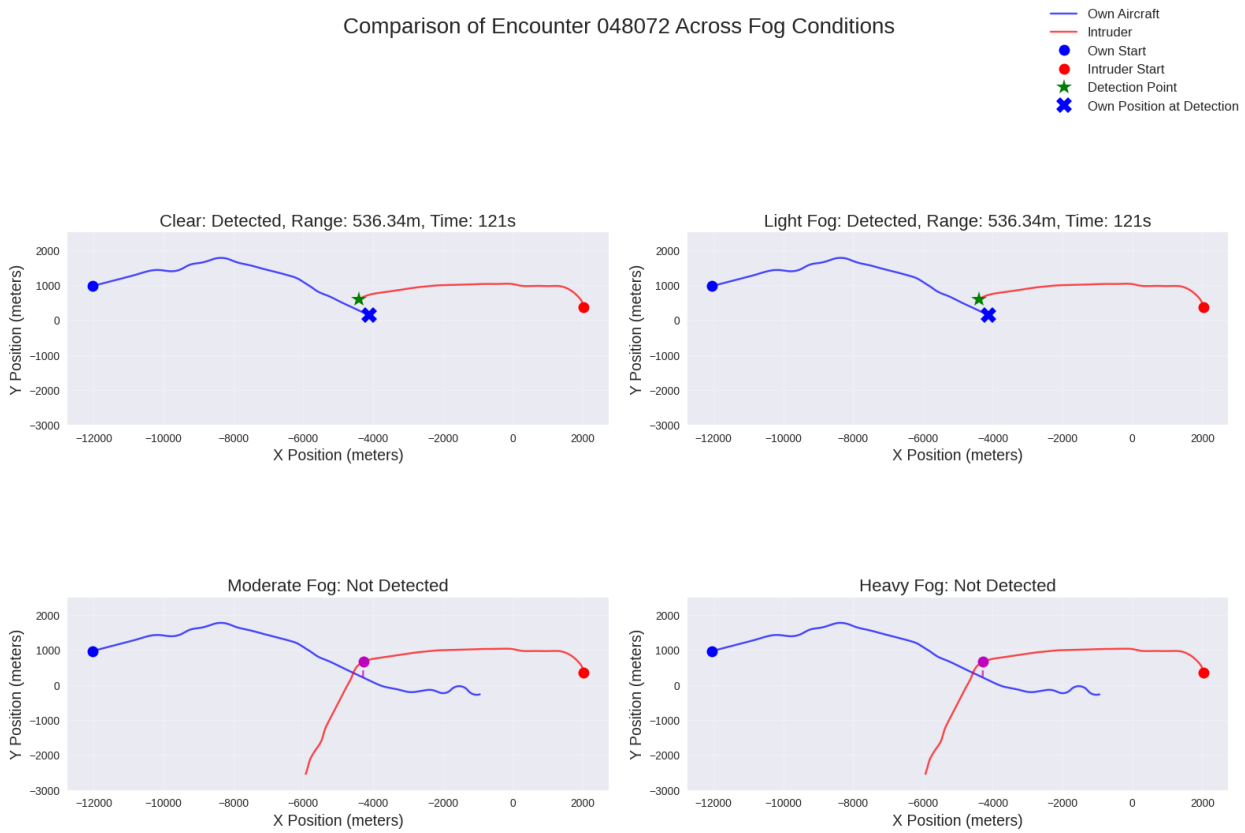

Figure 42. Detection outcomes for Encounter 048072 simulated under different fog conditions.

3 SUBTASK 2-2: SENSITIVITY ANALYSIS FOR DAA SYSTEMS AND OPERATIONS

The second subtask has the following description in the RTP:

> *"The performer will investigate the change in risk measures associated with DAA algorithms as caused by changes in the key model parameters of the DAA algorithm. The task will consist of conducting a sensitivity analysis, which may be performed in three distinct ways – using a mathematical model, simulation, or trial data. The resulting guidance from this task will drive model parameter selection and operating conditions for subsequent tasks/subtasks."*

Given the proposed alternative risk assessment methodologies in Section 2, this report includes a sensitivity analysis.

3.1 Sensitivity Analysis for Proposed Risk Assessment Method #2: DAA Timing Distribution Approach to PRA

The approach described in proposed risk methodology #2 in Task 2-1 yields a parameterized model for the instantaneous detection probability as a function of the instantaneous separation distance between the two aircraft, where the parameters capture system characteristics (*e.g.*, the camera resolution), and operating conditions (*e.g.*, fog and visual clutter). This model is obtained by using standard machine learning techniques on datasets that combine realistic flight trajectories with a detailed detection algorithm simulation. Specifically, there is a parameter space for system characteristics and operating conditions, which is sampled to estimate the probability of instantaneous detection under those particular conditions, and the machine learning algorithm yields a model of that detection probability over the entirety of the parameter space. The focus of this component of Task 2-2 is to explore the dependence risk measures of interest (*e.g.*, the instantaneous detection probability, the detection delay distribution, and the probability of detection before NMAC) upon operating conditions (camera resolution, fog, and visual clutter).

This project's goal is to design a framework that enables the prediction of critical timing under a variety of internal and external factors. To accomplish this, the research team will evaluate and test this data-driven framework in the Gazebo simulation environment using encounter samples that were not included in the model's training data. The team will first assess the independence of the timing function (*e.g.*, detection time) with respect to individual factors such as fog density or sensor resolution. Next, the team will evaluate the accuracy of the timing function derived from the proposed Bayesian framework, considering the combined effects of all relevant factors. Notably, during testing, the team will run complete encounter trajectories in the Gazebo environment and collect physics-based or ground truth data. The data-driven model is expected to accurately predict the timing distribution (*i.e.*, the ground truth outcomes) even before the two aircraft begin to interact, under any specific set of internal and external conditions.

3.1.1 Mathematical Sensitivity Analysis

This section presents a mathematical sensitivity analysis.

3.1.1.1 *Parameterized Detection Probability Model*

To enable sensitivity analysis across varying environmental conditions, the research team developed a parameterized sigmoid detection probability model that incorporates fog density as an explicit environmental variable. The model structure allows all sigmoid parameters to vary linearly with fog condition, providing a flexible framework for capturing environmental effects on detection performance.

The detection probability function is defined as:

$$P(detection \mid range, fog) = a/(1 + \exp(-b * (range - c))) + d$$

where each parameter is a linear function of fog density:

- $a = a_0 + a_1 \times fog$ (upper asymptote)

- $b = b_0 + b_1 \times fog$ (steepness of curve)
- $c = c_0 + c_1 \times fog$ (midpoint/inflection point)
- $d = d_0 + d_1 \times fog$ (lower asymptote)

This parameterization enables the model to capture the following sensitivity relationships:

Range sensitivity: The rate of change in detection probability with respect to aircraft separation distance reveals critical operational characteristics. As detailed in the mathematical derivation in Section A.8.2 of the Appendix, this sensitivity is maximized at the inflection point of the sigmoid curve and approaches zero at extreme ranges, indicating that detection probability is most sensitive to range changes at intermediate distances. This finding has important implications for operational planning, as small changes in separation distance have the greatest impact on detection success within the critical 800-1200 foot range.

Fog sensitivity: The rate of change in detection probability with respect to fog conditions quantifies the environmental impact on system performance. The mathematical analysis presented in Section A.8.3 of the Appendix demonstrates that fog sensitivity varies with range, being most pronounced at distances where the detection probability is transitioning rapidly (near the inflection point). This range-dependent environmental sensitivity explains why moderate fog conditions can have dramatically different impacts depending on the aircraft separation distance at the time of the encounter.

3.1.1.2 ***Parameter Estimation and Model Validation***

Using nonlinear least squares regression on the comprehensive Gazebo simulation dataset (40 fog levels from 0 to 0.02 density and 5000 encounter samples), the model parameters were estimated to minimize the sum of squared residuals between predicted and observed detection probabilities.

The fitted model demonstrates strong predictive capability across the parameter space, with the mathematical formulation enabling direct computation of sensitivity metrics without requiring additional simulations for each parameter variation. Figure 43 illustrates the three-dimensional detection probability surface, showing how the model accurately fits the empirical data across the complete parameter space. The visualization demonstrates the model's ability to capture both the range-dependent detection degradation and the fog-induced performance cliff, with particularly good agreement between predicted surface and observed data points at critical transition regions.

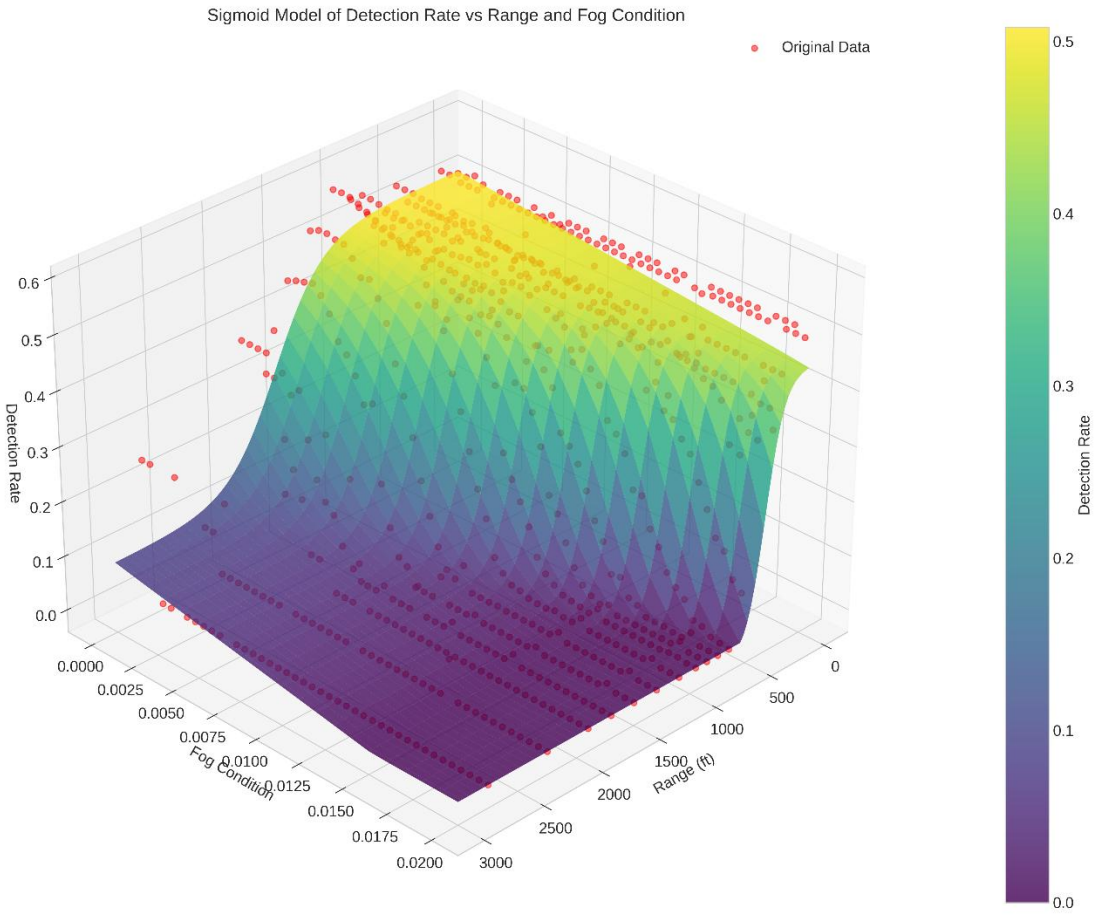

Figure 43. Sigmoid Model of Detection Rate vs Range and Fog Condition.

Figure 43 is a three-dimensional visualization of the fitted sigmoid detection probability model showing the relationship between aircraft separation distance (range), fog density, and detection rate. Red dots represent original simulation data points from Gazebo simulations.

3.1.2 Simulation-Based Sensitivity Analysis

This section provides a simulation-based sensitivity analysis.

3.1.2.1 *Experimental Design*

The simulation-based sensitivity analysis employed a comprehensive experimental design to systematically evaluate the impact of environmental conditions on DAA system performance:

- *Environmental Parameter Range:* Fog density varied from 0 (clear conditions) to 0.02 (heavy fog) across 40 discrete levels.
- *Encounter Dataset:* 5000 encounter trajectories sampled from the MIT LL Terminal Airspace Encounter Set.
- *Performance Metrics:* Average detection latency, detection distance, and NMAC rate.
- *Simulation Platform:* Gazebo environment with YOLO-based detection algorithm.

3.1.2.2 ***Detection Probability Surface Analysis***

The fitted sigmoid model reveals several critical sensitivity patterns:

Range-dependent sensitivity: Detection probability exhibits highest sensitivity to environmental changes at intermediate ranges (approximately 800-1200 feet). At very close ranges (< 400 feet), detection remains relatively robust even under adverse conditions. At long ranges (> 1500 feet), detection probability approaches zero regardless of fog condition.

Fog-dependent sensitivity: The model parameters demonstrate the following fog sensitivity characteristics:

- *Upper asymptote (a):* Decreases linearly with fog density, indicating reduced maximum detection probability;
- *Steepness (b):* Increases with fog density, creating sharper drop-offs in detection probability;
- *Inflection point (c):* Shifts toward shorter ranges with increasing fog, compressing the effective detection envelope;
- *Lower asymptote (d):* Remains near zero across all fog conditions.

3.1.2.3 ***Monte Carlo Simulation Results***

Using the parameterized detection model defined in Equations (15)-(16) of the Appendix, Monte Carlo simulations were conducted across 5000 encounter trajectories with 40 discrete fog levels ranging from 0.0 to 0.02 density. The comprehensive results demonstrate systematic performance degradation across multiple metrics.

3.1.2.3.1 Detection Rate Sensitivity

The overall detection rate follows a sigmoidal degradation pattern with fog density:

- *Clear conditions (fog = 0.000):* 98.68% detection rate;
- *Light fog (fog = 0.005):* 97.92% detection rate (0.77% reduction);
- *Moderate fog (fog = 0.010):* 92.44% detection rate (6.32% reduction);
- *Heavy fog (fog = 0.020):* 12.82% detection rate (87.01% reduction).

The overall detection rate follows a sigmoidal degradation pattern with fog density, as illustrated in Figure 44. The visualization clearly demonstrates the critical threshold behavior, with relatively stable performance above 98% for fog densities below 0.008, followed by a rapid decline.

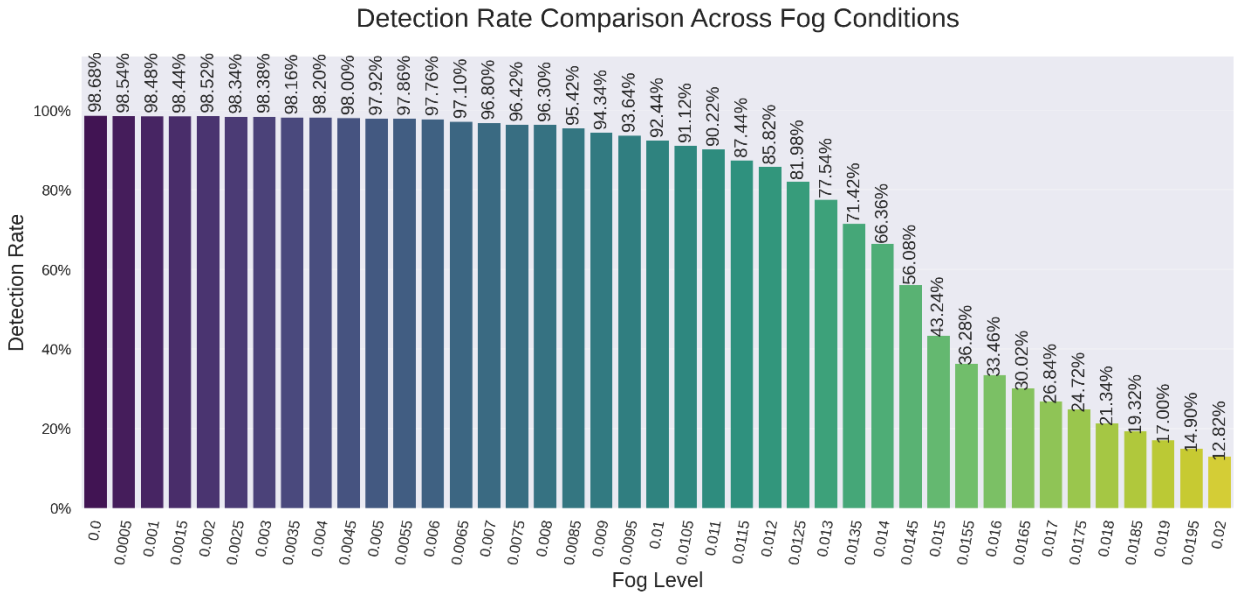

Figure 44. Detection rate performance across 40 fog density levels from Monte Carlo simulations of 5000 encounter scenarios.

The bar chart in Figure 44 demonstrates the systematic degradation of detection capability with increasing fog density, showing relatively stable performance (>98%) for fog densities below 0.008, followed by rapid exponential decline. The critical threshold at fog density ≈ 0.012 marks the transition from gradual to steep performance degradation, with detection rates dropping to 12.82% at maximum fog density (0.02).

3.1.2.3.2 Detection Distance Sensitivity

The average detection distance exhibits strong nonlinear sensitivity to fog conditions:

- *Clear conditions (fog = 0.000):* 1447.38 m average detection distance;
- *Light fog (fog = 0.005):* 1240.91 m average detection distance (14.3% reduction);
- *Moderate fog (fog = 0.010):* 996.35 m average detection distance (31.2% reduction);
- *Heavy fog (fog = 0.020):* 87.49 m average detection distance (94.0% reduction).

The average detection distance exhibits strong nonlinear sensitivity to fog conditions, as shown in Figure 45. The dramatic reduction from 1447.38m to 87.49m represents a 94% performance

degradation, confirming the exponential relationship between environmental conditions and detection capability.

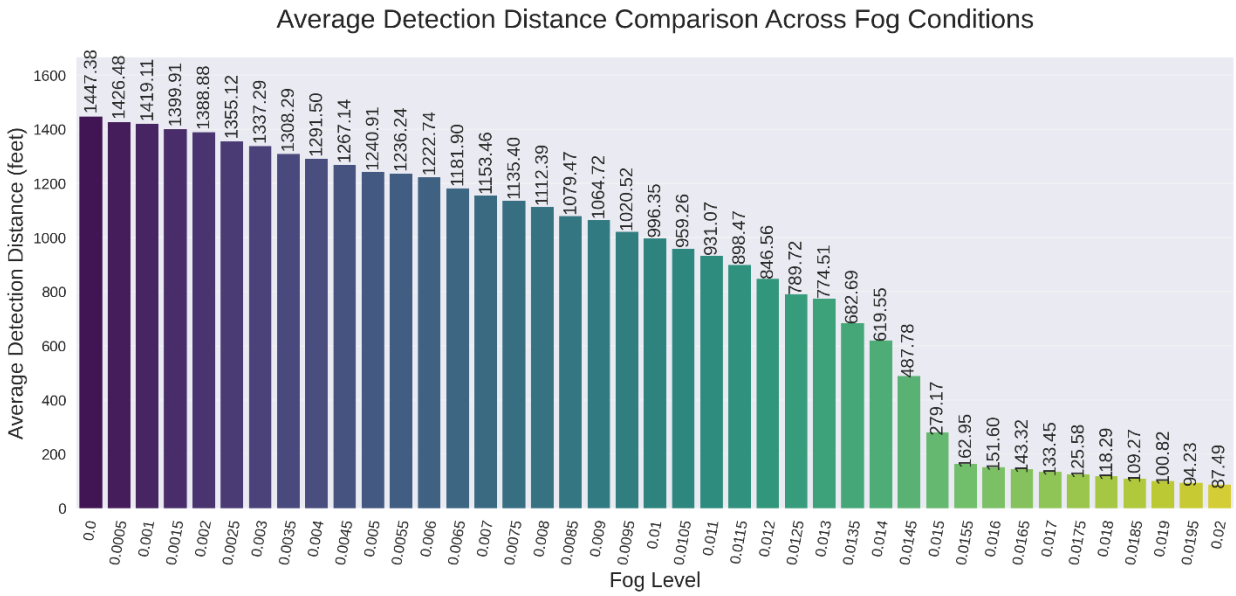

Figure 45. Average detection distance performance across fog density levels from Monte Carlo simulations.

The visualization in Figure 45 shows the dramatic reduction in effective detection range with increasing fog density, from 1447.38 feet in clear conditions to 87.49 feet in clear conditions to 87.49 feet in heavy fog (94% reduction). The nonlinear relationship demonstrates exponential decay in detection capability, with the steepest decline occurring beyond fog density 0.012, indicating a critical operational threshold.

3.1.2.3.3 Detection Latency Sensitivity

Average detection latency shows moderate but systematic sensitivity to environmental conditions:

- *Clear conditions (fog = 0.000):* 77.44 seconds average latency;
- *Light fog (fog = 0.005):* 81.26 seconds average latency (4.9% increase);
- *Moderate fog (fog = 0.010):* 88.56 seconds average latency (14.4% increase);
- *Heavy fog (fog = 0.020):* 113.18 seconds average latency (46.1% increase).

Average detection latency shows moderate but systematic sensitivity to environmental conditions, as presented in Figure 46. The nearly linear increase from 77.44 to 113.18 seconds demonstrates consistent degradation in response time across the fog spectrum.

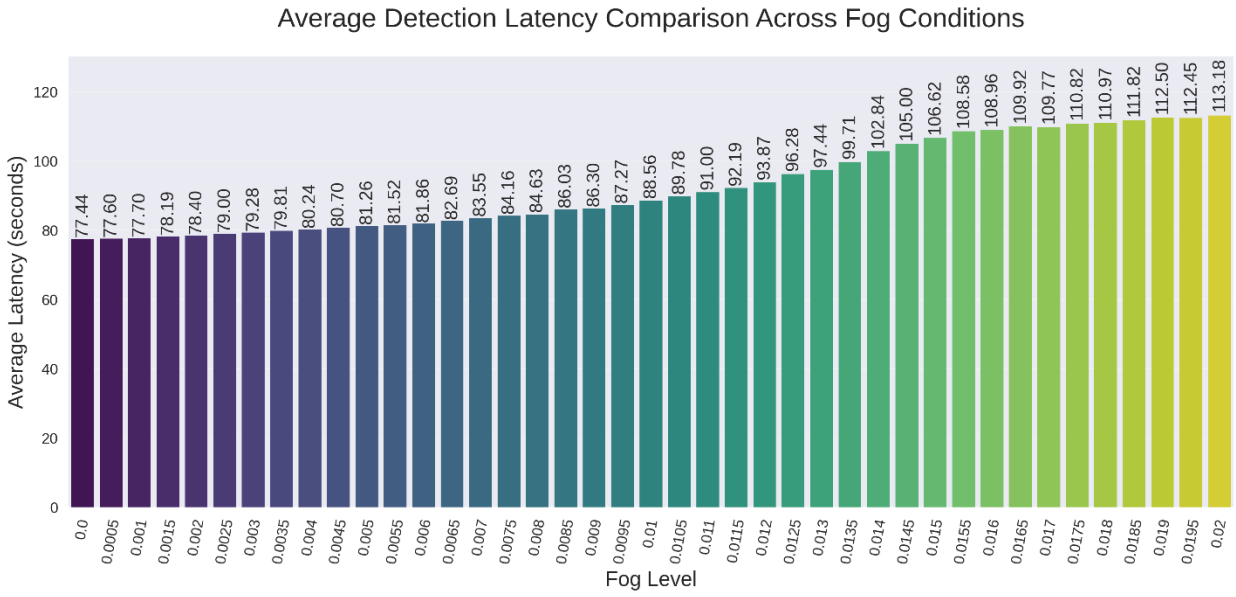

Figure 46. Average detection latency across fog density levels from Monte Carlo simulations.

The chart in Figure 46 illustrates the systematic increase in detection time with environmental degradation, rising from 77.44 seconds in clear conditions to 113.18 seconds in heavy fog (46.1% increase). Unlike detection rate and distance metrics, latency shows a more linear relationship with fog density, indicating consistent but gradual performance degradation across the fog spectrum.

3.1.2.3.4 NMAC Rate Sensitivity

The NMAC rate exhibits exponential sensitivity to fog conditions with a distinct threshold behavior:

- *Low fog conditions (fog < 0.010):* NMAC rates remain consistently low (0.02-0.22%);
- *Moderate fog (fog = 0.013):* 1.04% NMAC rate (5x increase from baseline);
- *High fog (fog = 0.015):* 2.70% NMAC rate (13x increase);
- *Heavy fog (fog = 0.020):* 13.48% NMAC rate (67x increase).

This exponential relationship, clearly visible in Figure 47, indicates that NMAC risk is highly sensitive to environmental degradation beyond a critical threshold around fog density = 0.012. The sharp transition from minimal risk (<0.5%) to significant risk (>1%) within a narrow fog density

range of 0.012-0.013 provides strong empirical evidence for establishing operational restrictions at this environmental threshold.

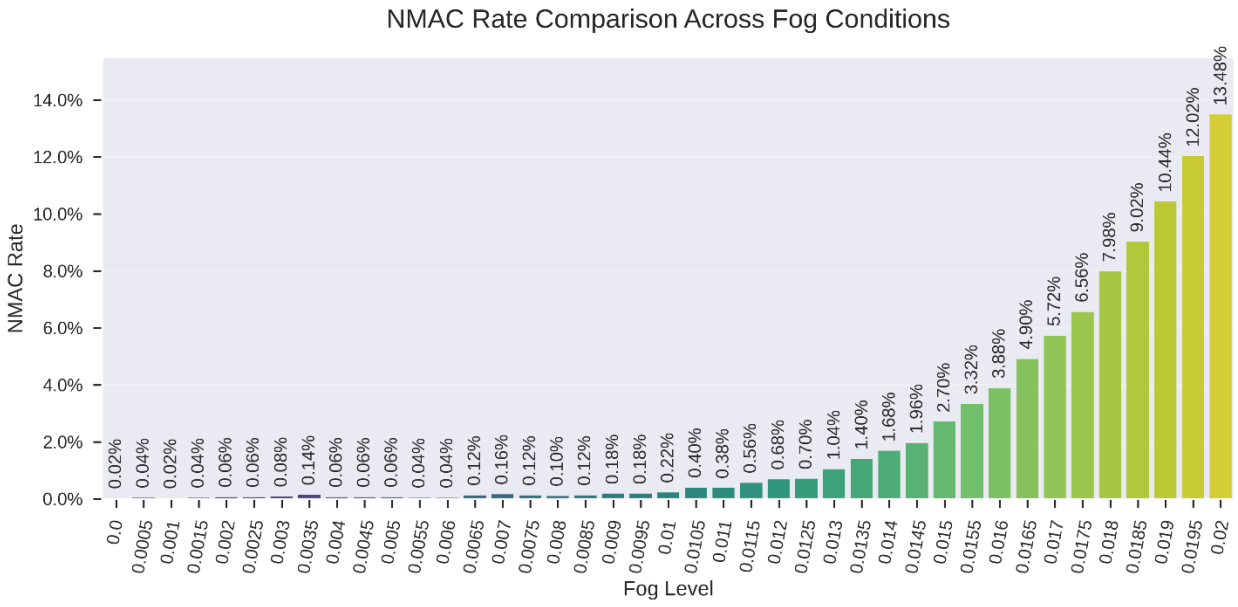

Figure 47. NMAC rate across 40 fog density levels from Monte Carlo simulations of 5000 encounter scenarios.

The visualization in Figure 47 demonstrates the exponential increase in collision risk with environmental degradation, showing minimal NMAC rates (<0.5%) for fog densities below 0.012, followed by a dramatic escalation to 13.48% at maximum fog density (0.02). This represents a 67-fold increase in collision risk, highlighting the critical safety implications of operating DAA systems in degraded visibility conditions. The sharp transition around fog density 0.012-0.013 confirms the identification of this threshold as a critical operational limit.

3.1.2.4 *Future Research Directions*

The sensitivity analysis framework establishes the foundation for several future research areas:

1. *Multi-parameter optimization:* Extending the analysis to simultaneous variations in fog, clutter, and system parameters using the combined probability model from Equation (16) of the Appendix.
2. *Real-time adaptation:* Developing adaptive algorithms that use the sensitivity coefficients to optimize system parameters in real-time based on environmental measurements.
3. *Certification support:* Using quantitative sensitivity relationships to support regulatory certification processes with data-driven safety demonstrations.

The comprehensive sensitivity analysis demonstrates that the proposed DAA timing distribution approach provides quantitative insights into system performance variability, enabling evidence-based operational decision-making and system design optimization. The mathematical framework

established in the Appendix provides the theoretical foundation for these practical applications, bridging the gap between academic research and operational implementation.

4 REFERENCE

[Amerson, 2024] D. Amerson, K. Ryker, C. White, C. Goodin, L. Dabbiru, K. Babski-Reeves, S. Lee, S. Gibson-Todd, A. LeGrand, and R. Sah, "ASSURE A65 – Detect and Avoid Risk Ratio Validation Final Report," Report No. A11L.UAS.105, July 12, 2024. https://www.assureuas.org/wp-content/uploads/2022/02/A65-Final-Report_v7.pdf

[ASTM, 2023] ASTM International, "Standard Specification for Detect and Avoid System Performance Requirements," F3442/F3442M − 23, 2023. https://store.astm.org/f3442_f3442m-20.html

[ASSURE A50, 2021] ASSURE, "Small Unmanned Aircraft System (sUAS) Traffic Analysis Initial Annual Report," A11L.UAS.91, 2021. https://assureuas.com/wp-content/uploads/2021/06/First-Annual-Report-Final-11-2-2022.pdf

[ASSURE A71 Task 1, 2024] ASSURE, A71 Task 1 Report, 2024.

[Aust, 2020] J. Aust and D. Pons, "A Systematic Methodology for Developing Bowtie in Risk Assessment: Application to Borescope Inspection," *Aerospace*, no. 7, pp. 86, 2020. https://doi.org/10.3390/aerospace7070086

[Bekmezci, 2013] I. Bekmezci, O. K. Sahingoz, and S. Temel, "Flying ad-hoc networks (FANETs): A survey," *Elsevier Ad Hoc Networks*, vol. 11, no. 3, pp. 1254–1270, 2013. https://doi.org/10.1016/j.adhoc.2012.12.004

[Bijjahalli, 2022] S. Bijjahalli, A. Gardi, N. Pongsakornsathien, R. Sabatini, R., and T. Kistan, "A unified airspace risk management framework for UAS operations," *MDPI Drones*, vol. 6, no. 7, pp. 184, 2022. https://doi.org/10.3390/drones6070184

[Bigazzi, 2022] L. Bigazzi, L. Miccinesi, E. Boni, M. Basso, T. Consumi, and M. Pieraccini, "Fast Obstacle Detection System for UAS Based on Complementary Use of Radar and Stereoscopic Camera," *MDPI Drones*, vol. 6, no. 11, pp. 361, 2022. https://doi.org/10.3390/drones6110361

[Campion, 2024] F. Campion, R. Danan, B. Hayes, J. Helleberg, and L. Levine, "Bowtie Analysis of Pilot Depression and Barrier-Based Risk Management," *MITRE Corporation*, DOT/FAA/AM-24/01, January 2024. https://doi.org/10.21949/1529630

[Cone, 2019] A. Cone, M. G. Wu, and S. Lee, "Detect-and-Avoid Alerting Performance for High-Speed UAS and Non-Cooperative Aircraft," *NASA*, 2019. https://ntrs.nasa.gov/citations/20190028640

[Costley, 2022] A. Costley, R. Christensen, R. C. Leishman, and G. N. Droge, “Sensitivity of Single-Pulse Radar Detection to Aircraft Pose Uncertainties,” *IEEE Transactions on Aerospace Electronic Systems*, vol. 59, no. 3, pp. 2286–2295, June, 2022. https://doi.org/10.1109/TAES.2022.3213793

[Du, 2024] S. Du, G. Zhong, F. Wang, B. Pang, H. Zhang, and Q. Jiao, “Safety Risk Modelling and Assessment of Civil Unmanned Aircraft System Operations: A Comprehensive Review”. *MDPI Drones*, vol. 8, no. 8, pp. 354, 2024 https://doi.org/10.3390/drones8080354

[EASA, 2016] European Union Aviation Safety Agency (EASA), "UAS safety risk portfolio and analysis," 2016. https://www.easa.europa.eu/en/document-library/general-publications/uas-safety-risk-portfolio-and-analysis

[FAA UTM, 2023] Federal Aviation Administration (FAA), "Unmanned Aircraft Systems Traffic Management (UTM) Implementation Plan," 2023. https://www.faa.gov/about/plansreports/congress/unmanned-aircraft-systems-traffic-management-utm-implementation-plan

[FAA 8040.4C, 2023] Federal Aviation Administration (FAA), "FAA Order 8040.4C – Safety Risk Management Policy," 2023. https://www.faa.gov/documentLibrary/media/Order/FAA_Order_8040.4C.pdf

[FAA 8040.6A, 2023] Federal Aviation Administration (FAA), “FAA Order 8040.6A – Unmanned Aircraft Systems (UAS) Safety Risk Management (SRM) Policy," 2023. https://www.faa.gov/documentLibrary/media/Order/Order_8040.6A.pdf

[Fang, 2024] A. Fang, S. Feng, B. Liang, B., and J. Jiang, "Real-time detection of unauthorized unmanned aerial vehicles using SEB-YOLOv8s," *Sensors*, vol. 24, no. 12, pp. 3915, 2024. https://doi.org/10.3390/s24123915

[Faturachman, 2023] A. Faturachman, D. Lestary, A. Agustono, and A. Satria, "Safety Risk Management Bow-Tie Analysis and Safety Promotion in the Operations of Small Unmanned Aircraft Systems," *Journal of Theoretical and Applied Information Technology*, vol. 101, no. 21, pp. 6843–6854, 2023. https://www.jatit.org/volumes/Vol101No21/16Vol101No21.pdf

[Fasano, 2023] G. Fasano and R. Opromolla, "Analytical Framework for Sensing Requirements Definition in Non-Cooperative UAS Sense and Avoid," *MDPI Drones*, vol. 7, no. 10, pp. 621. https://doi.org/10.3390/drones7100621

[Fern, 2015] L. Fern, R. C. Rorie, J. S. Pack, R. J. Shively, and M. H. Draper, "An Evaluation of Detect and Avoid (DAA) Displays for Unmanned Aircraft Systems: The Effect of Information Level and Display Location on Pilot Performance," *American Institute of Aeronautics and Astronautics*, 2015.

https://ntrs.nasa.gov/api/citations/20150018045/downloads/20150018045.pdf

[Fu, 2023] X. Fu, C. Zhi, and D. Wu, "Obstacle avoidance and collision avoidance of UAV swarm based on improved VFH algorithm and information sharing strategy," *Computers & Industrial Engineering*, vol. 186, pp. 109761, 2023.
https://doi.org/10.1016/j.cie.2023.109761

[Ghosh, 2023] S. Ghosh, J. Patrikar, B. Moon, M. M. Hamidi, and S. Scherer, "AirTrack: Onboard deep learning framework for long-range aircraft detection and tracking," *Proceedings of the IEEE International Conference on Robotics and Automation (ICRA)*, 2023.
https://arxiv.org/abs/2209.12849

[ICAO, 2020] International Civil Aviation Organization (ICAO), “UTM: A common framework with core principles for global harmonization,” 2020.
https://www.icao.int/safety/UA/Documents/UTM-Framework.en.alltext.pdf

[JARUS, 2019] Joint Authorities for Rulemaking on Unmanned Systems (JARUS), “JARUS guidelines on SORA, Annex C: Strategic Mitigation – Collision Risk Assessment,” Edition 1.0, 2019.
http://jarus-rpas.org/wp-content/uploads/2024/06/SORA-Annex-C-v1.0.pdf

[Johnson, 2015] M. A. Johnson, D. P. Thipphavong, E. R. Mueller, and C. Park, "Appendix A: NAS-Wide Encounter Rate Evaluation Using Historical Radar Data and the Airspace Concept Evaluation System (ACES)," Radio Technical Commission for Aeronautics (RTCA) Report No. ARC-E-DAA-TN23233, May 18, 2015.
https://ntrs.nasa.gov/citations/20190025098

[Khan, 2022] M. A. Khan, H. Menouar, A. Eldeeb, A. Abu-Dayya, and F. D. Salim, “On the Detection of Unauthorized Drones—Techniques and Future Perspectives: A Review,” *IEEE Sensors Journal*, vol. 22, no. 12, pp. 11439–11455, June 2022.
https://doi.org/10.1109/JSEN.2022.3171293

[Kochenderfer, 2008] M. J. Kochenderfer, L. P. Espindle, J. K. Kuchar, and J. D. Griffith, "A Bayesian Approach to Aircraft Encounter Modeling," *AIAA Guidance, Navigation and Control Conference and Exhibit*, Honolulu, Hawaii, August, 2008.
https://doi.org/10.2514/6.2008-6629

[Koeing, 2004] N. Koeing, and A. Howard, "Design and Use Paradigms for Gazebo, an Open-Source Multi-robot Simulator, " 2004 IEEE/RSJ International Conference on Intelligent Robots and Systems (IROS) (IEEE Cat No. 04CH37566), Sendai, Japan, 2004, pp. 2149-2154 vol.3.
https://ieeexplore.ieee.org/document/1389727

[Kopardekar, 2016] P. Kopardekar, J. Rios, T. Prevot, M. Johnson, J. Jung, J. and J. E. Robinson, "Unmanned aircraft system traffic management (UTM) concept of operations," *AIAA AVIATION Forum and Exposition* (No. ARC-E-DAA-TN32838), June, 2016.
https://doi.org/10.2514/6.2016-3292

[Kuru, 2023] K. Kuru, J. M. Pinder, B. J. Watkinson, D. Ansell, K. Vinning, L. Moore, C. Gilbert, A. Sujit, and D. Jones, "Toward Mid-Air Collision-Free Trajectory for Autonomous and Pilot-Controlled Unmanned Aerial Vehicles," *IEEE Access*, vol. 11, pp. 100323–100343, 2023. https://doi.org/10.1109/ACCESS.2023.3314504

[Leung, 2017] T. J. Leung and J. Rife, "Refining Fault Trees Using Aviation Definitions for Consequence Severity," *IEEE Aerospace and Electronic Systems Magazine*, vol. 32, no. 3, pp. 4–14, March, 2017.
https://doi.org/10.1109/MAES.2017.150171

[Lin, 2018] Z. Lin, L. Castano, H. Xu, "A fast obstacle collision avoidance algorithm for Fixed Wing UAS," *2018 International Conference on Unmanned Aircraft Systems (ICUAS)*.
https://doi.org/10.1109/icuas.2018.8453307

[Li, 2023] Q. Li, Q. Wu, H. Tu, J. Zhang, X. Zou, and S. Huang, "Ground risk assessment for unmanned aircraft focusing on multiple risk sources in urban environments," *Processes*, vol. 11, no. 2, pp. 542, 2023.
https://doi.org/10.3390/pr11020542

[Liang, 2023] C. Liang, L. Liu, and C. Liu, "Multi-UAV autonomous collision avoidance based on PPO-GIC algorithm with CNN–LSTM fusion network," *Neural Networks*, vol. 162, pp. 21-33, 2023.
https://doi.org/10.1016/j.neunet.2023.02.027

[MIT Lincoln Laboratory, 2021] MIT Lincoln Laboratory, "Bayesian Manned Aircraft Encounter Model (em-model-manned-bayes),", GitHub, 2021.
https://github.com/Airspace-Encounter-Models/em-model-manned-bayes

[MIT Lincoln Laboratory, 2025] MIT Lincoln Laboratory, Unmanned Aircraft Terminal Area Encounters, MIT LLTEM V1.0. Accessed: 1 May 2025.
https://www.ll.mit.edu/r-d/datasets/unmanned-aircraft-terminal-area-encounters

[Omeri, 2022] M. Omeri, R. Isufaj, and R. Moreno Ortiz, "Quantifying Well Clear for Autonomous Small UAS," *IEEE Access*, vol 10, pp. 68365–68383, 2022.
https://doi.org/10.1109/ACCESS.2022.3186025

[Open Source Robotics Foundation, 2025] Open Source Robotics Foundation (n.d.), "Tutorial: Sensor Noise Model," *Gazebo*, Retrieved April 30, 2025. [Online]. Available:
https://classic.gazebosim.org/tutorials?tut=sensor_noise

[OpenStreetMap, 2017] OpenStreetMap contributors, "Planet dump retrieved from https://planet.osm.org," *OpenStreetMap*, 2017. [Online]. Available:
https://www.openstreetmap.org

[OGRE Team, 2025] OGRE Team (n. d.), "fog_override," *OGRE Manual v1.8*, sec. 3.1.2, Retrieved April 30, 2025. [Online]. Available: https://www.ogre3d.org/docs/manual18/manual_16.html

[Pant, 2022] K. A. Pant, Z. Yang, J. M. Goppert, and I. Hwang, "An Open-source Gazebo Plugin for GNSS Multipath Signal Emulation in Virtual Urban Canyons," 2022. https://arxiv.org/abs/2212.04018

[Pascarella, 2022] D. Pascarella, G. Gigante, A. Vozella, P. Bieber, T. Dubot, E. Martinavarro, G. Barraco, and G. Li Calzi, "A Methodological Framework for the Risk Assessment of Drone Intrusions in Airports," *Aerospace*, vol. 9, no. 12, pp. 747, 2022. https://www.mdpi.com/2226-4310/9/12/747

[Prassinos, 2011] P. G. Prassinos, J. W. Lyver IV, and C. T. Bui, "Risk Assessment Overview," *Proceedings of the ASME 2011 International Mechanical Engineering Congress and Exposition (IMECE)*, Denver, Colorado, Nov. 11–17, 2011. https://ntrs.nasa.gov/api/citations/20110016003/downloads/20110016003.pdf

[Primatesta, 2020] S. Primatesta, A. Rizzo, and A. la Cour-Harbo, "Ground risk map for unmanned aircraft in urban environments," *Journal of Intelligent & Robotic Systems*, vol. 97, pp. 489-509, 2020. https://doi.org/10.1007/s10846-019-01015-z

[Ray, 1999] J. K. Ray, M. E. Cannon, and P.C. Fenton, "Mitigation of static carrier-phase multipath effects using multiple closely spaced antennas," Navigation, 46(3):193-201, Sep 1999. https://citeseerx.ist.psu.edu/document?repid=rep1&type=pdf&doi=dc99e55abbba1f0706f15ebc4a64b06fadd1cbef

[Redmon, 2016] J. Redmon, "You Only Look Once: Unified, Real-time Object Detection, " In Proceedings of the IEEE Conference on Computer Vision and Pattern Recognition, Las Vegas, NV, USA, 27-30 June, 2016. https://ieeexplore.ieee.org/document/7780460

[Redmon, 2018] J. Redmon and A. Farhadi, "YOLOv3: An incremental improvement," *arXiv preprint arXiv:1804.02767*, 2018. Available: https://arxiv.org/abs/1804.02767

[Seidaliyeva, 2023] U. Seidaliyeva, L. Ilipbayeva, K. Taissariyeva, N. Smailov, and E. T. Matson, “Advances and Challenges in Drone Detection and Classification Techniques: A State-of-the-Art Review,” *Italian National Conference on Sensors*, vol. 24, no. 1, Jan. 2023. https://doi.org/10.3390/S24010125

[Semenyuk, 2024] V. Semenyuk, I. Kurmashev, A. Lupidi, D. Alyoshin, L. Kurmasheva, and A. Cantelli-Forti, “Advance and Refinement: The Evolution of UAV Detection and Classification Technologies,” *arXiv*, 2024. https://doi.org/10.48550/ARXIV.2409.05985

[Serres, 2022] C. Serres, B. Gill, P. Reheis, and M. Edwards, "RTCA detect and avoid phase 2: Safety risk management modeling and simulation final report," *MIT Lincoln Laboratories*, 2022 https://apps.dtic.mil/sti/trecms/pdf/AD1197090.pdf

[Singh, 2024] A. Singh, S. Kumar, and D. Choudhury, "Deep Learning Driven Real-Time Airspace Monitoring Using Satellite Imagery," *Scalable Computing: Practice and Experience*, vol. 25, no. 6, October 2024. https://doi.org/10.12694/SCPE.V25I6.3101

[Sumi, 2024] Y. Sumi, B. K. Kim, T. Ogure, M. Kodama, N. Sakai, and M. Kobayashi, "Impact of Rainfall on the Detection Performance of Non-Contact Safety Sensors for UAVs/UGVs," *Italian National Conference on Sensors*, vol. 24, no. 9, May 2024. https://doi.org/10.3390/S24092713

[Sun, 2024] X. Sun, Y. Hu, Y. Qin, and Y. Zhang, "Risk assessment of unmanned aerial vehicle accidents based on data-driven Bayesian networks," *Reliability Engineering & System Safety*, vol. 248, pp. 110185, 2024. https://doi.org/10.1016/j.ress.2024.110185.

[Sun, 2018] J. Sun, W. Wang, Q. Da, L. Kou, G. Zhao, L. Zhang, and Q. Han, "An intrusion detection based on Bayesian game theory for UAV network," *European Alliance for Innovation (EAI) International Conference on Mobile Multimedia Communications*, 2018. https://doi.org/10.4108/eai.21-6-2018.2277054

[Tirri, 2014] A. E. Tirri, G. Fasano, D. Accardo, and A. Moccia, "Particle Filtering for Obstacle Tracking in UAS Sense and Avoid Applications," *The Scientific World Journal*, No. 280478, 2014. https://doi.org/10.1155/2014/280478

[Truong, 2020] D. Truong and W. Choi, "Using machine learning algorithms to predict the risk of small Unmanned Aircraft System violations in the National Airspace System," *Journal of Air Transport Management*, vol. 86, pp. 101822, 2020. https://doi.org/10.1016/j.jairtraman.2020.101822

[Virtanen, 2020] P. Virtanen et al. 'SciPy 1.0: fundamental algorithms for scientific computing in Python', *Nature Methods*, vol. 17, no. 3, pp. 261–272, 2020. https://doi.org/10.1038/S41592-019-0686-2

[vvoovv, 2025] vvoovv, *BLOSM documentation* [Computer software documentation], GitHub. Retrieved April 30, 2025. Available: https://github.com/vvoovv/blosm/wiki/Documentation

[Wang, 2024] Y. Wang and X. Yue, "Aviation Safety Risk Analysis Based on Bayesian Network Modeling," *Highlights in Science, Engineering and Technology (EMIS)*, vol. 81, pp. 623–630, 2024. https://doi.org/10.4028/p-c5s5dh

[Wang, 2021] K. Wang, K., M. Song, and M. Li, "Cooperative multi-UAV conflict avoidance planning in a complex urban environment," *Sustainability*, vol. 13, no. 12, pp. 6807, 2021. https://doi.org/10.3390/su13126807

[Weinert, 2018] A. Weinert, S. Campbell, A. Vela, D. Schuldt, and J. Kurucar, "Well-Clear Recommendation for Small Unmanned Aircraft Systems Based on Unmitigated Collision Risk," *Journal of Air Transportation*, vol. 26, no. 3, pp. 113–122, 2018. https://arc.aiaa.org/doi/10.2514/1.D0091

[Wu, 2023] Wu, J., Wang, C., & Liang, H. (2023). Bayesian quickest detection-based spectrum sensing for cognitive UAV networks," *Transactions on Emerging Telecommunications Technologies*, vol. 34, no. 5, pp. 4750, 2023. https://doi.org/10.1002/ett.4750

[Xiao, 2023] Q. Xiao, Y. Li, F. Luo, and H. Liu, "Analysis and assessment of risks to public safety from unmanned aerial vehicles using fault tree analysis and Bayesian network," *Technology in Society*, vol. 73, pp. 102229, 2023. https://doi.org/10.1016/j.techsoc.2023.102229

[Zeng, 2023] J. Zeng, Z. Wu, M. D. Todd, and Z. Hu, "Bayes risk-based mission planning of unmanned aerial vehicles for autonomous damage inspection," *Mechanical Systems and Signal Processing*, vol. 187, pp. 109958, 2023. https://doi.org/10.1016/j.ymssp.2022.109958

[Zhang, 2023] X. Zhang, Y. Liu, Z. Gao, J. Ren, S. Zhou, and B. Yang, "A ground-risk-map-based path-planning algorithm for UAVs in an urban environment with beetle swarm optimization," *Applied Sciences*, vol. 13, no. 20, pp. 11305, 2023. https://doi.org/10.3390/app132011305